Towards identifying New Human Ribonucleases that Cleave microRNA Using a High-Throughput Method

by

Suhua Ye

B.Sc., University of Ottawa, 2007

THESIS SUBMITTED IN PARTIAL FULFILLMENT OF
THE REQUIREMENTS FOR THE DEGREE OF
MASTER OF SCIENCE
IN
MATHEMATICAL, COMPUTER AND PHYSICAL SCIENCE
(CHEMISTRY)

THE UNIVERSITY OF NORTHERN BRITISH COLUMBIA

July 2011

Library and Archives Canada

Published Heritage Branch

395 Wellington Street
Ottawa ON K1A 0N4
Canada

Bibliothèque et Archives Canada

Direction du Patrimoine de l'édition

395, rue Wellington
Ottawa ON K1A 0N4
Canada

Your file Votre référence
ISBN: 978-0-494-87574-2

Our file Notre référence
ISBN: 978-0-494-87574-2

Abstract

Endoribonucleases were once thought of as only being key enzymes responsible for the degradation of prokaryotic mRNAs. They are now believed to play critical role in initiating eukaryotic/mammalian RNA decay and hence RNA abundance. To date, only few mammalian endoribonucleases that cleaved mRNA have been identified and studied. It is unknown if mammalian endoribonucleases can control microRNA (miRNA) abundance. The major goal of this MSc thesis was to develop a high-throughput method to identify new human endoribonucleases that cleave miR155.

The first objective of this thesis was to develop a high-throughput method to express and purify human recombinant proteins from the hEx1 human fetal brain library. This was followed by development of a high-throughput fluorescence-based assay to screen purified recombinant proteins for activity against fluorogenic miR155 substrate. Through a series of optimization experiments, we have successfully established a high-throughput procedure and the criteria in selecting a preliminary list of positive candidates.

Table of Contents

Chapter 5 - General discussion

List of Tables

List of Figures

Acknowledgements

I would like to thank my MSc. Thesis supervisor Dr. Chow Lee for his guidance, support and encouragement during the course of this thesis. I would also like to thank my supervisory committee members, Dr. Stephen Rader and Dr. Brent Murray for their helpful suggestions and insights in carrying out this research. Special thanks to Maggie Li for her help and guidance in conducting the experiments. Also, I would like to extend my thanks to all members of the Lee lab for their encouragement and technical support, and friends in Prince George for the support and friendship.

Most importantly, I would like to thank my parents, Ye Huan-Cai and Tang Wei-Min for their unending love, support and encouragement throughout my life, especially during this ten-year student journey in Canada.

Candidate's Publications Relevant to this Thesis

Abstracts

Ye, S., Woodbeck, R., Li, W.M., Lee, C.H. Towards Discovering New Mammalian RNA Cleaving Enzymes Using a High Throughput Screening Method. RiboWest Conference, Prince George BC (2009)

Chapter 1

Introduction

In Eukaryotic cells, gene expression is a tightly regulated process with key players guarding at different steps. This chapter briefly describes the general key players involved in the post-transcriptional control of gene expression with an emphasis on human endoribonucleases and microRNAs.

1.1 Mechanisms in the control of Eukaryotic gene expression

In eukaryotic cells, gene expression can be controlled at transcriptional and post-transcriptional levels. At the transcriptional level, gene regulatory proteins containing DNA binding motif bind to the regulatory sequence of the target gene and regulate the time and frequency of gene transcription. For example, p53 and GATA-1 recognize two different DNA sequences in target genes in mammalian cell (Alberts *et al.* 2002). On the other hand, transcription can also be turned off completely upon DNA methylation (Alberts *et al.* 2002).

In the post-transcriptional stage, RNA turnover which dictates mRNA abundance can directly control the abundance of protein (Fan *et al.* 2002; Raghavan *et al.* 2002). Conventional mRNA decay pathways such as polyA deadenylation, 3'-5' decay and 5'-3' decays were generally believed to be the major mode of mRNA degradation (Parker and Song 2004). However, this dogma has been challenged by the mRNA specificity of few endoribonucleases (Li *et al.* 2010) and the recent discoveries of endoribonucleases that demonstrated endoribonuclease activity of a number of proteins known to be involved in exonucleolytic degradation (Tomecki *et al.* 2010; Lebreton *et al.* 2008; Schaeffer *et al.* 2009). Differences and similarities between these two pathways are illustrated in Figure 1.

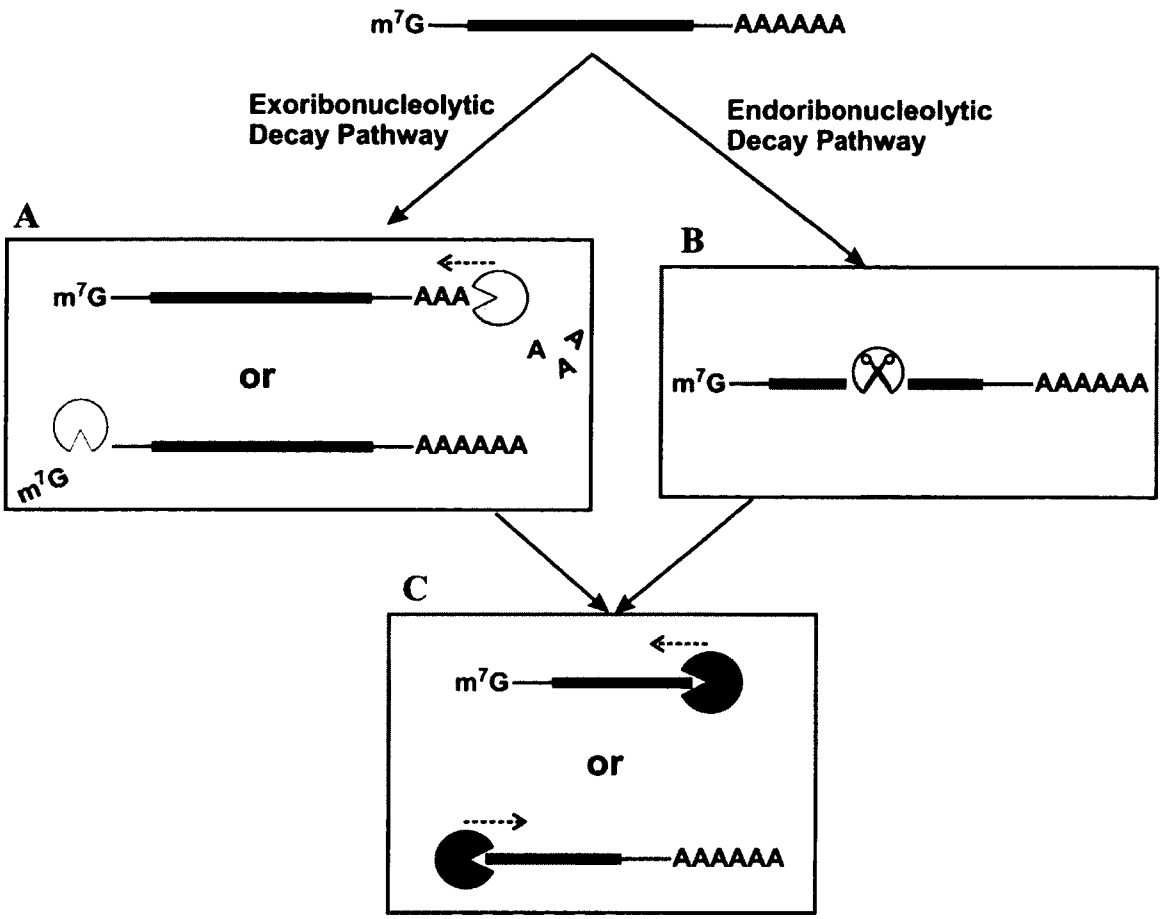

Figure 1. A schematic diagram of conventional exoribonucleolytic decay pathway and hypothetical endoribonucleolytic decay pathway that control stability of mRNA. (A) Two major exoribonucleolytic decay pathways. Top: Deadenylase leads to the shortening of polyA tail as the initial step of 3'-5' mRNA exoribonucleolytic decay. Bottom: Removal of 5'-cap by decapping proteins decreases the susceptibility of degradation. **(B)** Endoribonuclease cleaves mRNA in the middle and accelerates further degradation of target mRNA. **(C)** Further degradations are executed by 3'-5' and 5'-3' exoribonucleases (Parker and Song 2004; Garneau *et al.* 2007).

CH 1 INTRODUCTION

1.2 Key players in the control of RNA degradation

1.2.1 Enzymes – decapping enzymes, exoribonucleases, endoribonucleases and RBP

Decapping enzymes

Decapping enzymes are enzymes that remove the 5'- cap structure of transcript (Fillman and Lykke-Andersen 2005). Well studied decapping enzymes include Dcp1/2 and DcpS. Dcp 1/2 is part of a processing body complex that hydrolyzes the cap structure m^7Gppp. Removal of the protective cap leads to further degradation of the mRNA. The ability to bind to specific RNA is also essential for the decapping function as exemplified by hDcp2 (Li *et al.* 2008).

Exoribonucleases

In the past, exoribonucleases were thought to be the major players in RNA degradation. A number of exoribonucleases have been studied in different mRNA decay pathways. Exoribonucleolytic degradation takes place after the decapping or dephosphorylation of the transcript, from either 5'-3' or 3'-5' direction (Figure 1). Some well known examples of exoribonucleases associated with cancers are CCR4b, PARN and XRN1.

CCR4b, a component of human Ccr4-Not complexes, exhibits 3'-5' poly(A) exoribonuclease and ssDNA exonuclease activities (Lau and MacRae 2009; Chen *et al.* 2002; Morita *et al.* 2007). It regulates the mRNA level of a tumor suppressor gene p27Kip1. Depletion of CCR4b can increase the p27Kip1 mRNA level and impair cell growth (Morita *et al.* 2007). Poly (A)-specific ribonuclease (PARN) is another exoribonuclease that

cleaves from 3'-5' direction. As its name suggests, PARN preferably cleaves the poly (A) tails from 3'-direction. It also interacts with the 5'- end cap for a more efficient degradation of the poly (A) tails (Gao *et al.* 2000; Martinez *et al.* 2001). It participates in nonsense-mediated mRNA decay and degradation of mRNAs containing AU-rich elements (AREs) in their 3'-UTR (Lai *et al.* 2003).

Besides deadenylase, the 5'-3' exoribonuclease representative XRN1can also promote mRNA decay. In conventional mRNA decay pathways, upon the decapping of mRNA, XRN1 degrades the decapped mRNA from 5'-3' (Mitchell *et al.* 1997). It was also found to be an important factor in the spatial regulation of mRNA decay in mouse (Bashkirov *et al.* 1997). In the absence of XRN1, polyA$^+$ mRNAs accumulate at the processing bodies in mammalian cells (Cougot *et al.* 2004). The XRN1 gene is also a novel candidate tumour suppressor gene in osteogenic sarcoma (Mullen *et al.* 2008; Zhang *et al.* 2002).

Endoribonucleases

Researchers in the RNA field started to rethink the position of these two types of RNases in term of RNA metabolism after more work on endoribonucleases was done. Compared to exoribonucleolytic decay, endonucleolytic cleavages demonstrate higher sequence specificity (Rodgers *et al.* 2002, Stevens *et al.* 2002, van Dijk *et al.* 2000). One important aspect to consider is that many RNA therapeutic approaches, such as antisense therapy and therapeutic RNA interference, involve specific RNA sequence and endoribonucleolytic activity.

Many of the known endoribonucleases are discovered by chance. A recent review on endoribonuclease concludes that no share protein domains for endonucleolytic RNA cleavage were found in most of the 13 enzymes discussed; structural diversity was found for those that did have identified ribonuclease domains (Li *et al.*, 2010). Regardless of their dissimilarity, these known endoribonucleases have been found to play important roles in essential cellular processes such as RNA interference, ER stress response, viral defence, aberrant RNA surveillance, microRNA biogenesis, tRNA processing, signalling and angiogenesis.

Associations between endoribonucleases and cancers have been shown previously by several examples such as Argonaute 2, IRE1, APE1 G3BP, Drosha and Dicer (Kim *et al.* 2009). These examples provided evidence that induction or suppression of such enzymes control toward the development of diseases such as cancers. More detailed descriptions of relevant human endoribonucleases are discussed in Section 1.4.

RNA-binding proteins (RBP)

Beside the enzymes that cleave RNA, RBPs also play important role in post-transcriptional control of gene expression. One of the main functions of these proteins are to block the interaction of the target mRNA with other proteins. AU-rich mRNAs are often the target of RNA binding protein regulation. Studies have found one single enzyme, tristetraprolin (TTP), to be the key regulator of a group of 63 genes which have AU-rich mRNA and are implicated in cellular growth, invasion and metastasis (Al-Souhibani *et al.* 2010). Furthermore, exemplified by transactivation-responsive RBP/ TRBP, RBP is also found to post-transcriptionally control the biogenesis of microRNA (Chendrimada *et al.* 2005; Melo *et al.* 2009; Paroo *et al.* 2009).

RBPs can bind to protect and control stability of the target RNA. For instance, HuR plays an important role in the growth of cancer cells. In MCF7 human breast cancer cell lines, it increases the stability of GATA3 and ER mRNA (Licata *et al.* 2010; Pryzbylkowski *et al.* 2008). In human conventional renal cell carcinoma (CRCC), HuR is overexpressed and stabilizes mRNA for proteins that are crucial for human CRCC tumorigenesis (Danilin *et al.* 2010).

The c-myc coding region determinant-binding protein (CRD-BP) is another example of RBP found highly expressed in various types of human cancer including breast, colon, skin, ovary, lung, brain and testicular cancer (Doyle *et al.*, 2000; Ioannidis *et al.*, 2003; Dimitriadis *et al.*, 2007; Ross *et al.*, 2001; Kobel *et al.*, 2007; Hammer *et al.*, 2005; Ioannidis *et al.*, 2005; Elcheva *et al.*, 2008; Ioannidis *et al.*, 2004). CRD-BP has been shown to bind to and stabilize a number of mRNAs implicated in cancers. The mRNA targets of CRD-BP are *c-myc*, CD44, βTrCP1, IGF-II, β-catenin, GLI1, and MDR1 (Ioannidis *et al.* 2005; Sparanese and Lee 2007; Vikesaa *et al.* 2006; Noubissi *et al.* 2006; Leeds *et al.* 1997; Gu *et al.* 2008; Noubissi *et al.* 2009).

While HuR and CRD-BP promote the growth of cancer cells, there are RBPs that play the opposite role by suppressing cancer growth. They are exemplified by proteins in the quaking family which is composed of multifunctional mRNA regulators that function as tumour suppressors (Biedermann *et al.* 2010).

1.2.2 Cellular structures involved in mRNA degradation

Stress granule (SG)

SGs belong to a type of the RNA granule groups involved in RNA translational regulation and decay. The SGs rapidly accumulate within 15-30 minutes as a stress response upon environmental stresses (Anderson and Kedersha 2006). The stability of specific mRNAs is regulated by the selective recruitment into the SGs, and the translational rate is subsequentially controlled (Anderson and Kedersha 2002). Components of SG include a wide range of protein classes such as ribosomal, translational proteins, proteins involved in RNA stability, RNA-binding proteins, exonucleases and enzymes from the RNAi pathway (Anderson and Kedersha 2006; Kedersha *et al.* 2005; Kedersha *et al.* 2002; Kedersha *et al.* 1999; Wilezynska *et al.* 2005; Stoecklin *et al.* 2004; Gallouzi *et al.* 2000; Thomas *et al.* 2005; Hua and Zhou 2004; Tourriere *et al.* 2003).

Processing-body (PB)

PB is one of the major compartments involved in mRNA degradation in cytoplasm. They interact closely with the SGs. mRNA marked by destabilizing factors may be transferred from SGs to PBs for degradation (Anderson and Kedersha 2008). It is also a site for RNA interference to take place (Lian *et al.* 2006; Jakymiw *et al.* 2005).

PBs contain enzymes which carry out the mRNA degradation functions including deadenylation, decapping, exoribonucleolytic and endoribonucleolytic decay (Eulalio *et al.* 2007; Franks *et al.* 2008; Parker and Sheth 2007). The degradation function begins with deadenylation of the poly A tail of the target transcript by the Ccr4p/Pop2p/Not complex, which is required for the PB formation (Parker and Sheth 2007; Zheng *et al.* 2008). After

deadenylation, two major decays take place from either direction of the transcript: 3' to 5' degradation carried by exosome and 5' to 3' degradation by exoribonuclease Xrn1p following removal of the m7Gppp cap by Dcp1/2 (Gu *et al.* 2004; Parker and Sheth 2007) or DcpS (Gu and Lima 2005). PBs are also composed of microRNA repression factors such as Argonautes and RNA binding proteins and translation repressors (Parker and Sheth 2007).

RNA-Induced Silencing Complex (RISC)

The RISC has received a great deal of attention since its discovery in 1985, due to its ability to repress target gene expression by degrading respective mRNA transcript (van den Berg *et al.* 2008; Rosenberg *et al.* 1985). It is a multi-protein complex that controls gene expression in translational level. Minimal components of RISC include a main catalytic component Argonaute 2 and a guide strand RNA that is either a microRNA or siRNA. The guide strand is either partially or completely complimentary to the target mRNA. Pairing of these two strands will result in translational repression or mRNA degradation (Huntzinger and Izaurralde 2011). The cleaved mRNA is then released and subjected to further exoribonucleolytic degradations.

Exosome

The exosome, also called PM/Scl complex, is a well known and characterized complex cellular structure that degrades RNA in 3'-5' direction. Specific exoribonucleases in the exosome are hRrp4p, hRrp40p, hRrp41p, hRrp46p, hMtr3p, Hrrp42p, oIP2, PM/Scl-75, PM/Scl-100 and Rpp14 (Raijmakers *et al.* 2004). Beside its main role in exoribonucleolytic activity, it is recently found that the exosome also contains proteins

with specific endoribonuclease and cytoplasmic mRNA decay activities (Schaeffer *et al.* 2009). The complex is also composed of proteins with RNA binding, 3'-5' hydrolytic exoribonuclease, 3'-5' phosphorolytic exoribonuclease, RNA helicase and nucleotide binding activities (Raijmakers *et al.* 2004).

In eukaryotes, the exosome is known to contribute to ribosomal RNA and small RNAs processing, pre-mRNA quality control and mRNA turnover (Raijmakers *et al.* 2004). Exosome mediated RNA degradation is sequence specific. For example, mRNAs with AU-rich elements are targeted by the exosome mRNA degradation (Mukherjee *et al.* 2002).

1.2.3 non-coding RNA

Another group of trans-acting factors that control the expression of genes is the non-coding RNAs (ncRNAs). They are abundant in mammalian cells (Mattick and Makunin 2006). RNAs that belong to this group include rRNA, tRNA, snRNA, snoRNA, microRNA and siRNA (Mattick *et al.* 2006). They fall into two categories according to their function: infrastructural ncRNAs (rRNA, tRNA, snRNA and snoRNA), and small regulatory ncRNA (snoRNA, microRNA and siRNAs) (Mattick *et al.* 2006). Increasing evidence indicates the association of ncRNAs with different types of cancers, which warrant their possible use as therapeutic target (Mallardo *et al.* 2008).

1.3 Significance of microRNA in the control of gene expression

MicroRNAs are a type of non-coding RNAs with the length of 18 - 24 nt that post-transcriptionally regulate the expression of genes. This group of small RNA has gained

great attention after its discovery in 1993, mainly due to its important role in the regulation of gene expression in the RISC.

1.3.1 MicroRNA Biogenesis

MicroRNAs are produced in a highly regulated manner (Siomi and Siomi 2010). They are generated from a microRNA gene or from the intron of a protein coding gene that is also called a mirtron (Chekulaeva and Filipowicz 2009; Kim *et al.* 2009). Four complexes (the microprocessor complex, the nuclear export complex, the Dicer complex and the RISC) are involved in the biogenesis and action of microRNA. In the nucleus, primary microRNA or pri-microRNA is generated, through the tailoring of Drosha containing microprocessor complex (Han *et al.* 2004; Gregory *et al.* 2004; Denli *et al.* 2004). Pri-microRNA is cropped by Drosha to form the hairpin shaped pre-microRNA. The pre-microRNA is then transported out of the nucleus to the cytoplasm by the nuclear export complex composed of Exportin 5 and RAN. In the cytoplasm, the Dicer complex further cuts the pre-microRNA into its mature form; the mature microRNA is functional as part of the RISC (Ryan *et al.* 2010; Ahluwalia *et al.* 2009).

1.3.2 Regulatory roles of microRNA

MicroRNAs control gene expression through either translational repression or degradation of mRNA (Cai *et al.* 2010; Esslinger *et al.* 2009). They have a huge impact on the global expression of proteins (Baek *et al.* 2008); about half of all mammalian protein coding genes are predicted to be controlled by these versatile regulatory elements (Krol *et al.* 2010). Targets of microRNAs include functionally related effector genes, regulators of transcription and regulators of alternative splicing (Makeyev and Maniatis 2008).

MicroRNAs have also been found to be involved in skin morphogenesis (Yi and Fuchs 2010), signal transduction (Inui *et al.* 2010) and glucose and lipid metabolism (Lynn 2009).

1.3.3 Role of microRNA in cancer

MicroRNAs are broadly implicated in various types of diseases, particularly cancer. The role of microRNA in cancer can be placed into two categories - oncogenic and tumour suppressor microRNA (Zhang *et al.* 2007). Oncogenic microRNAs that capture much of the attention are over-expressed in many types of cancers; this is exemplified by miR155 as the first oncogenic microRNA discovered (Tong and Nemunaitis 2008; Tam and Dahlberg 2002). MiR155 was found to inhibit apoptosis by suppressing Caspase-3 and apoptosis related enzymatic activity (Ovcharenko *et al.* 2007; Gironella *et al.* 2007). It is up-regulated in several types of cancers including CLL (chronic lymphocytic leukemia), breast cancer, Burkitts lymphoma, Hodgkins lymphoma, B-cell lymphoma, lung cancer, and pancreatic cancer (Iorio *et al.* 2005; Faraoni *et al.* 2009; Zhang *et al.* 2007; Rai *et al.* 2008; Tong and Nemunaitis 2008; Yue and Tigyi 2006; Wiemer 2007). Because of the widely distributed oncogenic activity of miR155 in a number of malignancies, it serves as an excellent target for cancer therapy. Thus, miR155 was chosen as a target RNA in this research.

1.3.4 Regulation of microRNA abundance

Though much evidence has shown the regulatory roles of microRNA in a wide variety of cellular activities, the expression and turnover of microRNAs are also under sophisticated regulations. The microRNA abundance can be controlled in two major ways: through the regulation of microRNA biogenesis and microRNA decay.

CH 1 INTRODUCTION

Primary microRNAs (pri-miRNA) are generated from microRNA gene transcription by RNA polymerase II (Kim *et al.* 2009). The transcriptional control of the microRNA gene is quite similar to the protein-coding gene. These two types of gene share similar features in the promoter regions, such as GpG islands, TATA box sequences, initiation elements and histone modifications (Ozsolak *et al.* 2008; Corcoran *et al.* 2009). These similarities suggest that transcription factors (TFs), enhancers, silencing elements and chromatin modifications are the key controllers in microRNA gene transcription (Krol *et al.* 2010).

After transcription, pri-miRNAs are cleaved by Drosha in the microprocessor complex in the nucleus (Han *et al.* 2004; Gregory *et al.* 2004; Denli *et al.* 2004). Pri-miRNAs become precursor microRNAs (pre-miRNAs) after removal of part of the stem. The pre-miRNAs are then exported from the nucleus. In the cytoplasm, pre-miRNAs are further processed by Dicer to remove the loop to generate a major and a minor mature microRNA. The major strand is loaded onto Argonaute located in the RISC as a guide for gene silencing. Differential expressions of microRNAs in different tissues and during different developmental stages suggest that microRNA biogenesis can be regulated (Davis *et al.*, 2009; Ding *et al.*, 2009; Ambros *et al.*, 2003; Wulczyn *et al.*, 2007).

Besides regulation of microRNA biogenesis, the microRNA abundance is also controlled by their turnover. Compared to biogenesis and regulatory control of microRNA, current available information regarding the control of microRNA stability is still very limited. Nonetheless, some progress has been made to find the key players in microRNA degradation. Several studies have found evidence of acceleration and regulation in selected microRNA turnover (Krol *et al.* 2010; Hwang *et al.* 2007; Buck *et al.* 2010; Sethi and

Lukiw 2009; Rajasethpathy *et al.* 2009). The first two exoribonucleolytic degradation models of microRNA decay were found in studies using model species, *Arabidopsis thaliana* and *Caenorhabditis elegans*. In *A. thaliana*, small RNA degrading nuclease 1 (SDN1) acted directly toward single stranded miR173 *in vitro* (Ramachandran and Chen 2008). Increased stability of several microRNAs (miR159, miR167, and miR173) after knockdown of the members from this 3'-5' exoribonuclease family indicated that these microRNAs may share a similar RNA decay pathway (Ramachandran and Chen 2008). 5'-3' Exoribonuclease 2 (XRN-2) from *C. elegans* is the second exoribonuclease discovered (Chatterjee and Großhans 2009). It is a 5'-3' exoribonuclease that carries out the degradation of mature *let-7* microRNA *in vivo* (Chatterjee and Großhans 2009). This function of XRN-2 depends on the target availability; the 5'-end of microRNA has to be released from miRISC in order to be accessible for XRN-2 (Chatterjee and Großhans 2009).

The evidence of microRNA degradation by exoribonucleases was also found in human cells. In a recent study conducted with human melanoma cells, miR221 was shown to be degraded by a 3'-5' exoribonuclease, human polynucleotide phosphorylase/*hPNPase*$^{old\text{-}35}$ (Das *et al.* 2010). Another recent study using human embryonic kidney 293 cells revealed involvement of the exosome in the degradation of miR382 (Bail *et al.* 2010).

RBP also play a role in the abundance of microRNA. This is exemplified by a human nuclear factor named TDP-43 (Buratti *et al.* 2010). It can up- or downregulate different microRNAs base on the position it binds to. It stabilizes the let-7b by binding to the mature form sequence, and decreases the abundance of mature form miR663 by binding

to its hairpin precursor (Buratti *et al.* 2010). Binding to Argonaute proteins in the RISC is also thought to protect the microRNA from degradation (Chatterjee and Großhans 2009).

Furthermore, a small number of *cis*-acting elements that affect the microRNA stability have also been identified. In animals, 3'-terminal adenylation by GLD-2 was found to stabilize mature miR122, but not pre-miR122 (Katoh *et al.* 2009). In plants, both 2'-O-methylation and adenylation at 3'- terminal demonstrated stabilizing effect on microRNA (Yu *et al.* 2005; Lu *et al.* 2009). Known key players regulating animal microRNA turnover are shown in Figure 2. It is believed that microRNA degradations are likely to be similar to those of mRNAs (Krol *et al.* 2010).

Mature microRNA levels do not always correlate with their pri- or pre-mRNAs. The evidence of selected mature microRNA turnover strongly supports the existence of post-transcriptional mechanisms that control the level of mature microRNA. It is possible that endoribonucleolytic cleavage plays a role in the process of microRNA degradation. However, due to the lack of information in this area, other key players in microRNA decay have yet to be identified and characterized.

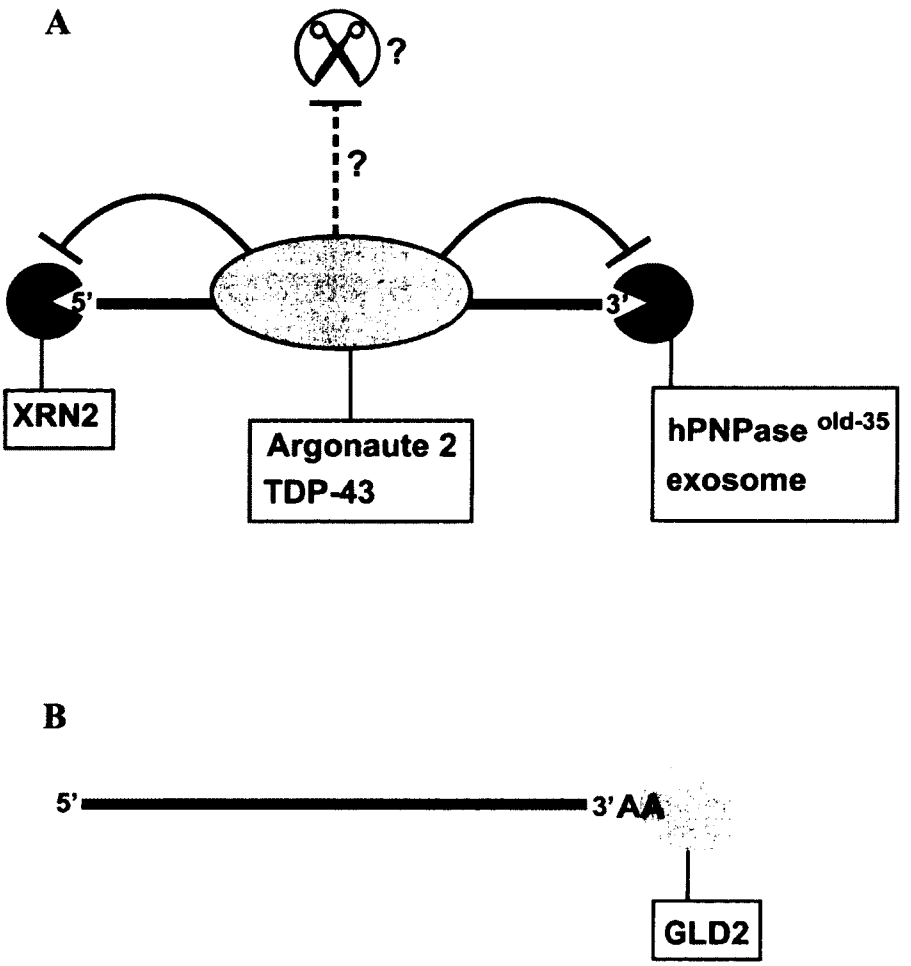

Figure 2. Schematic diagram summarizing key factors regulating animal microRNA turnover. (A) Binding of RBP (Argonaute 2 or TDP-43) prevents the exoribonucleolytic decay from either ends by exoribonucleases (XRN2 or hPNPaseold-35) or exosome. It may also compete with unknown endoribonucleases and prevent them from cleaving in the middle of microRNA. **(B)** Adenylation at the 3'-end stabilizes microRNA.

1.4 Human endoribonuclease

One of the reasons for our limited knowledge on mammalian endoribonucleases is the lack of tools used to identify them. Most of the recent endoribonuclease discoveries were quite random. A recent review has focused on comparing the different eukaryotic endoribonuclease. It was found that some of the enzymes with known domains demonstrate

structural diversity (Li *et al.*, 2010). Endoribonucleases can be associated with a wide variety of cellular functions; they may have different mRNA targets, and possess different cleavage specificity (Li *et al.*, 2010). In this section, mRNA targets, cleavage specificity and cellular functions of known human endoribonucleases are briefly introduced.

1.4.1 Human endoribonuclease implicated in cancers

Argonaute 2 (Ago2)

Ago2, also called Eukaryotic translation initiation factor 2C 2 (eIF-2C 2), is an important component in RISC and required for RNA mediated gene silencing (Liu *et al.* 2004). Ago2 binds to a guide RNA, either a microRNA or siRNA, in the RISC to target a complementary mRNA (Liu *et al.* 2004; Kim *et al.* 2009; Carthew and Sontheimer 2009; Jinek and Doudna 2009). The binding of the complementary mRNA with the RISC will then result in gene silencing by inhibiting the translation or cleaving the complementary mRNA (Hutvágner and Zamore *et al.* 2002; Jinek and Doudna 2009). The interaction of Ago2 with Dicer also suggests a role in microRNA biogenesis (Maniataki and Mourelatos 2005; O'Carroll *et al.* 2007). Increased level of Ago2 was found in aggressive breast tumours (Blenkiron *et al.* 2007). Also, increased cell proliferation was observed in Ago2 transfected MCF7 cell line (Adams *et al.* 2008).

Inositol-requiring enzyme 1 (IRE1)

IRE1 is also called endoplasmic reticulum-to-nucleus signalling protein. It is a bi-functional protein that has both endoribonuclease and serine/threonine-protein kinase activity (Tirasophon *et al.* 1998). In mammalian cells, IRE1 is required for a stress response pathway functioning under ER stress (Tirasophon *et al.* 1998). It carries out

translational repression by cleaving 28S ribosomal RNA under ER stress (Iwawaki *et al.* 2001). IRE1 plays both tumorigenic and tumour suppression roles in tumorigenesis through the activation of unfolded protein response by the IRE1-XBP1s pathway (Kim and Lee 2009). The IRE1 activity was found to increase the cancer survival and progression in several types of cancer, including breast cancer, liver cancer and myeloma (Lin *et al.* 2007; Gomez *et al.* 2007; Davies *et al.* 2008; Shuda *et al.* 2003; Li *et al.* 2007; Carrasco *et al.* 2007). Several observations demonstrating the ability of IRE1 in inducing cancer cell death and inhibition supported the tumor suppression role of IRE1 in cancer (Kim and Lee 2009; Davenport *et al.* 2007; Guichard *et al.* 2006; Little *et al.* 2007; Kraus *et al.* 2008; Joung *et al.* 2007; Gao *et al.* 2008).

RNase L

RNase L, commonly named 2-5A-dependent ribonuclease, is a 2'-5'-oligoadenylate- dependent ribonuclease that cuts single stranded RNA (Liang *et al.* 2006). It functions as a viral defense following the activation of interferon (IFNs) pathway through a combination of mechanisms by directly degrading viral RNAs and rRNA, and inducing apoptosis and other antiviral genes (Le Roy *et al.* 2001).

RNase L also contributes to tumor suppressor activities such as stress mediated apoptosis cell proliferation and regulation of protein synthesis (Liang *et al.* 2006, Madsen *et al.* 2008). Mutated RNase L was related to the increased risk of head and neck, uterine cervix, breast and prostate cancer (Madsen *et al.*, 2008; Carpten *et al.*, 2002).

CH 1 INTRODUCTION

APE1

Apurinic/apyrimidinic (A/P) DNA endonuclease APE1, also called APEX-1 in humans, is commonly known as a DNA repair enzyme that cleaves A/P DNA in base excision repair mechanism. Other known functions of APE1 include redox activation of transcription factors, 3'-phosphodiesterase, 3'-5' exonuclease, 3' phosphatase, and RNase H activities (Chou and Cheng 2002, Tell *et al.* 2005). It was recently discovered as an endoribonuclease that binds to a coding region of c-myc mRNA called the coding region determinant (CRD) and preferentially cleaves phosphodiester bonds between UA, CA and UG dinucleotides (Barnes *et al.* 2009). The cancer types previously reported to be associated with APE1 are myeloma, osteosarcoma, hepatocellularcarcinoma, breast carcinoma, colon adenocarcinoma, lung adenocarcinoma and leiomyoma (Kim and Lee 2009; Tell *et al.* 2005; Yang *et al.* 2007; Wang *et al.* 2004; Pardini *et al.* 2008; De Ruyck *et al.* 2007; Orii *et al.* 2002). The implications of APE1 with cancer may be linked to its ability to control *c-myc* gene expression level by cleaving its mRNA (Kim and Lee 2009; Barnes *et al.* 2009).

Drosha and Dicer

Drosha and Dicer are both members of the RNase III family. Drosha processes primary microRNA (pri-microRNA) as a component of the microprocessor complex in the nucleus (Han *et al.* 2004; Gregory *et al.* 2004; Denli *et al.* 2004). It cleaves double stranded pri-microRNA at the 3'- and 5'- ends and produces precursor microRNA (pre-microRNA) (Lee *et al.* 2003). Dicer comes in to carry out dsRNA cleavage and generate siRNA or premature microRNA by cleaving the hairpin pre-mRNA (Fortin *et al.* 2002, Nicholson

and Nicholson 2002, Doi *et al.* 2003, Zhang *et al.* 2004). A recent study also suggests that Drosha and Dicer are involved in rRNA biogenesis (Liang, 2011). The major implication of Drosha and Dicer in cancer mainly comes from their functions in microRNA processing and biogenesis by increasing the levels of oncogenic microRNA (Nakamura *et al.* 2007; Davis *et al.* 2008; Iorio *et al.* 2005; Roldo *et al.* 2006; Slaby *et al.* 2007; Dillhoff *et al.* 2008; Markou *et al.* 2008; Connolly *et al.* 2008; Chiosea *et al.* 2006; Chiosea *et al.* 2007; Chiosea *et al.* 2008; Flavin *et al.* 2008; Kaul *et al.* 2004).

G3BP

G3BP was identified as a cytosolic protein that binds to Src homology 3 (SH3) domain of GTPase-activating protein (GAP) (Parker *et al.* 1996). It binds to GAP only in proliferating cells where Ras is in the activated state (Parker *et al.* 1996, Tourriere *et al.* 2001). Endoribonucleolytic activity of G3BP occurs at the phosphodiester bond in between CA dinucleotide of 3' UTR of c-myc mRNA (Tourriere *et al.*, 2001). Its high-affinity binding to polyA mRNAs sequence appears to allow the mRNA to decay with specificity as exemplified by the cleavage of 3'UTR of human c-myc mRNA (Tourriere *et al.* 2001, Gallouzi *et al.* 1998). Two isoforms of this RNase, G3BP1 and G3BP2 also bind to p53 both *in vitro* and *in vivo*, and results of the knockdown experiment suggest their negative regulation of p53 by regulating a p53 regulator MDM2 (Kim *et al.* 2007). Expression of G3BP is also closely related to lymph node metastasis in esophageal squamous carcinoma (Zhang *et al.* 2007).

CH 1 INTRODUCTION

Angiogenin

Angiogenin, also known as RNase 5, belongs to the pancreatic ribonuclease family with 65% homology to pancreatic ribonucleases RNase A (Saxena *et al.* 1992). Compared to RNase A and other known eukaryotic endoribonuclease, Angiogenin has much weaker activity (Li *et al.* 2009; Kelemen *et al.* 1999). However, despite its weak enzymatic activity, Angiogenin has great biological significance. It is a cytotoxic RNase that inhibits protein synthesis by degrading cellular tRNAs, and both 28S and 18S ribosomal RNA (Saxena *et al.* 1992; Lee and Vallee 1989; Shapiro *et al.* 1986). The level of angiogenin is found to be elevated in prostate cancer, gastric carcinoma and melanoma (Katona *et al.* 2005; Chen *et al.* 2006; Vihinen *et al.* 2007).

Flap structure-specific endonuclease 1 (FEN1)

FEN1, similar to APE1, is an important multi-functional protein in DNA repair and base-excision repair (Robins *et al.* 1994; Shen *et al.* 1996; Guo *et al.* 2008). It also exhibits 5'-3' exonuclease activity toward double stranded DNA, RNase H activity and endonucleolytic cleavage of RNA at 5' endogenous stem structures (Robins *et al.* 1994; Shen *et al.* 1996; Guo *et al.* 2008; Stevens *et al.* 1998). Its association with cancer has been linked to its DNA endonuclease activity (Kim and Lee 2009). However, its endoribonuclease activity has not been associated with cancer.

Poly[U]-specific endoribonuclease

This protein is also called Placental protein 11 (PP11), as it is placental specific (Bohn and Winckler 1980; Bohn *et al.* 1981). It belongs to the ENDOU family and cleaves single stranded RNAs and results in products containing 2'-3'- cyclic phosphate termini

(Laneve *et al.* 2008). PP11 is a tumour marker with diagnostic significance (Grundmann *et al.* 1990), and has been found to express in various type of cancer including mucinous and serous cystadenocarcinoma (Inaba *et al.* 1982), breast cancer (Inaba *et al.* 1981), and gastric cancer (Inaba *et al.* 1980).

1.4.2 Human endoribonucleases that belong to a complex

Some endoribonucleases take part in a complex to achieve their functions. The endoribonucleases Argonaute 2, Dicer and Drosha that have already been mentioned in Section 1.4.1 also belong to this group. Both Argonaute 2 and Dicer are components of the microRNA loading complex (miRLC) of RISC and are required for biogenesis and recruitment of microRNA (MacRae *et al.* 2008), while Drosha is part of the microprocessor complex (Han *et al.* 2004; Gregory *et al.* 2004; Denli *et al.* 2004). The rest of this group is exemplified by CPSF3, SMG6 and Rrp44.

CPSF3

CPSF3 is a component of the cleavage and polyadenylation specificity factor (CPSF) complex. It possesses both endoribonuclease and exoribonuclease activities. CPSF3 plays a key role in the histone 3'-end pre-mRNA processing by cleaving the histone pre-mRNAs and carrying out exoribonucleolytic degradation of the downstream cleavage product from the 5' to 3' direction (Ryan *et al.* 2004; Kolev *et al.* 2008; Mandel *et al.* 2006). It also recognizes the AAUAAA signal sequence and interacts with PolyA polymerase and other factors to implement the cleavage and polyA addition (Kaufmann *et al.* 2004).

SMG6

SMG6, also called Telomerase-binding protein EST1A, is part of the telomerase ribonucleoprotein (RNP) complex. It functions as an endonuclease and cleaves single stranded RNA, but not double stranded RNA or single stranded DNA (Snow *et al.* 2003; Glavan *et al.* 2006). It exemplifies the involvement of endoribonucleases in the mRNA surveillance mechanism by cleaving nonsense mRNA in human cells (Eberle *et al.*, 2009).

Rrp44

Rrp44 (Ribosomal RNA-processing protein 44, also called Dis3-like 1), is a component of the exosome complex that plays key role in RNA processing and turnover. It has recently been discovered that Rrp44 has both 3'-5' exoribonuclease and endoribonuclease activities (Tomecki *et al.* 2010).

1.4.3 Other human endoribonucleases

RNase κ

RNase κ is a relatively new ribonuclease. The human ortholog of RNase κ is a 98 amino acid protein that cleaves specifically at ApU and ApG phosphodiester bonds, and also UpU at a lower rate (Economopoulou *et al.* 2007).

ARD-1/NIPP-1

ARD-1 (Activator of RNA decay) is a site-specific Mg^{2+} dependent endoribonuclease that has a similar cleavage functionally resembling RNase E from *E. coli*; it cleaves the same substrate as RNase E *in vitro* at the same cleavage site. ARD-1 was first

discovered in the expression of human cDNA copy of *ARD-1* (Claverie-Martin *et al.* 1997), and it was later found to be an isoform to NIPP-1 encoded from the same gene by alternative splicing (Chang *et al.* 1999).

Pancreatic RNase

The pancreatic ribonuclease family is probably the most extensively studied RNase across different species. The RNase A superfamily is one of the most intensively studied ribonuclease with diverse members from RNase 1-13, which are mainly responsible for host defense (Dyer and Rosenberg 2006). Other biological processes that RNase A contributes to are neurotoxicity, angiogenic activity, immunosuppression and anti-tumour activity (Beintema *et al.*, 1988; Di Donato *et al.*, 1993).

1.4.4 Summary

It is believed that endoribonucleases closely regulate the abundance of mRNA or microRNA in cells. However, very little information is known regarding the specific mRNA and microRNA endoribonucleases regulate. Only a few human endoribonuclease described in the earlier sections possess specificity toward a particular mRNA. For instance, IRE1 specifically cleave XBP1 mRNA during splicing to generate a new C-terminus as an unfolded protein response (Iwakoshi *et al.*, 2003; Lee *et al.*, 2002). In addition, IRE1 also cleave non-mRNA, 28S ribosomal RNA. APE1 is shown to cleave *c-myc* mRNA at its CRD region (Barnes *et al.*, 2009). As mentioned above, G3BP binds and cleaves the 3'-UTR of c-myc mRNA (Tourriere *et al.* 2001, Gallouzi *et al.* 1998), while Angiogenin possess substrate specificity toward cellular tRNAs, and both 28S and 18S ribosomal RNA (Saxena *et al.* 1992; Lee and Vallee 1989; Shapiro *et al.* 1986).

To date, no endoribonuclease has been found to cleave on microRNA directly in cells. For the endoribonucleases that have been shown to carry substrate specificity, it still remains unknown whether these enzymes can act on other RNAs and influence biological functions relevant to the RNA. Therefore, a better understanding of mammalian endoribonucleases is required for us to answer these questions.

1.5 Research objectives

There is an increasing interest in the regulatory roles of microRNAs in cancers. To date, characteristics of inhibitory and regulatory targets of microRNAs have been the main focus of microRNA research. In contrast, less effort has been put in finding the key players in the regulation of microRNA abundance, especially the degradation of microRNA. It is already known that exoribonucleases can catalyze the degradation of microRNA as described in Section 1.3.4. No research has been done to find out whether any endoribonucleases play a role in accelerating the decay of microRNAs.

One of the major hindrances to identifying endoribonucleases is the difficulty in detecting mRNA or microRNA cleavage products. Hence, despite the increasing importance of mammalian endoribonucleases, a great proportion of information about them still remains unknown. To this end, this thesis was undertaken in an effort to develop a robust fluorescence-based system to identify new human endoribonuclease that can potentially degrade oncogenic microRNA.

The first objective of this thesis was to develop a high-throughput fluorescence-based method to screen a library of human recombinant proteins for endoribonclease activity. To achieve this goal, we chose miR155 as the microRNA target in the high-

throughput screen. Five 96-well sets containing clones of the human fetal brain cDNA library, hEx1 were randomly chosen. In the first part of this objective, we optimized some experimental conditions in the high-throughput system. The second part of this objective was to obtain a list of positive hits. Following were the questions that we aim to answer as we accomplish the objective: 1. Is the substrate designed suitable based on the screening results? Given that there is no known endoribonuclease that cleaves microRNA, is it feasible to use microRNA as a substrate for endoribonuclease screen? 2. What is the average rate of positive hits from one set? Is it possible that the tested clones are going to be all negative or all positive? 3. How do we distinguish between positive and negative hits?

The second objective of this thesis was to verify the positive hits obtained from the primary screen in the first objective. The primary screen step has the potential to pull out endoribonuclease, exoribonuclease and RBP, but our primary goal is to find novel endoribonucleases. The first part of the second objective, which was essentially our secondary screen process, was accomplished by determining the inducibility and purity of clones, by further repeating the fluorescence-based assay to reproduce the data from primary screen, and obtaining identity and integrity of clones. The second part of the second objective was carried out by performing electrophoretic assays using three radiolabeled substrates. Two of these radiolabeled substrates used in the electrophoretic assay resemble the fluorescence-based substrates used in the primary screen. To find out whether the candidate was a potential exoribonuclease, a fourth substrate composed of 15 adenosine monophosphates was used.

Chapter 2
Development of a High-Throughput System to express and purify a library of recombinant proteins

2.1 Introduction

A high-throughput system (HTS) is a type of experimental design that allows parallel assay with multiple samples. It is commonly used in drug discovery, chemical, biological and biochemical compound discovery.

2.1.1 Protein Functional Screen

High-throughput methods that have been proven to be useful for protein functional analysis are in increasing demand. In the past, several *in vitro* protein functional screens were successfully developed by different labs (Galicia-Vázquez *et al.* 2009; Kijanka *et al.* 2009; Mouratou *et al.* 2002; Woo *et al.* 2005; Proudfoot *et al.* 2008). Nucleic acid related enzymatic functions that have been screened for in these studies include endonuclease activity toward DNA substrate, nucleic acid binding and methyltransferase acitvities. In the endonuclease and methyltransferase studies, enzymatic activities were screened using biotin and digoxingenin labeling methods and determined by ELISA (Mouratou *et al.* 2002; Woo *et al.* 2005). All of these studies involved substrate labeling. This indicates the common use of substrate labeling in protein functional screen.

2.1.2 cDNA expression library

The cDNA expression library, hEx1 (prefix MPMGp800, Imagenes GmbH), used in this project contains 35,000 clones that express His-tagged human fetal brain

recombinant proteins (Bussow *et al.* 2000). It was made by inserting cDNAs generated from human fetal brain tissue directionally into an expression plasmid, pQE30NST, in between restriction sites *SalI* and *NotI* (Figure 3). The hEx1 clones were placed in 384-well plates. Each plate contained 4 sets (A-D). In this thesis, the code of hEx1 clones is in a format that the first three letter/digits represent position of the clone in the 384 plate and the last three digits represent the plate number. For example, "I23512" is clone I23 from plate 512.

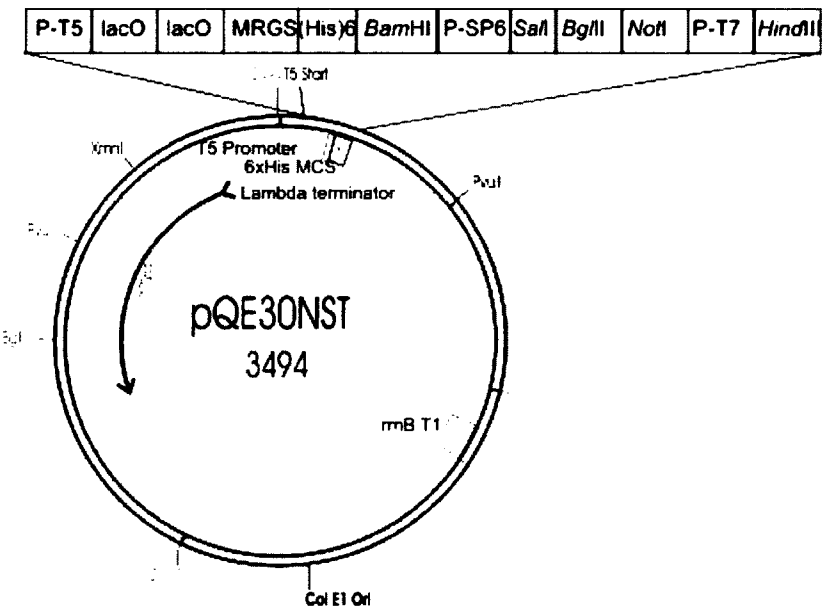

Figure 3. Map of the pQE30NST plasmid.

The hEx1 library was designed and shown to be suitable for protein characterization of the human proteome (Bussow *et al.* 2004). Another study also showed the application of hEx1 recombinant proteins in a high-throughput screen for antibody binding specificity (Kijanka *et al.* 2009).

There are several potential advantages in using hEx1. First, as some tumor suppressor genes and oncogenes are found to be expressed only during fetal development (Dean 1998), using proteins expressed in human fetal brain may increase the chance of finding endoribonuclease implicated in cancer. Second, as the expression-ready cDNA is already inserted in the plasmid, cloning step is not necessary. Third, it is known that some hEx1 proteins may be in truncated form (Bussow 2000). Hence, it is possible to produce portions of proteins which are soluble and possess endoribonucleolytic activity.

2.1.3 Expression and purification of sets 512A, 517A, 523C, 525A and 568D

We developed a high-throughput method to express and purify 480 hEx1 clones from selected sets 512A, 517A, 523C, 525A and 568D, through the optimizations of recombinant protein induction, purification, dialysis, and cell lysis. The development of this high-throughput system for generating recombinant proteins used in the functional screen is described in this chapter.

2.2 Methodology

2.2.1 Protein expression using two different sets of media

1) Preparations

2YT and SB broth

Inoculation of the *E.coli* bacterial culture was performed using a 96-pin replicator to transfer a set of frozen hEx1 clones from 384-well stock plate to four 96-well tissue culture plates. Each of the 96 well contained 100 μL 2YT with perspective antibiotics (100 μg/mL ampicillin and 15 μg/mL kanamycin). Glucose (2%) was added to the broth to

ensure the healthy growth of small size cultures. These starter cultures were incubated in a 37°C shaker at a speed of 200 rpm overnight. On the second day, the 100-μL starter culture was then transferred to a bigger culture sets containing 900 μL SB in each well. The SB broth contained Vitamin B1 (20 μg/mL) and 1x KPB to improve the growth of small size culture. Cultures were grown to OD_{600} of 0.5 before induction.

LB broth

The *E.coli* culture was grown in LB broth under similar conditions as above. Starter culture was grown overnight at 37°C with 100 LB medium containing 100 μg/mL of ampicillin, 15 μg/mL kanamycin and 2% (w/v) glucose. The next day, each clone of a 96-clone set was grown in 900 mL LB medium 100 μg/mL of ampicillin, 15 μg/mL kanamycin and 20 μg/mL vitamin B1 at 37°C for 3 hours to a OD_{600} of 0.5 in 96 deep-well plate microplates (UNIPLATE, Whatman®) at 200 rpm before induction.

Table 1. Ingredients of broth used for *E.coli* culture in this project.

Broth / Reagent	Ingredients
LB	1.0 % (w/v) BactoTryptone, 0.5 % (w/v) yeast extract, 1.0 % (w/v) NaCl, pH7.4
2YT	1.6 % (w/v) BactoTryptone, 1.0 % (w/v) yeast extract, 0.5 % (w/v) NaCl, pH 7.4
SB	1.2 % (w/v) BactoTryptone, 2.4 % (w/v) yeast extract, 0.4 % (v/v) Glycerol
1x KPB	4.6 % KH_2PO4, 24.3 % K_2HPO_4

Induction

All clones were induced with IPTG at final concentration of 1 mM at 37°C for 6 hours.

Cell lysis

After induction, bacterial cell pellets were collected by spinning the deep-well plate at 3000xg for 10 minutes (Beckman Coulter®). Cells were lysed for 5 cycles of complete freezing and thawing. The lysed cells were then subjected to immunoblotting.

2) Western blots

Lysed cells were transferred to a piece of nitrocellulose membrane using a 96 Solid Pin Multi-Blot Replicator (408, V&P Scientific). Western blot described previously was performed to visualize the presence of His-tagged proteins in the cell lysate.

2.2.2 HTS induction optimization

A 96 Solid Pin Multi-Blot Replicator (VP408, V&P Scientific, San Diego, CA) was used to transfer and inoculate 96 bacteria at a time. It is capable of inoculating 4 sets of clones from one 384-well stock plate. Prior to every application, metal tips of the replicator were dipped briefly in a 10% bleach solution, then into a series of two autoclaved milliQ water baths, followed by a 99% isopropanol bath. Between baths, the liquid on the pin tips was removed by light tapping on a piece of lint-free blotting paper (VP522, V&P Scientific, San Diego, CA). The pins were then air dried. In addition to the sterilization steps, pins were washed with wash buffer provided (V&P Scientific, San Diego, CA).

An induction test was performed by comparing expression of the same set of clones induced under two different conditions: incubation for 16 hours at 16 °C and 6 hours at 37°C. Proteins expressed under these two sets of conditions were purified. Four elutions

were collected and concentrations of proteins in each elution were compared to determine the best condition for small culture parallel purification.

2.2.3 Methods to lyse bacterial cells for use in HTS and individual cell growth

A 150 mL *E.coli* culture of clone F20568 was divided into three parts. Cell pellets from 50 mL cell cultures were each resuspended in 4 mL NPI-10 followed by the following lysis methods:

1) Enzymatic method - cells were incubated in a final concentration of 1 mg/mL lysozyme for 1 hour;

2) Sonication method - resuspended cells were sonicated 5 times at setting 4 (Fishers Scientific Sonic dismembrator Model 100) for 10 seconds each, with 1 minute time period on ice in between each sonication;

3) Freeze and thaw method - the resuspended cells underwent 5 cycles of freezing on dry ice for 5 minutes and thawing in 37°C water bath for 3 minutes.

SDS-PAGE

Two 12% polyacrylamide gels were typically made together. Resolving gels were made by mixing 3.33 mL 30% acrylamide/0.8% bisacrylamide, 2 mL of 4x lower gel buffer (pH8.8), 2.67 mL of autoclaved water and 16 µL of 20% ammonium persulfate (APS), and 4.8 µL of TEMED (Sigma) and pouring into a gel apparatus (Biorad, Hercules, CA) at about 2/3 full immediately after mixing. The rest of the space was filled with water to flatten the top surface of the stacking gel. The water was removed after 30 minutes. The

5% SDS-PAGE stacking gel was made by mixing 0.48 mL 30% (w/v) acrylamide/0.8% (w/v)bisacrylamide, 0.75 mL of 4x lower gel buffer (pH 6.9), 1.77 mL of autoclaved water and 7.5 μL 20% (w/v) ammonium persulfate (APS), and 3 μL of TEMED (Sigma) and quickly pouring it on top of the resolving gel after mixing.

Before loading to the SDS-PAGE, each protein sample was processed by adding 16 μL to 4 μL of 5x Sample buffer with 5 % (v/v) of β-mercaptoethanol. Mixed samples were then heated in boiling water for 5 minutes. As a reference, 5-10 μL of molecular weight markers (Bio Basic, Inc., Markham, ON) was loaded to each gel. Gels with loaded samples were then run in 1x running buffer at 200V for about 35 minutes until the bromophenol blue dye reached the edge of the gel.

Table 2. List of reagents used in SDS-PAGE.

Reagents	Ingredients
4 x Lower Gel Buffer	1.15 M Tris-HCl, 0.4% SDS, pH 8.8
4 x Upper Gel Buffer	0.38 M Tris-HCl, 0.4% SDS, pH 6.9
5 x Sample Buffer	249.75 mM Tris-HCl, pH6.8, 10% SDS, 30% glycerol, 0.012% bromophenol blue
1x Running Buffer	20 mM Tris-HCl, 0.1 % SDS, 0.2 M Glycine
Coomassie brilliant blue	50 % methanol, 10% acetic acid, 0.1% Coomassie brilliant blue R-250
Destain Buffer	20% methanol, 10% glacial acetic acid

2.2.4 HTS purification optimization

Unclarified cell lysates were directly applied to a 96 unit HTS parallel His-tag recombinant protein purification system (His MultiTrap™ HP, GE Healthcare). The system was preloaded with 500 μL of 10% highly cross-linked spherical agarose, precharged with Ni^{2+} ions (GE Healthcare). Prior to adding the lysates, His MultiTrap™ HP filter plates

were spun down at 500 x g for 2 minutes to remove the storage solution from the matrices. Five hundred microlitres of autoclaved milliQ water were then added, followed by two rinses with 500 μL binding buffer containing 20 mM imidazole at 500 x g for 2 minutes each. The unclarified cell lysates were incubated with the matrices for at least 3 minutes, followed by centrifugation for 4 minutes at 100 x g. Unbound proteins were removed by adding 500 μL of wash buffer containing 40 mM imidazole and spinning down at 500 x g for 2 minutes twice. His-tagged recombinant proteins were eluted out in a 96-well collection plate (Corning) by adding 50 μL of elution buffer containing 500 mM imidazole to each well and mixing for 1 minute, and were subsequently spun down at 500 x g for 2 minutes. Components of buffers required for the HTS protein purification are listed in Table 3.

Table 3. Reagents used in HTS protein generation.

Reagents	Ingredients
HTS lysis buffer	20 μg/mL DNase I, 1 mM MgCl2, 1 mM PMSF, 20 mM sodium phosphate, 500 mM NaCl, 20 mM imidazole, pH 7.4
HTS binding buffer	20 mM sodium phosphate, 500 mM NaCl, 20 mM imidazole, pH 7.4
HTS elution buffer	20 mM sodium phosphate, 500 mM NaCl, 500 mM imidazole, pH 7.4

1) Quantification of purified proteins

Concentrations of protein samples were tested using the Bradford protein assay. The Dye Reagent Concentrate was diluted 5 times with distilled, deionized (DDI) water and filtered through a Whatman #1 filter paper. Duplicates of 9 dilutions of BSA (Thermo Fisher Scientific Inc., Waltham, MA) protein standard (0.03125, 0.0625, 0.125, 0.25, 0.5,

0.75, 1, 1.5 and 2mg/mL) and a blank (DDI water) were used to generate the standard curve. Ten microlitres of each protein from the original collection plate were added to a clear 96-well tissue culture plate. Two hundred μL of the reagent was then added to each well of the microtiter plate. The microtiter plate with a mixture of the purified protein sample and reagent was gently shaken for a better mixing and left at room temperature for about 5 minutes to allow the colour to develop. Absorbance of the colour was then measured in a spectrophotometer (Multiskan, Thermo Scientific) at 600nm.

2) Immunodetection of His-tagged recombinant proteins

Western blots were performed to visualize the presence of His-tagged recombinant proteins before and after the purification. A multi-pipettor was used to transfer 1 μL of each purified protein from the 96-well storage plate to a piece of nitrocellulose membrane with the same order as in the 96-well storage plate. The nitrocellulose membrane was allowed to dry on the bench before putting in 1x TBS buffer containing 10mM Tris-HCl (pH 7.4), 0.15 M NaCl and 5% (w/v) skim milk for blocking overnight at 4°C. Following the blocking step, the membrane was incubated with 1° antibody (monoclonal anti-His antibody raised in rabbit, Affinity Bio Reagents, Golden, CO) diluted to 1/1000 in TBST buffer containing 10mM Tris-HCl (pH 7.4), 0.15 M NaCl, 0.1% (v/v) Tween 20 and 1% skim milk for 1 hour at room temperature. The membrane was quickly rinsed once with 20 mL of TBST buffer immediately after the incubation. Each of three additional washes with the same buffer was done at room temperature for 10 minutes. The membrane was then incubated with 2° antibody (anti-rabbit, Promega, Madison, WI) diluted to 1/2000 in TBST with 1% skim milk for 1 hour at room temperature. After the incubation, the membrane was then washed three times as described previously. Blot detection was developed by

incubating the membrane with SuperSignal West Pico Chemilluminescent substrate (Pierce, Rockford, IL) for 1 minute and visualized under ChemImager (Alpha Innotech, San Leandro, CA).

2.2.5 HTS Dialysis Optimization

Endoribonucleolytic activity of APE1 (44 ng) was shown to be inhibited in the presence of 500 mM imidazole (Oh, 2010). In two separate studies (Lunts 1976; Wolff 1993) imidazole is also found to inhibit various enzymatic activities, and that a thorough dialysis step to exchange the buffer content is therefore necessary.

To successfully exchange the buffer content using HTS micro-dialysis, we first need to develop a method to quickly determine the imidazole concentration and the time required for dialysis, and estimate the potential protein loss.

(i) Using Nanodrop® spectrophotometer to estimate imidazole concentration

A method of using wavelength spectrum peak position to estimate approximate concentration of imidazole present in a solution was discovered unexpectedly during the measurement of protein concentration using the Nanodrop spectrophotometer. Samples with different concentrations of imidazole in elution buffer were tested. The positions of absorbance peak on the wavelength spectrum were measured as a function of imidazole concentration. This test was repeated twice.

(ii) Minimum time required to remove imidazole using dialysis

Minimum time required to remove imidazole from the protein solution was assessed. We used different sample volume sizes (50, 100 and 200 μL) and tested with and without the presence of 1 mg/mL of bovine serum albumin (BSA) to assess how these two factors affect the dialysis speed.

(iii) Test for protein loss during dialysis

Pre-dialysis and post-dialysis concentrations of 0.5 mg/mL BSA and purified recombinant proteins were measured to determine the possible protein loss during dialysis.

2.3 Results and discussions

2.3.1 Comparison of protein expression in LB and SB

To test whether there are any major differences in protein expression using the commonly employed LB broth and the special broths, 2YT and SB (2YT/SB), the same set of bacterial clones were grown in these media. Using Western blots to detect the presence of His-tagged proteins in *E.coli* grown in LB and 2YT/SB (Figure 4), we found that most of the proteins in LB-grown cells were also detectable in 2YT/SB-grown cells. Although some dots were comparatively more intense in cells grown in LB, in general there were no major differences in protein expression in cells grown using these two different broths.

Since this test was done after all five sets of clones had been purified, and LB medium is more convenient and common to use in the lab, it was later used as the growth medium for larger cultures, where special broth 2YT/SB were not necessary. Due to the

fact that this test was done after the high-throughput purification of several sets of clones was already performed, 2YT/SB were used continuously for all clone sets so as to keep the experimental conditions consistent. When growing bigger cultures at the post-screening stage, LB broth was used as it was suitable for growing higher volume of culture.

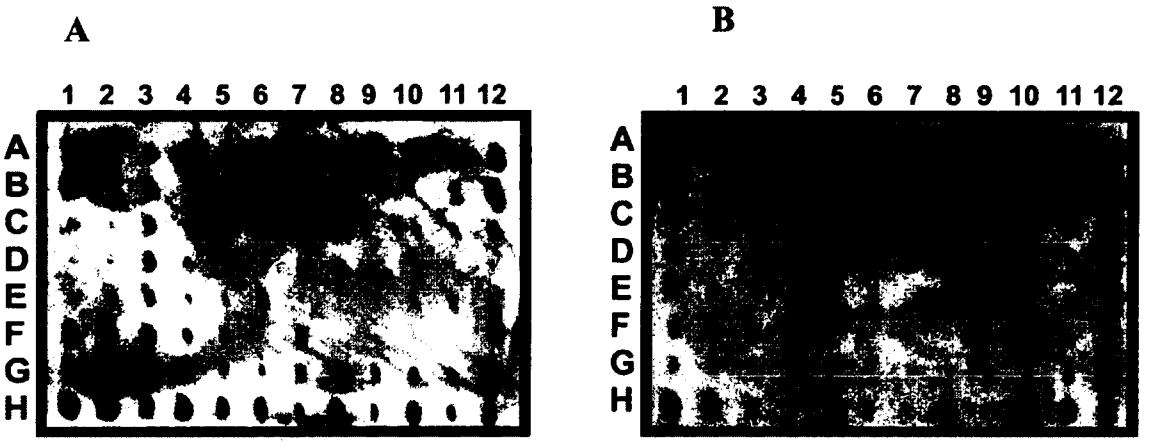

Figure 4. Western blots showing the expression of His-tagged proteins in the cells grown in different media. A) LB **and B)** 2YT/SB. More than 80% of clones show apparent expression of His-tagged proteins. No major differences in expression were found using these two sets of broths.

2.3.2 Optimizing HTS bacterial induction step

The average concentration of each elution (elution 1 - 4) and the total average of all elutions are shown in Table 4. Within all elutions, the 16-hour induction at 16°C appeared to produce a higher average of protein concentration. Elution 2 of both induction methods had a higher average protein concentration amongst all elutions. Not all of the proteins induced for 16 hours at 16°C had a higher concentration than the 6-hour induction at 37°C. Most of the clones produced higher protein concentration after 16 hours of induction at 16°C. Another advantage of inducing proteins at a lower temperature and longer time is

that it allowed a higher chance of proper folding of proteins. Hence, all clones in this project were induced at 16°C for 16 hours.

Table 4. Purified protein yields comparison of proteins induced with IPTG for 6 hours at 37°C and 16 hours at 16°C.

	Average concentration of clone set 517A (mg/mL)			
Condition	**Elution 1**	**Elution 2**	**Elution 3**	**Elution 4**
6 hours @ 37 °C	0.184	0.231	0.050	0.100
16 hours @ 16 °C	0.236	0.346	0.077	0.126

2.3.3 Choice of cell lysis method

Amongst the three cell lysis methods tested, the enzymatic lysis method might be the least vigorous for purifying recombinant proteins. However, when compared with the other two physical cell lysis methods, the protein yield was much lower. Between the two physical cell lysis methods, sonication was the most effective in lysing the *E.coli* cells as shown by the abundant target protein bands on the SDS-PAGE gel (Figure 5C, Lane 7). Despite its cell lysis effectiveness, the target protein produced under this cell lysis method also appeared to have a lower protein purity. As shown in Figure 5C, unwanted protein bands with various sizes are present in Elution 2. Another reason for the unsuitability of lysing cells using sonication is that some proteins may be sensitive to the vigorous vibration, and hence may be denatured. Taken together, the freezing and thawing method of lysing cells was the best cell lysis method. This method produced sufficient yields and was considered gentle.

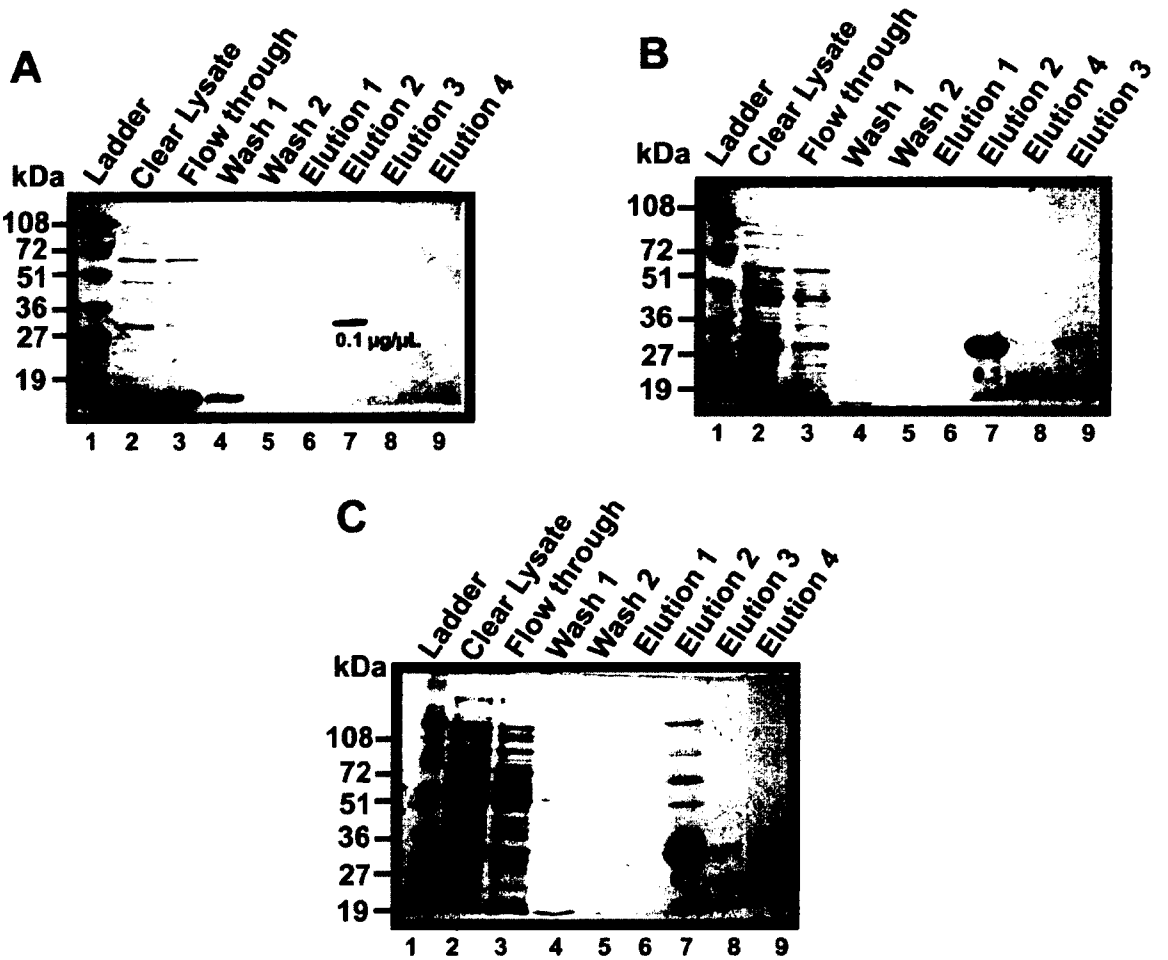

Figure 5. SDS-PAGEs showing different fractions of 568F20 in the purification process after cell lysis with three different methods. A) Enzymatic cell lysis; **B)** Physical cell lysis using 5 freeze and thaw cycles; **C)** Physical cell lysis using sonication. A small size band shown in Part (A) indicates the presence of lysozyme in clear lysate, flow through and wash 1. The protein concentrations of elution 2 were estimated with NanoDrop Spectrophotometer.

2.3.4 Optimizing HTS protein purification step

To determine whether all clones produced similar His-tagged protein yield, an anti-His-tagged immunoblotting was performed using cell lysates and post-dialysis protein samples. The Western blots show the corresponding His-tagged proteins were present in all cell lysate of set 517A (Figure 6A), but not all were present after purification (Figure 6B).

This might due to the proteins being in inclusion bodies and therefore not purified under native conditions.

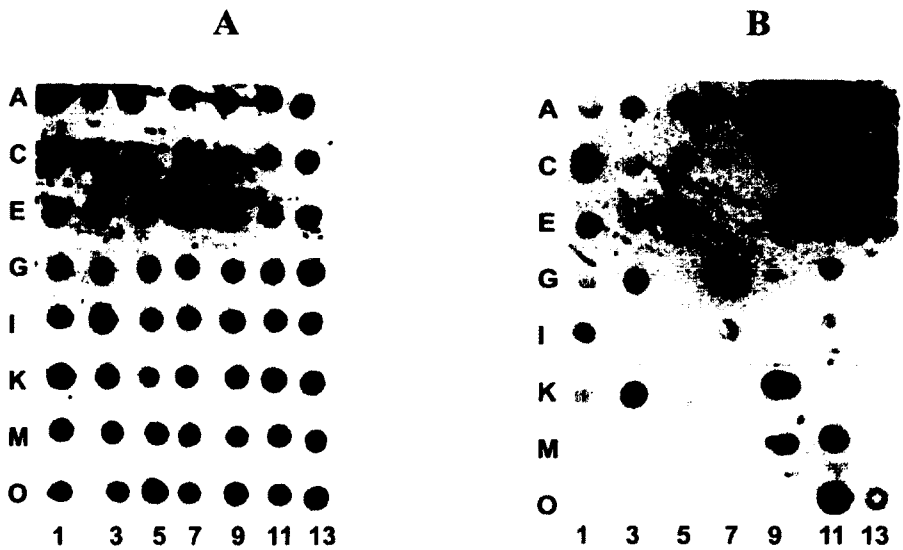

Figure 6. Western blots showing His-tagged proteins from set 517A in cell lysate and after dialysis. One microlitre of each protein sample was transferred to the nitrocellulose membrane. **(A)** All of these clones show expression of His-tagged recombinant protein. **(B)** Only 34 out of 56 clones were able to produce detectable amount of purified recombinant protein. Data is adapted from unpublished report (Oh 2009).

2.3.5 Using Nanodrop spectrophotometer to estimate imidazole concentration

While measuring protein concentration using the spectrum peak position of a Nanodrop spectrophotometer wavelength, we discovered a method to assess the concentration of imidazole present in the solution. The absorbance peak's positions on the wavelength spectrum were measured as a function of the imidazole concentration. This test was repeated twice.

The results show that the shift of the absorbance peak's position was consistent with the increased imidazole concentration (see Figure 7). According to this standard curve,

the concentration of imidazole can be estimated. For example, if the peak is located at around 228nm, imidazole in the solution would be approximately 0.5 M. Identical data from duplicated readings demonstrated the reliability of this method in estimating the imidazole concentration. This quick detection method using NanoDrop spectrophotometer allowed us to measure the concentration of imidazole and assess the effect of dialysis on imidazole concentration in the original buffer.

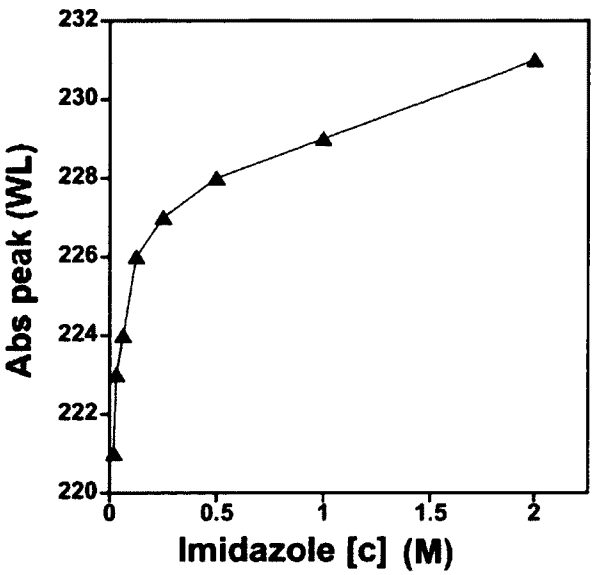

Figure 7. Position of absorbance peak shifting to the right on wavelength spectrum (increasing in wavelength) as imidazole concentration in the sample increases.

2.3.6 Assessing the minimum time required for dialysis

Figure 8 shows the effect of dialysis on the concentration of the imidazole, with and without BSA. In both conditions, the imidazole concentration dropped significantly after 30 minutes, and remained constant after 120 minutes of constant buffer exchange with all sample volumes. Smaller sample volumes tend to have better chances of removing

imidazole from the buffer as indicated by a lower imidazole concentration of all time points. Hence, 50 µl dialysis sample size and 120 minute dialysis time were chosen for the HTS dialysis system.

Another phenomenon was observed during the experiment. When the protein concentration was increased, the detected concentration of imidazole using the NanoDrop method was also increased at the same time. Two explanations are possible for this observation. First, the BSA proteins were partially blocking the membrane and subsequently decreasing the exchanging rate of buffers. Second, the presence of BSA was interfering with the absorbance measurement. This could be due to the similarity of ring structures present in both imidazole and some amino acids such as histidine.

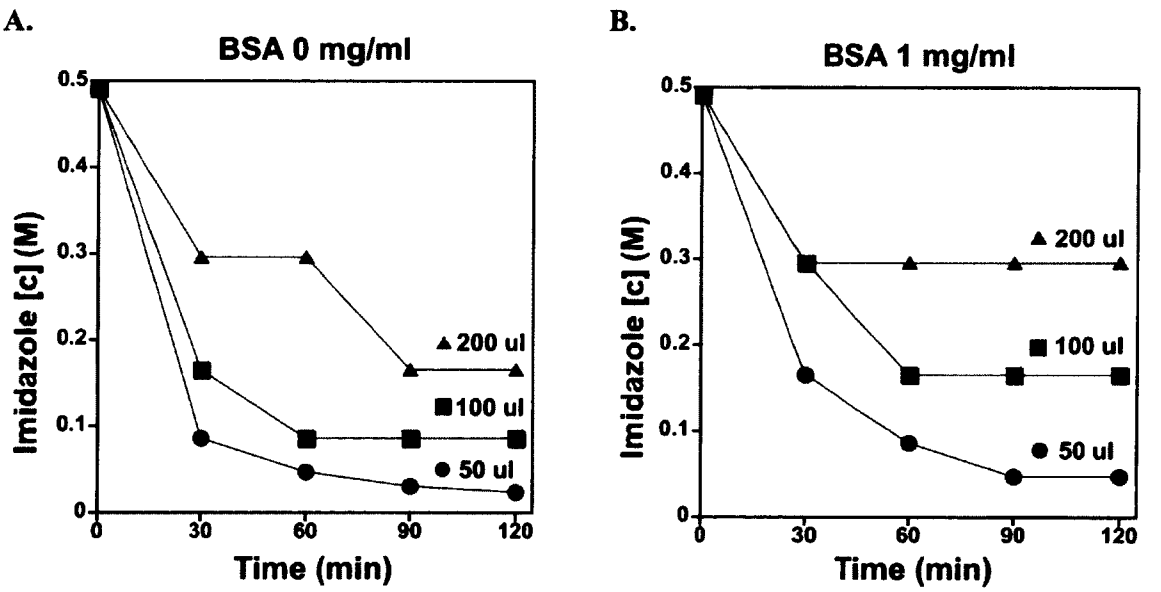

Figure 8. Determining the time required to decrease imidazole concentration during dialysis. (A) Test run using 0 mg/ mL BSA; **(B)** Test run using 1 mg/mL BSA.

2.3.7 Determining the amount of protein loss during dialysis

We anticipated that certain amounts of protein loss may occur during dialysis. Two trials were run using 96 BSA samples and 36 recombinant proteins from set 517A respectively. The concentration was estimated by Bradford protein assay. Concentrations of BSA after dialysis were very similar to their pre-dialysis concentration of 0.5 mg/mL. The average concentration of BSA after dialysis was 0.554 mg/mL, with a low standard deviation of 0.038. Hence, the dialysis had not caused any significant protein loss in the BSA samples.

Table 5. Purified protein sample concentrations (mg/mL) of before (A) and after (B) dialysis, and percentage (%) decrease of concentration (C). Clones tested were from rows K, M and O, and columns 1, 3, 5, 7, 9, 11, 13, 15, 17, 19, 21 and 23 of plate 517.

A

	1	3	5	7	9	11	13	15	17	19	21	23
K	0.112	0.113	0.111	0.071	0.071	0.087	0.023	0.094	0.090	0.140	0.131	0.006
M	0.126	0.166	0.141	0.204	0.140	0.117	0.114	0.126	0.155	0.085	0.105	0.003
O	0.077	0.173	0.170	0.095	0.150	0.099	0.138	0.117	0.098	0.132	0.097	0.039

B

	1	3	5	7	9	11	13	15	17	19	21	23
K	0.037	0.050	0.043	0.033	0.038	0.045	0.028	0.077	0.061	0.104	0.079	0.020
M	0.066	0.105	0.064	0.094	0.079	0.057	0.049	0.050	0.061	0.041	0.053	0.001
O	0.042	0.086	0.081	0.045	0.073	0.053	0.084	0.062	0.049	0.068	0.051	0.049

C

	1	3	5	7	9	11	13	15	17	19	21	23
K	66.9	55.9	61.2	53.9	47.0	48.1	-21.7	17.7	32.6	25.6	39.4	-258.7
M	47.7	36.6	54.7	54.1	43.4	51.4	56.9	60.1	60.4	51.3	49.8	56.2
O	45.4	50.6	52.3	52.8	51.0	46.2	38.9	46.7	49.7	48.3	47.0	-26.2

In contrast, the 2 hour dialysis seemed to have a significant effect on the concentration of the recombinant proteins. The majority of the protein concentration

dropped after dialysis in comparison to their pre- and post-dialysis concentrations (Table 5, panel A & B). The average concentration of purified proteins before dialysis was 0.109 mg/mL with a maximum of 0.204 mg/mL and a minimum of 0.003 mg/mL. The average concentration of purified proteins after dialysis was 0.058 mg/mL, with a maximum of 0.105 mg/mL and a minimum of 0.001 mg/mL. The average percentage decrease in concentration was 35.9%, with a maximum of 66.9% and a minimum of -258.7%. As observed in Table 5C, the concentrations dropped uniformly for most of the clone after dialysis with the exceptions of clones K13, K23, and O23. This may be due to the different size of each clone. As compared to most of these clones, BSA is relatively bigger, with the size of about 68 kDa. In summary, concentration of recombinant protein is expected to decrease about half after dialysis.

Chapter 3

High-Throughput Functional Screen

3.1 Introduction

The real-time fluorescence-based assay previously developed in Dr. Lee's lab has been shown to be valid for the measurement of endoribonuclease activity of APE1 (Kim *et al.* 2010). The principle of this method is based on the signal of a fluorophore attached to 5'- end of the substrate (Figure 9). Increase in fluorescence signal subsequently occurs upon cleavage of the substrate and separation of the fluorophore from the quencher. The signal is picked up by the fluorescence multiplate reader (Varioskan Flash Multimode Reader, Thermo Scientific). Similar fluorescence-based assay has been conducted, supporting the effectiveness of this method in accessing ribonuclease activity (Wang and Hergenrother 2007).

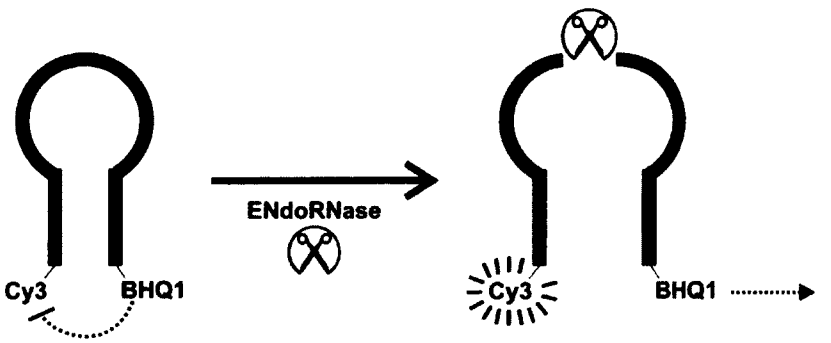

Figure 9. Principle of fluorescence-based assay used in high-throughput screen. The left hand side of the figure shows fluorescence signal of fluorophore Cy3 being quenched by the nearby quencher BHQ1 when the substrate is uncleaved. The right hand side of the figure shows an enzymatic reaction with the presence of endoribonuclease causing separation of BHQ1 from Cy3 and hence dequenching.

CH 3 HIGH-THROUGHPUT SCREEN

3.2 Methodology

3.2.1 HTS 96 parallel protein expression and purification

1) HTS small culture production

Inoculation

Two special media, 2YT and SB, with 100 μg/mL of ampicillin and 15 μg/mL kanamycin, were used according to the recommended conditions for small size culture (Lueking, 1999; Bussow, 1998). Two percent (w/v) glucose was added to 2YT and 20 μg/mL vitamin B1 and 1x KPB was added to SB to ensure the healthy growth of small size cultures.

The ingredients in these two broths are listed in Table 1. A 96-well plate was used to grow the starter culture. The starter culture of each clone was incubated in two sets of 100 μL 2YT overnight in a 37°C shaker at a speed of 200 rpm. On the second day, 100 μL starter culture was transferred to each of the two bigger culture sets containing 900 μL SB in each well.

Bacterial culture

For sets 517A, 523C, 525A and 568D, clones were grown in two 96-well deep microplates (UNIPLATE, Whatman) new cultures by incubating for 3 hours to the OD_{600} of 0.5 before induction. To evaluate the possible advantage of using higher culture volume, set 512A was grown in four 96-well deep microplates instead of two. A final concentration of 1mM IPTG was put into the culture to induce the recombinant protein expression. Bacterial cell pellets were collected by spinning the deep-well plate at 3000 x g for 10

minutes (Beckman Coulter). Pellets were stored in capped deep-well plate at -80°C until the cell lysis step.

2) HTS parallel cell lysis

Mechanical cell lysis method was used to lyse all cells simultaneously. Cell pellets were re-suspended in 250 μL HTS lysis buffer using a multichannel pipettor (Fisher). Re-suspended cell pellets of the same clones were combined in one plate, followed by a series of at least five freezing and thawing cycles done at - 80°C and 37 °C respectively. Unclarified cell lysates were produced after the cell lysis.

3) HTS recombinant protein purification

Recombinant proteins were purified as described in Chapter 2. Typically, 4 fractions were collected for each purification procedure. Purified His-tagged proteins were then subjected to dialysis or kept at -80°C until proceeding to dialysis.

3.2.2 HTS dialysis and quantification

1) HTS dialysis

All second elution fractions were subjected to dialysis using a 96-well microdialyzer (Spectra/Por) to exchange a buffer for 96 proteins at a time. In this process, 500 mL of dialysis buffer, with a pH of 7.4, contained 50 mM of Tris and 10 mM of $MgCl_2$ was used. For two hours the buffer was continuously exchanged from one buffer chamber via a tube to a lower buffer chamber. The dialyzed proteins were then stored in another new sterile collection plate and stored at -80°C.

2) Quantification of dialyzed proteins

The concentrations of protein samples were measured by performing the BioRad protein assay as described in Chapter 2.

3.2.3 HTS protein functional screen

To identify candidate recombinant proteins capable of cleaving miR155, a dual labeled substrate was synthesized based on the mature form of miR155 (Figure 10). It was attached with a fluorophore (Cy3) and a quencher (BHQ1) to the 5'- and 3'- end, respectively (IDT, Coralville, IA). Screening results using the miR155 substrate were compared with Oligo CG, CU, and UA as controls to detect sequence specific endoribonuclease activity. The predicted secondary structures of these control oligonucleotides are shown in Figure 11. The sequence of each substrate is shown in Table 6.

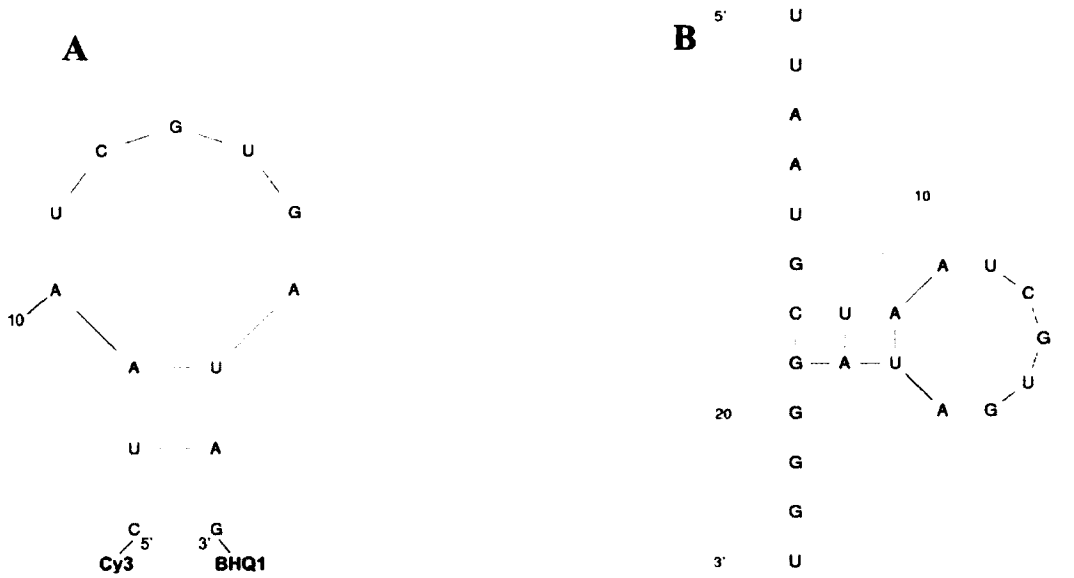

Figure 10. Secondary structure of the miR155 substrate used in the fluorescence-based assay, which was designed based on one of the mature miR155 secondary structures. (A) miR155 substrate; **(B)** mature miR155. RNA structures were predicted by Mfold RNA folding program.

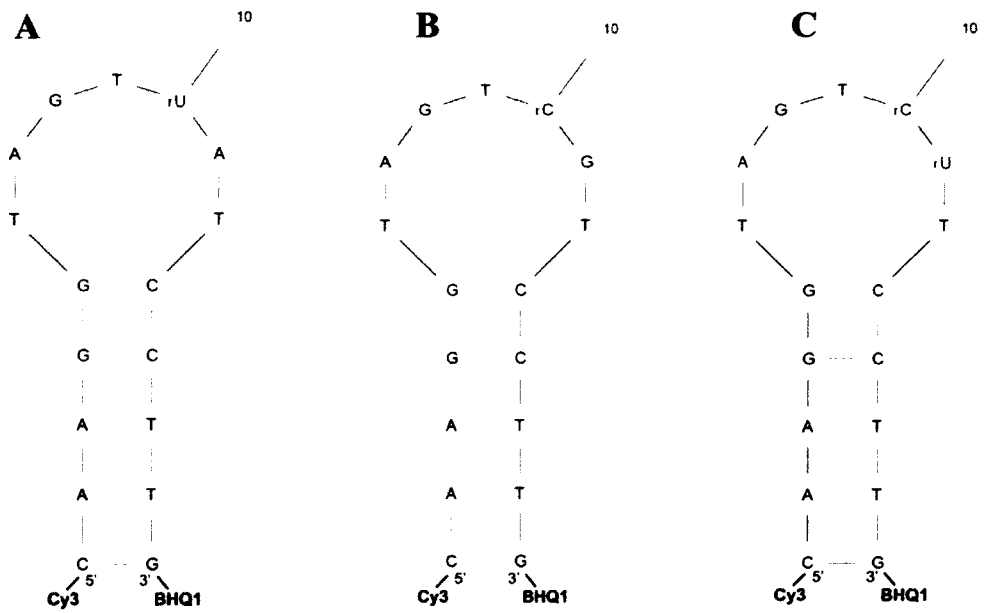

Figure 11. Secondary structures of substrates used as controls. Structures were predicted by Mfold RNA folding program. **(A)** Oligo UA; **(B)** Oligo CG; **(C)** Oligo CU. The prefix "r" denotes ribonucleotide. The rest of the substrate is composed of deoxiribonucleotides.

Table 6. List of substrates used in the fluorescence-based assay and their sequences.

Substrate	Sequence*
miR155	Cy3 – 5'-rCrUrArArUrCrGrUrGrArUrArG-3' – BHQ1
Oligo UA	Cy3 – 5'-CAAGGTAGTrUATCCTTG-3' – BHQ1
Oligo CG	Cy3 – 5'-CAAGGTAGTrCGTCCTTG-3' – BHQ1
Oligo CU	Cy3 – 5'-CAAGGTAGTrCrUTCCTTG-3' – BHQ1

Note: * The prefix "r" denotes ribonucleotide.

A total of 480 clones from 5 unbiasly selected sets (512A, 517A, 523C, 525A and 568D) were tested for the validation of the HTS screening test. A fluorescence-based assay was performed to screen for positive hits from the candidate pool of these 480 clones.

The fluorescence-based assay contained 20 nM of the miR155 substrate (Figure 10 A) and 5μL of protein in a total volume of 80 μL containing 50mM Tris and 2 mM $MgCl_2$ at pH 7.4. The fluorophore was excited at a wavelength of 533 nm and fluorescence is absorbed at 563 nm every 30 seconds for 30 cycles. The RFU readings were measured over a time period of 15 minutes. RNase A cleaves specifically at the 3'side of U and C on both single and double strand RNA (delCardayré *et al.* 1995) and was therefore used as a positive control. DEPC-treated water was used as negative control. Ingredients of each fluometric assay reaction are shown in Table 7.

Table 7. Components in fluorescence-based assay reaction.

Content		Final amount/concentration in reaction	Volume (μL)
miR155 substrate		20 nM	1
Protein		Various (0-3.37 mg)	5
Reaction Buffer (pH7.4)	Tris	50 mM	74
	MgCl2	2 mM	
Positive control (RNase A)		0.01 μg	1
Negative control (DEPC-treated Water)		Not applicable	1

3.3 Results and discussions

3.3.1 Protein concentrations

The average concentration of all sets as measured by the Bradford method was 0.06 mg/mL; the lowest concentration was 0 mg/mL, and the highest concentration was 0.674 mg/mL. Set 512A had a higher average concentration (0.1 mg/mL) because clones from this set were grown in four 96-well plates with a total of 4 mL culture for each clone, instead of two plates for the rest of the sets.

3.3.2 HTS fluorescence-based assay

There are five possible ways to select positive hits from the above screens: 1) "Manual selection" picks up clones that stand out and created an obvious increase of RFU as a function of time; 2) "Last RFU method" uses the value of last RFU as criteria of selection; the higher the last RFU, the stronger the signal; 3) "Last RFU normalized to the protein concentration" method uses the value of last RFU divided by the concentration of the respective clone to detect enzymatic activity; 4) "Percentage change method" measures

the percentage change from the first RFU to the last RFU, the higher the percentage change, the stronger the signal; 5) "Percentage change normalized to the protein concentration" method uses the RFU percentage change of a clone from method 4 over its own concentration.

The manual method (method 1) was the fastest amongst all the five methods as it did not require calculations, sorting and normalization of the data. However, using merely visualization to select positive hits may increase the risk of missing some true positives. Moreover, RFUs in all wells increased in some screens. This is one of the reasons why using method 1 is not feasible, because if the maximum RFU value is very high within the run (as obtained with the positive control RNase A), the baseline is pushed down to the bottom of the graph and tends to look flatter. The increase of the RFU is less observable in this case therefore some positive hits may be missed using this method.

Method 4 and 5 were not used for a technical reason. The reaction captured in a graph may vary depending on the activity of the enzymes. Two hypothetical fluorescence signal curves representing two activity levels are shown in Figure 12. Time point "a" and "b" represent the first and last reading in fluorescence-based assay. Due to technical reason, there is often a gap between the zero time point and the first reading. When the RFU value of a strong enzyme such as RNase A already reaches a very high level at time point "a", a low percentage change in RFU is obtained and therefore would be missed in the screen. Hence, method 4 and 5 were not suitable for identifying very active enzymes.

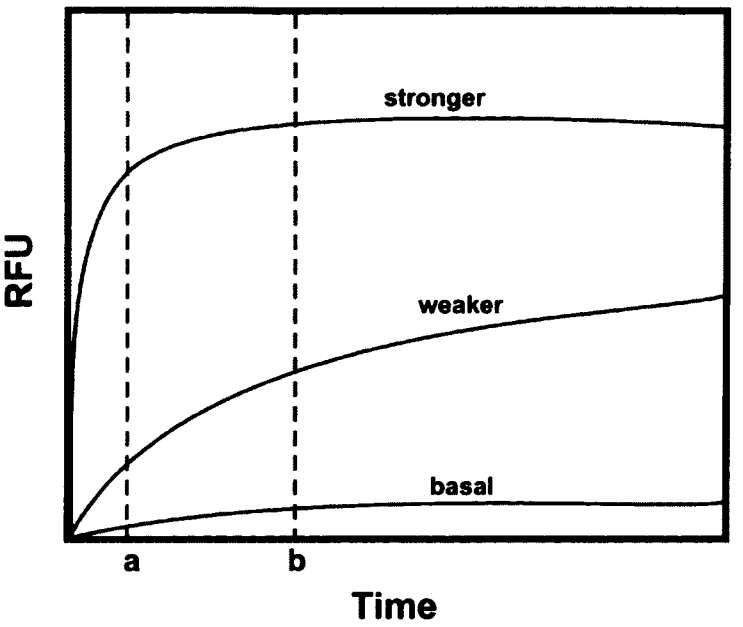

Figure 12. Kinetics curves of enzymes of diffferent activities. RFUs from time points "a" to "b" are representing the relative fluorescence units capture in one fluorescence-based assay. RFU at time point "b" is a better representation of the activity strength than the percentage RFU increase from "a" to "b".

Method 3 and 5, both using the protein concentrations to normalize the fluorescence signals, can be problematic as some of the clones had produced very small amounts of proteins. If these small values were used to normalize the RFU values obtained in the fluorescence assay, these candidate proteins would be erroneously identified as having strong enzyme activity. Furthermore, as demonstrated in Figure 12, last RFU is more suitable in representing the signal strength. Because of the above reasons, method 2 using the last RFU was selected to identify candidates for further analysis. Using this method, clones were categorized into 3 groups based on their activity: high, low or negative. Clones that belong to the "high" activity group are clones with the last RFU higher than two standard deviations above the average RFU for the clone set. Clones that have "medium"

activity have their last RFU higher than one standard deviation above the average RFU. The rest of the clones are considered to be negative.

A representative primary fluorescence screen for a set of 96 clones (517A) is shown in Figure 13. Using the last RFU method, clones with high and medium activity were identified and indicated by H and M respectively. The top ten clones that produced the highest amount of protein are indicated by an asterisk (*). It is worth noting that these clones did not necessarily produce high signals in the assay. As exemplified in this set of data, most of the positive hits (either H or M) appear to be cleaving both the miR155 and Oligo UA substrate (e.g. A17 and C07). It is interesting to note that the RFU value obtained for RNase A in the assay are often decreasing with time during the measured time period due to fluorescence bleaching.

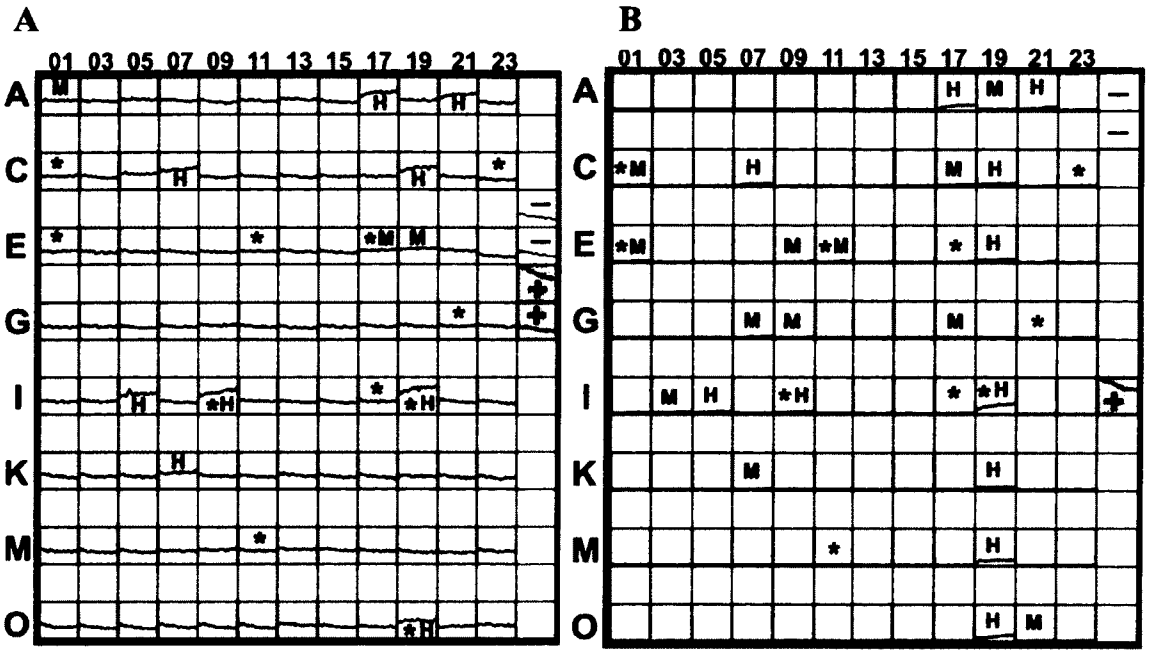

Figure 13. Representative results of fluorescence-based assay to screen for activity against the miR155 substrate and Oligo UA. (A) Screen against miR155; **(B)** screen against Oligo UA. Each square represents the RFU signals plotted as a function of time in a 15-minute time period after the addition of the respective substrates to proteins purified from the clone set 517A. All RFU values presented were normalized to the maximum value obtained with 5 μg of RNase A, which was included as a positive control (+) in each assay. DEPC-treated water was included in each assay as negative control (-). Reactions with "H" indicate ranking with high signal and reactions with "M" indicate ranking with medium signal as according to the ranking method used. The top ten high concentration clones are marked with an asterisk. High = last RFU > average RFU of each set +2x standard deviation; Medium = last RFU > average RFU of each set + 1 x standard deviation. Average RFU for the set was calculated using the last RFU values from all the clones except the clones that produced obviously high signal in the assay (eg. I19).

The list of positive hits is longer than what we anticipated. Average rate of positive hit for one set was about 23 %. It is very possible that a considerable portion of these "hits" are false positives due to contamination. There are two hypothetical approaches to eliminate the false positive. The first approach is to compare the reproducibility of screening results. Screens of sets 517A, 525A and 568D were repeated at least one more

time. When the different screen was compared, only some hits were reproducible in both lists. As shown in Table 8, not all hits are reproducible and the number of reproducible positive hits only covered less than half of all hits from two combined trials. However, repetitive screen was not performed with sets 512A and 523C due to the insufficient amount of protein samples. Although this approach was not applied to all clone sets and hence was not used to eliminate false positive, we were aware of this problem.

In the second approach used to eliminate the false positives we focused on hits that were positive only toward miR155 but not Oligo CG and CU or Oligo UA (Oh 2010; Woodbeck 2010). We reasoned this may be a suitable way to quickly eliminate false positives based on the possibility that some bacterial RNase may contaminate the protein samples. This method can also help us focus on clones that may possess substrate specificity toward miR155. A total of 25 positive candidates selected for all sets (Table 9) were subjected to further post-screening or secondary screen analysis. These clones appeared to be positive in at least one trial.

Table 8. Comparison of positive lists from two repeated screens (Trial 1 and 2).

517A		525A		568D	
Trial 1	**Trial 2**	**Trial 1**	**Trial 2**	**Trial 1**	**Trial 2**
A01		**A01**	**A01**		B04
	A05		A03	B06	
	A07	A05		B08	
A17	**A17**	**A09**	**A09**	B16	
A21	**A21**	**A15**	**A15**	B18	
C07		**A17**	**A17**		B22
	C17	**A19**	**A19**	D18	
C19	**C19**		A21	**D22**	**D22**
E17		C09		D24	
E19	**E19**	**C15**	**C15**	F06	
I05	**I05**		E01	**F08**	**F08**
I09		**E15**	**E15**	**F20**	**F20**
I19	**I19**		E17		F22
K07			E23		H02
	K17	**G03**	**G03**		H04
	M01	**I05**	**I05**	H06	
	M17	**I15**	**I15**		H12
	O05	**I23**	**I23**		H14
O19	**O19**	M01		H18	
		M09		H20	
		M11	**M11**		H22
		M15	**M15**	J10	
			M23	**J16**	**J16**
		O01		J20	
				L20	**L20**
				N10	
				N12	**N12**
					N14
				N20	
					N22
				P02	
				P16	
				P22	

Note: Reproducible positive hits are bolded and shown in both columns (e.g. A17 and A21 in set 517A). In set 517A, 7 positive hits were reproducible; in set 525A, 13 positive hits were reproducible; in set 568D, 6 positive hits were reproducible.)

Table 9. List of clones exhibiting specificity toward miR155 substrate.

Clone MPMGp800. .	Signal Ranking *	Reproducibility**
C19512	Medium	N/A
E15512	Medium	N/A
I23512	Medium	N/A
O13512	Medium	N/A
O23512	Medium	N/A
A01517	Medium	N
E17517	Medium	N
B01523	Medium	N/A
F01523	High	N/A
L01523	High	N/A
N01523	High	N/A
P07523	Medium	N/A
P09523	High	N/A
A15525	High	R
C15525	Medium	R
E15525	High	R
G03525	Medium	R
B06568	High	N
D24568	Medium	N
F06568	Medium	N
F20568	High	R
H06568	Medium	N
J10568	Medium	N
J16568	Medium	R
N10568	Medium	N

Note: * RFU signals in fluorescence assay: High = last RFU > average RFU of each set +2x standard deviation; Medium = last RFU > average RFU of each set + 1 x standard deviation. ** R- reproducible hit, N- not reproducible, N/A- data not available.

Chapter 4

Post Screening Analysis of the Positive Hits

4.1 Introduction

4.1.1 Rationale for carrying out secondary screen

Post screening analysis (secondary screen) is necessary because the positive hits obtained from the high-throughput screen (primary screen) might contain false positives, especially with such a high percentage of total positive hits (23%) initially identified in Chapter 3. Several factors may contribute to the occurrences of false positives.

First, cross contamination amongst clones in 96-well plates during the bacterial growth is possible and can introduce a second recombinant protein into adjacent protein samples during the handling of clones in 96-well plates. In this case, an inactive clone can be contaminated with an adjacent active clone and be selected as a positive hit. Second, since the recombinant protein is grown in the *E.coli* cells, the bacterial host itself can be a source of contamination. Third, during the high-throughput cell lysis, a batch of DNase I (Roche, Switzerland) was added to the lysis buffer according to the manufacturer's protocol (Table 5). We later found out that this batch of DNase I powder contained RNase activity. The RFU was increased with the increased amount of this DNase I (data not shown). Although this contaminant may not remain with the purified protein, this finding cautioned us about the possibility of false positive signal in the screen when this batch of DNase I was included in the primary screen. Lastly, it was also possible that some of the positive hits selected were not endoribonucleases. Exoribonuclease and RNA binding protein could also alter the stem loop structure of miR155 substrate (Figure 10A) and

subsequently cause the Cy3 to be distant from BHQ1. Therefore, post screening analysis must involve electrophoretic assay which can distinguish these possibilities.

4.1.2 Electrophoretic assay to characterize positive hits

The fluorescence-based screen was designed for quick detection of potential ribonuclease activity, but it could not provide details of the activity. The electrophoretic assay was used to access the RNA cleaving activity and the RNA cleavage sites generated by candidate enzymes. Electrophoretic assays with four different substrates were carried out to further understand and characterize the possible enzymatic activity of the selected proteins. By radiolabeling the substrate at either end, the nature of the cleavage products can be determined when the substrate was cleaved.

Two substrates were designed based on the mature miR155 sequences, and they differed by nucleotide length. The 13 nucleotide substrate (miR155_13nt, Figure 14A) was identical to the substrate sequence used in the screen, except that it had no fluorophore and quencher attached. As mentioned in Chapter 3, the 13-nt substrate was an artificial substrate derived from the mature form of miR155 and fits the technical criteria of fluorescence-based assay. After all, it is not the actual mature miR155 itself. Therefore, it is deemed important to include the second 24-nt full length (miR155_24nt) which more closely mimics the biological structure. The most stable predicted secondary structure of miR155_24nt is shown in Figure 14B.

Substrate Oligo CU-aR (Figure 15) was used as a control for two reasons. First, it was used as a criterion to eliminate false positives in the screening step. Second, using a different substrate could provide more RNA cleavage information and possibly answer the

question as to whether enzymatic activity was sequence specific. The Oligo CU-aR substrate used in electrophoretic assay was composed entirely of ribonucleotides instead of the hybrid form used in the primary screen. The suffix "aR" indicates ribonucleotide composition in the substrate, distinguishing it from the fluorogenic substrate Oligo CU. To further determine whether the candidate enzyme possesses exoribonucleolytic activity, Poly $(A)_{15}$ substrate was used.

To be consistant with the primary screen, RNase A was used as a positive control. Clone E01517 was include as a negative control, because it did not cleave miR155 in the primary screen and had a relatively high protein yield.

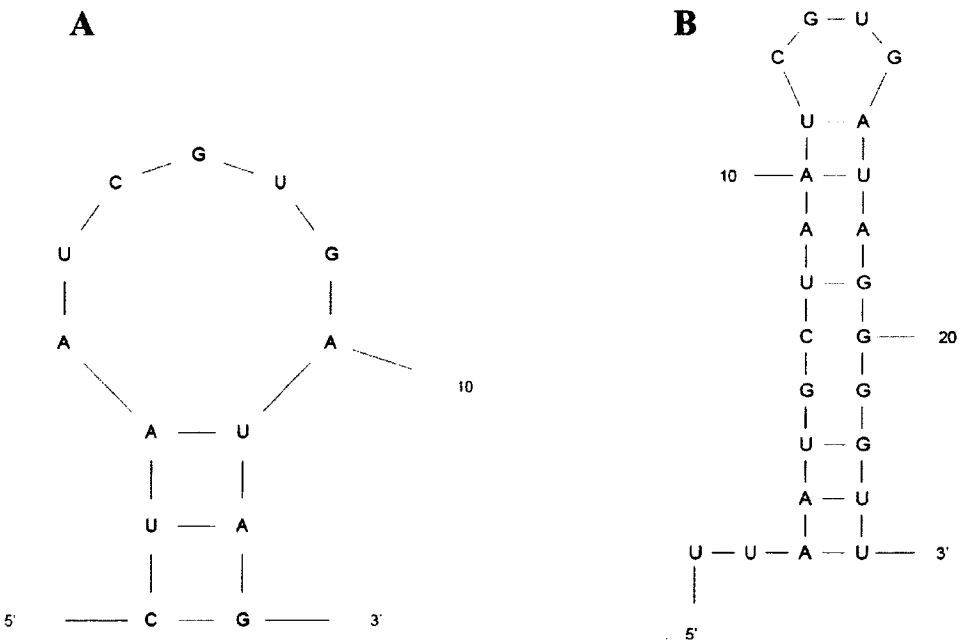

Figure 14. Secondary structures of electrophoretic assay substrates miR155_13nt and miR155_24nt. (A) Structure of short form substrate miR155_13nt; **(B)** structure of full length substrate miR155_24nt. These structures were predicted by mfold RNA folding program (Zuker 2003). The initial loop free energies dG are 2.2 kcal/mol and -0.1 kcal/mol for miR155_13nt and miR155_24nt respectively.

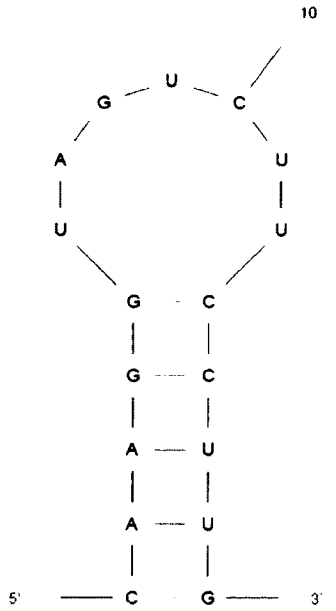

Figure 15. Secondary structure of electrophoretic assay control substrate Oligo CU-aR. This folding was predicted by mfold RNA folding program (Zuker 2003). The initial loop free energy dG is - 4.00 kcal/mol.

4.2 Methodology

4.2.1 Induction test of positive clones

1) Individual clone production

Two 50 mL cultures were grown for each positive candidate, one of which was induced by IPTG at 16°C for 16 hours, and another one without IPTG. Both were incubated until OD_{600} reached 0.5. After induction, cells were spun down after the induction and 2 mL of cell lysis buffer was added into each tube to re-suspend the bacterial pellet. All tubes were subjected to at least 5 cycles of freezing on dry ice and thawing at 37°C to lyse the cells. Clear cell lysates were obtained after spinning the lysed cells at 3000xg for 20 minutes. The uninduced control samples were subjected to identical procedures.

2) SDS-PAGE

SDS-PAGE gels were made following the protocol described in Section 2.2.4. Sixteen- microlitres clear cell lysate were mixed with 4 μL of 5x sample buffer containing 5% of β-mercaptoethanol. Samples were then boiled at 95°C for 3 minutes prior to loading to a 12% gel. The SDS-PAGE was run at about 200 volts for 35 minutes or until the dye reached the bottom of the gel. The SDS-PAGE gel was then stained in Coomassie brilliant blue for 15 minutes and destained in destaining buffer for a minimum of 2 hours. Purity of the His-tagged protein was measured by the ratio the density of this protein to the density of the whole sample including background.

4.2.2 Expression and purification of positive clones

1) Individual recombinant protein purification

Bacterial culture

For each positive clone, 200 mL culture was typically grown in LB broth containing 100 μg/mL Ampicillin and 25 μg/mL Kanamycin to an OD_{600} of at least 0.5, and induced with 0.1 mM IPTG at 16°C for 16 hours. *E.coli* cells were collected by spinning at 3000xg for 25-30 minutes after induction; 4 mL of cell lysis buffer was added into each tube to resuspend the pellet. All tubes were subjected to at least 5 cycles of freezing on dry ice and thawing at 37°C to lyse the cells. Clear cell lysates were obtained after spinning the lysed cells at 3000xg for 20 minutes. To remove the cell debris, lysed cells were centrifuged in Eppendorf tubes at 10,000 xg for 20-30 minutes.

CH 4 POST SCREENING ANALYSIS

Gravity flow purification

Four-mililitre clear cell lysate was then incubated with 2 mL of 50% Ni-NTA slurry (Qiagen, Valencia, CA) in a 15 mL capped column on an orbital shaker at 4°C for about 1 hour. Resin with bound proteins was then washed twice with 4 mL wash buffer to remove proteins that unspecifically bound to the matrices. His-tagged proteins are then eluted out four times with 0.5 mL elution buffer in each elution. All flow-through fractions were collected for SDS-PAGE analysis purpose.

During the preparation of Ni-NTA column, 2 mL of 50% precharged nicol resin Ni-NTA (Qiagen, Valencia, CA) was rinsed twice with five volumes of autoclaved milliQ water and equilibrated by rinsing twice with five volumes of lysis buffer. Resins were used up to a maximum of five times before being discarded.

The purification procedure described above was slightly modified from the Qiagen "The QIAexpressionist™" 6x His- tagged protein purification protocol. Contents of reagents used are described in Table 10.

Table 10. List of reagents used in gravity flow purification.

Reagents	Ingredients
Lysis buffer	50 mM NaH_2PO_4, 300 mM NaCl, 10 mM imidazole, pH 8.0
Wash buffer	50 mM NaH_2PO_4, 300 mM NaCl, 20 mM imidazole, pH 8.0
Elution buffer	50 mM NaH_2PO_4, 300 mM NaCl, 500 mM imidazole, pH 8.0

2) Dialysis

To remove the high concentration of imidazole in the elution buffer, two 100-µL protein samples from the elution with the highest concentration of protein were dialyzed with 50 mL of dialysis buffer containing 50mM Tris, 2 mM MgCl2 and 20% (w/w) glycerol with pH of 7.4 for a total of five hours. Buffer was changed once after 2.5 hours of dialysis. After dialysis, proteins in exchanged dialysis buffer were then collected in individual Eppendorf tubes and stored at -80 °C.

4.2.3 Secondary screen using fluorescence-based assay

A secondary screen using fluorescence-based assay was performed to confirm the positive hits as found in the primary screen. Similar to the primary screen, each reaction contained a total volume of 80 µL. One microgram of purified recombinant protein was added to the fluorescence assay buffer containing 20nM of the dual-labeled miR155 substrate. RNase A (0.25ng) was used as a positive control; DEPC treated water (1 µL), DNase I (2 U) and clone E01517 (1 µg) were used as negative controls.

4.2.4 Identity of Positive Hits

1) Growing bacterial culture for plasmid extraction

A 5 mL *E.coli* bacteria culture was grown in LB medium with 25 µg/mL Ampicillin overnight at 37°C; the inoculation was done directly from the original 384 well plate by pipette tip picking. Bacterial cells were pelleted by spinning at 17,900 x g for 10 - 15 minutes and subjected to plasmid purification as per manufacturer's instruction.

CH 4 POST SCREENING ANALYSIS

2) Plasmid extraction

The plasmids from relevant clones were extracted using QIAprep® Spin Miniprep Kit. Amounts of all buffers were doubled corresponding to the high copy of plasmid in the 5 mL culture as recommended by the manufacturer's protocol.

Cell pellet was first resuspended in 500 μL Buffer P1 with RNase A and then transferred to two Eppendorf tubes. Next, 250 μL of Buffer P2 was added to each tube and mixed with the previous solution by inverting 6 times. Immediately after 350 μL Buffer N3 was added to the previous mixture, the tube was inverted 6 times for a thorough mix. Cell debris was then pelleted by spinning the tubes at 17,900 x g for 10 minutes. Supernatants from the previous spinning were then transfer to and spun through the QIAprep spin column (Qiagen, Valencia, CA) for 60 seconds each tube. 0.5 mL of Buffer PB was added to the spin column followed by washing of 0.75 mL Buffer PE to wash out unwanted residual. The spin column was spun at 17,900 x g for 60 seconds after each wash. An additional 1-minute spin was applied to remove excess wash buffer. The plasmid was eluted with 50 μL milliQ water by incubating for one minute and then centrifuging for another minute (Qiagen).

Plasmids were then sent to MACROGEN (Seoul, Korea) for clone identification by DNA sequencing. Two universal primers, SP6 and T7, were first used for DNA sequencing. Identities of clones were determined using BLAST (National Center for Biotechnology Information). We later realized it was necessary to precisely determine the entire sequence of the clones. Although we were able to find protein matches using the sequencing results obtained using SP6 and T7, we could not determine whether the His tagged protein was in

frame since they were both located downstream of the 6xHis tag (Figure 3). Plasmids from the positive clones of first priority were then subjected to another round of DNA sequencing.

The second round of DNA sequencing was performed using two different primers (pQE-F and pQE-Nhe1-R) to determine the entire sequence and to check whether the cDNA inserts were in frame as pQE-F anneals to a location upstream of the His-tag. Sequences of all four primers used in DNA sequencing are shown in Table 11.

Table 11. List of primers and their sequences used in cDNA sequencing.

Primers	Sequence
SP6	5'-ATTTAGGTGACACTATAG-3'
T7	5'-TAATACGACTCACTATAGGG-3'
pQE-F	5'-CCCGAAAAGTGCCACCTG-3'
pQE-Nhe1-R	5'-CAAGCTAGCTTGGATTCT-3'

4.2.5 Dephosphorylation of miR155 substrates (13nt and 24 nt) for use in electrophoretic assay

MiR155_13nt and miR155_24nt oligonucleotides were both dephosphorylated at the 5' end by the same procedure. The substrates were incubated in 37°C for 1 hour with a final concentration of 15.6 pmol/μL. The 80 μL reaction mixture contained 1 μL of 40 U/ μL RNasin® (Promega, Madison, WI), 1 μL of 2 U/ μL Calf Intestine Phosphatase/CIP (New England Biolabs, Beverly, MA), 8 μL of 10x NEBuffer 3 (New England Biolabs, Beverly, MA), 1 μL of 10 nM DTT (Promega, Madison, WI). The rest of the volume was adjusted with DEPC treated water. The reaction was stopped by adding 20 μL of 10% SDS, 4 μL of 5M NaCl, 1 μL of 0.5 M EDTA (pH8.0), and 120 μL of DEPC treated water.

Following the dephosphorylation, the substrates were subjected to the standard phenol/chloroform extraction.

4.2.6 Standard phenol/chloroform extraction and ethanol precipitation

1) Phenol/Chloroform extraction

DEPC-treated water was added to bring the volume of dephosphorylated substrate to 200 µL. One hundred microlitres of phenol (100 µL, pH 6.7, Sigma) and 100 µL of chloroform:isoamylalcohol ($CHCl_3$:IAA = 4:1, Fluka) were added to the sample and mixed by gentle inverting. The mixture was then centrifuged at 12,000 rpm for 5 minutes at 4°C. The aqueous layer was transferred to a new tube and the volume of it was estimated. One volume of chloroform:isoamylalcohol ($CHCl_3$:IAA = 4:1, Fluka) was added to the tube and mixed by gentle inverting. The mixture was centrifuged at 12,000 rpm for 5 minutes. The aqueous layer was then transferred to another new tube.

2) Ethanol precipitation

Two volumes of 100% ethanol and 1/10 volume of 10x Glycogen (pH 5.2) were added to the tube. The tube was mixed well and left at -20 °C for at least 30 minutes. Precipitated RNA was then pelleted by spinning the tube at 12,000 rpm for 10 minutes. Supernatant was gently pipetted out from the tube. The pellet was then rinsed by adding 200 µL of 70% ethanol and spun down at 12,000 rpm for another 5 minutes. The pellet was dried by pipetting the ethanol out, left inside a running fume hood for 20 minutes, and resuspended by adding 30 µL of DEPC treated water. All extracted dephosphorylated substrate was stored at -80°C.

4.2.7 Production of 5' radiolabeled substrates for use in electrophoretic assay

1) 5' labeling reaction

Concentrations of dephosphorylated RNA determined using the NanoDrop® Spectrophotometer (Thermo Scientific). Samples were diluted to 5pmol/μL. A 12.5 μL reaction mixture contained 2.5 μL dephosphorylated RNA (5 pmol/ μL), 1.25 μL 10xPNK buffer, 1 μL of 40 U/ μL RNasin® (Promega, Madison, WI), 1 μL of 100 mM DTT (100mM) (Promega, Madison, WI), 1 μL of 1U/ μL T4 PNK, 3.8 μL γ-^{32}P-ATP (10 μCi/ μL/3.32 pmol, PerkinElmer Inc., Waltham, MA) and 1.95 μL DEPC treated water. The reaction mixture was mixed and incubated at 37°C for 1 hour. The reaction was stopped by adding 15 μL RNA stop dye in each tube. Labeled substrates were either kept at -20°C immediately or proceeded to gel purification step.

2) Gel purification of radiolabeled substrate

The 15% denaturing polyacrylamide gel was made by adding 48 mL pre-made 15% poly acrylamide containing 7M urea with 65 μL of TEMED (N,N,N',N'-tetramethylethylenediamine) and 180 μL 20% APS, and poured to the thin space in between two assembled glass plates immediately after. A 17-comb spacer was used to create sample loading wells. The gel was left to solidify in room temperature for about 30 minutes.

After loaded into the 15% denaturing polyacrylamide gel, radiolabeled substrates were separated from any degraded fragments and excess free γ-^{32}P-ATP by running at 25 mAmp for 50 minutes. The intact substrates were excised directly from the gel.

The gel slice was then put into an RNase DNase free sterile Eppendorf tube and grinded using a sterile pestle (Argos Technologies Inc., Elgin, IL) into fine pieces. To elute the substrate out of the ground gel slice, 200 μL DEPC treated water was added to the tube and the mixture was then transferred directly to a prepared PERFORMA® DTR (Dye Terminator Removal) Gel Filtration Cartridge (EdgeBio). The DTR columns are prepared by spinning the storage buffer in the column for 3 minutes at 850x g. To avoid breakdown of sensitive substrate, incubation under high temperature was eliminated from the instructed DTR gel filtration cartridge protocol. After loaded with ground gel mixture, the DTR gel filtration cartridge was spun down at 850x g for 3 minutes and eluted substrates were collected in a new 1.5 mL Eppendorf tube. The eluted substrate was then further subjected to phenol-chloroform precipitation. Dried radiolabeled RNA pellet was resuspended by adding 30 μL DEPC treated water. The sample was either put in a -20°C freezer or subjected to scintillation counting.

4.2.8 Assessing the endoribonucleolytic activity of positive hits

The radioactivity (count per minute/ CPM) of the labeled RNA was typically measured using 1 μL of the RNA sample. The radiolabeled RNA was further diluted to about 100,000 CPM / μL before use in the endonucleolytic assay. A larger volume of reaction mixture was freshly made and divided into 18 μL aliquots prior to the reaction. For each reaction, 1 μL of 5' labeled substrate (100,000CPM) was incubated at 37°C in 18 μL reaction buffer containing 0.2 μL of 1M Tris (pH 7.4), 0.4 μL of 100 mM DTT, 0.4 μL of 100 mM MgOAc and 17 μL of DEPC-treated water. Typically, about 0.5 - 1.0 μg of purified proteins were used in the assay and the typical incubation time for a concentration dependent experiment was 20 minutes.

4.2.9 Determination of RNA cleavage products

1) Negative controls

Two types of negative controls were included in every set of experiment (Input and None). "Input" negative control was prepared by adding 1 μL of labeled substrate (100,000CPM) with 40 μL RNA stop dye; the "None" negative controls differed from "Input" by addition of 18 μL of reaction buffer. There was no incubation required for "Input", while "None" had different incubation times that matched up with the reactions incubated with the protein samples. In concentration dependent experiments, negative control reactions labeled as None 0' and None 20' represented incubation time of 0 and 20 minutes, respectively.

2) Markers

To identify the cleavage sites generated by candidate enzymes, three markers were run in parallel (Alkaline hydrolysis ladder, RNase A and RNase T1).

Alkaline ladder

The alkaline ladder was produced by incubating 7 μL of labeled substrate (100,000CPM) with 1 μL of 10x alkaline buffer and 2 μL of DEPC treated water at 95°C for 3 minutes, and subsequently placed on ice for 1 minute before adding 20 μL of RNA stop dye.

RNase A

RNase A ladder was produced by incubating 1 μL of labeled substrate (100,000CPM) with 1 μL 10x Structure buffer (Ambion, Austin, TX), 1 μL of active

RNase A (0.025ng/ μL, Ambion, Austin, TX) and 7 μL DEPC treated water at room temperature for 5 minutes. Reaction was stopped by adding 20 μL of RNA stop dye.

RNase T1

RNase T1 ladder was prepared by incubating 1 μL of labeled substrate (100,000CPM) with 3 μL of active RNase T1 (Roche Diagnostics Inc, Mannheim, Gemany) and 4 μL of 1x Sequence buffer (Ambion, Austin, TX) at room temperature for 5 minutes. Reaction was stopped by adding 20 μL of RNA stop dye. Components in each reaction in electrohphoretic assay are presented in Table 12.

Table 12. Comparison of contents in each reaction in the endoribonucleolytic reaction assay.

Reactions		Rxn Buffer (μL)	Protein (μL)	Radiolabeled Substrate (μL)	Incubation Time
Input (In)		0	0	1	0
None (Non)		18	0	1	0 - 20 mins
Reaction with protein		18	0.1 -2 μg	1	0 – 60 mins
Ladders	Alkaline hydrolysis	1 μL 10x Alkaline buffer, 2 μL DEPC water	N/A	7	3 min at 95°C, 1 min on ice
	RNase A	1 μL 10x Structure buffer, 7 μL DEPC water	1	1	5 mins
	RNase T1	4 μL 1x Sequence buffer	3	1	5 mins

Note: "N/A" not applicable.

4.2.10 Exoribonucleolytic Reactions

1) Negative controls

Negative controls include the "Input" and "None". "Input" negative control was prepared by adding 1 μL of labeled Poly $(A)_{15}$ (100,000 CPM) with 40 μL of RNA stop dye. Two "None" reactions with incubation time of 5 minutes and 20 minutes were

prepared with 18 μL of reaction buffer and 1 μL of labeled Poly $(A)_{15}$ (100,000 CPM), and stopped by adding 40 μL RNA stop dye.

2) Candidate enzymes

In each reaction, 0.5 μg of candidate enzyme (e.g. RPS2) was incubated in 18 μL of reaction buffer in the presence of 1 μL of labeled Poly $(A)_{15}$ (100,000CPM). Four reactions with different incubation time periods (0, 5, 10 and 20 minutes) were made simultaneously. Reactions were stopped by adding 40 μL of RNA stop dye.

3) Snake Venom Phosphatase Reaction

Snake Venom Phosphatase/SVP reactions were included as positive controls. Reactions with two incubation periods of 5 and 20 minutes were performed by mixing 1 μL SVP ($3x\ 10^{-5}$ units, Sigma, St. Louis, MO) with 12 μL SVP buffer (99 mM Tris, 14 mM $MgCl_2$, 100 mM NaCl) in the presence of 2 μL labeled Poly $(A)_{15}$ (100,000CPM). Reaction was stopped by adding 40 μL of RNA stop dye.

4.2.11 3'- end radiolabeling of substrates

The 3'- end labeling was performed by mixing 10 pmol of each substrate with 5 μL 3x pCp buffer in the presence of 1 μL 100 μM ATP, 10 pmoles γ-^{32}P-pCp (10mCi/mL, Perkin Elmer), 1 μL T4 RNA ligase and 1 μL RNasin at 4°C overnight. The following day, reaction was stopped with 1 μL of phenol and 20 μL of RNA stop dye. The sample was loaded into a 15% polyacrylamide gel for gel purification. Gel purification procedure with the 3' labeled probes was performed as described in Section 4.2.7 (2). List of reagents used for 3'-radiolabeling is presented in Table 13.

Table 13. Components of reagents used in 3'-radiolabeling procedure.

Reagents	Ingredients
3x pCp buffer	150 mM Hepes (pH 7.5), 60 mM $MgCl_2$, 9.9 mM DTT, 30% (v/v) DMSO and 30 μg/mL BSA
SVP buffer	99 mM Tris, 14 mM $MgCl_2$, 100 mM NaCl
10x Alkaline buffer	500 mM sodium bicarbonate pH 9.2 and 10 mM EDTA
RNA stop dye	9M Urea, 0.01% bromophenol blue, and 0.01% xylene cyanole FF
½ x TBE	44.5 mM Tris-HCl, 44.5 mM Boric Acid, 1 mM EDTA (pH 8.3)

4.2.12 Reactions with 3'- radiolabeled substrates

Time dependent experiments were performed using 3'-radiolabled substrates miR155_13nt and Poly $(A)_{15}$. The reactions using 3'-radiolabled miR155_13nt were the same as the 5'-radiolabeled substrate. Time course experiments were performed.

4.2.13 Sample loading and gel running

All reactions, except for the alkaline hydrolysis digestion, had been normalized to equal CPM radioactivity. Since not all reactions had the same volume, the CPM per μL concentrations varied. It was important to have the same radioactivity in all lanes to visualize and compare the reactions at different time points or with different protein concentration. Since the purpose of including the markers (Alkaline ladder, RNase T1 and RNase A reactions) was to assign the nucleotide position, the CPM count was not critical to their enzymatic function. The CPM of all lanes loaded in the 15% poly acrylamide gel, except for the markers, were normalized by adjusting the sample volumes loaded to the well.

CH 4 POST SCREENING ANALYSIS

After loading samples to each well, the gel was run at 15 mAmp for 1 hour and 30 minutes in 0.5x TBE buffer. The gel was put in a -80°C freezer on one glass plate with a Phosphor Screen (Packard, Meriden, CT) on top immediately after the gel finished running to prevent the RNA fragment in the gel from diffusing. Exposure was typically done over night in the freezer. The following day, the gel image was scanned using a Cyclone Phosphor Imager (PerkinElmer, Waltham, MA). Post editing of the images was done using CorelDRAW software (Corel, Ottawa, ON).

4.3 Results and discussions

4.3.1 Induction test

To ensure that we can proceed to the secondary screening step, we tested the inducibility of the selected positive hits (See Table 9) obtained from the primary screening step (Chapter 3). Clones from set 517A are shown as examples of the inducibility test (Figure 16). Only one of the two positive hits from 517A appears to be inducible. This is indicated by an extra protein band.

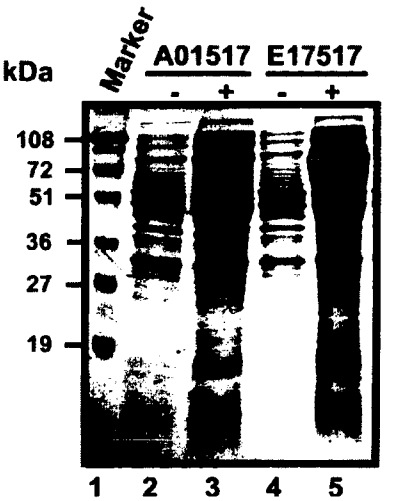

Figure 16. SDS-PAGE showing inducibility of positive hit from set 517A. Ten microlitres of each sample were loaded on the 12% SDS-PAGE gel. The gels were run at 200 volts for about 30 minutes. "-" indicates lane from uninduced clone, "+" indicates lane from clones induced with final concentration of 1 mM IPTG. Inducible recombinant protein bands are marked with an asterisk.

Twelve of these selected positive hit clones mentioned in Chapter 3 were found to be detectable by SDS-PAGE. The clones that appeared to have extra visible band and were selected as inducible clones according to the SDS-PAGE were: C19512, I23512, O13512, E17517, B01523, N01523, P09523, A15525, F06568, F20568, H06568, and N10568. The protein expression shown on the SDS-PAGE was ranked into four catergories by the thickness of the induced band: "high", "medium", "low" and "no" expression. However, to ensure the sufficient protein yield to work with in the later stage of the analysis, we only selected clones with inducibility ranking of "high" and "medium" for further purification: C19512, I23512, E17517, B01523, N01523, A15525, and F20568 (Table 14). The inducibility of these clones along with negative control E01517 was further confirmed in the process of purifying the proteins for further analysis.

Table 14. Inducibility of positive hits that underwent induction test and their ranking.

Clone MPMGp800..	Inducibility Ranking
C19512	Medium
E15512	No
I23512	Medium
O13512	Low
O23512	No
A01517	No
E17517	High
B01523	Medium
F01523	No
L01523	No
N01523	High
P07523	No
P09523	Low
A15525	Medium
C15525	No
E15525	No
G03525	No
B06568	No
D24568	No
F06568	Low
F20568	High
H06568	Low
J10568	No
J16568	No
N10568	Low

Note: Names of the selected clones for further analysis are bolded.

4.3.2 Purity of recombinant proteins

To assess the purity and to determine size of the purified recombinant proteins after dialysis, 8 μL of each sample was loaded onto a 12% SDS-PAGE gel. Protein purity was obtained by comparing the recombinant protein band, which was the most abundant protein band, to the protein background on SDS-PAGE (Figure 17).

Some clones produced extra protein bands besides the main recombinant protein band. Clone A15525 appeared to have two protein bands on the SDS-PAGE (Figure 17,

Lane 5). The appearance of the lower band may be due to protein degradation. Other clones that have significant amount of extra bands were C19512, E17517, B01523, F20568 and the negative control E01517.

Clone F20568 had a significant recombinant protein yield as shown on the SDS-PAGE (Figure 17, Lane 2). According to the size estimated from SDS-PAGE (Table 16), the clone purified had a size close to the complete TCTP protein sequence. Lane 2 in Figure 17 shows that some larger proteins have been purified along with the recombinant protein. The sizes of these extra faint bands were estimated to be 108, 80, 60 and 40 kDa. These extra bands may be bacterial proteins that have mild affinity for the Ni-NTA column.

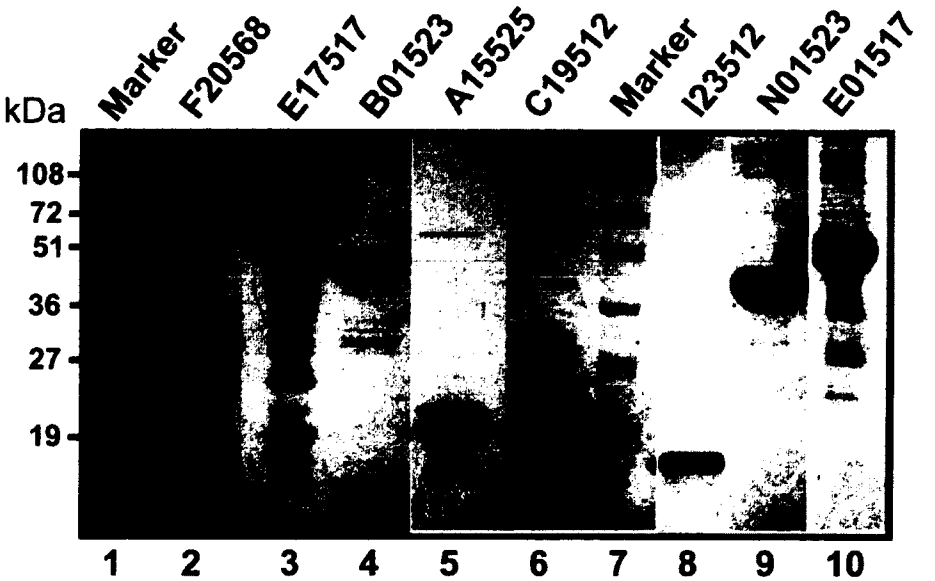

Figure 17. Purity of recombinant proteins after purification and dialysis. Eight microlitres of each purified recombinant proteins F20568, H06568, N10568, E17517, B01523, A15525, C19512, I23512, N01523 and E01517 (negative control) were run on a 12% SDS-PAGE. Ten microlitres of protein marker were loaded to Lane 1; five microlitres of protein marker were loaded to Lane 10. *A15525 appears to have two protein products (Lane 5).

4.3.3. Secondary screen using fluorescence-based assay

To confirm the results obtained from primary screen, a secondary screen was conducted using the similar fluorescence-based assay used in the primary screen. The fluorescence-based assay of each of the remaining seven clones was repeated four times with 1μg recombinant protein. Clone E01517 was included as the negative control.

As shown in Figure 18, I23512, F20568, C19512 and A15525 were found to be the top four active proteins in terms of their ability to cleave the miR155 substrate in all four trials of the fluorescence assay.

On the other hand, E17517, B01523 and N01523 were found to produce results close to the negative controls (E01517, DNase I, dialysis buffer and DEPC H_2O). Therefore, these clones were eliminated from further investigation.

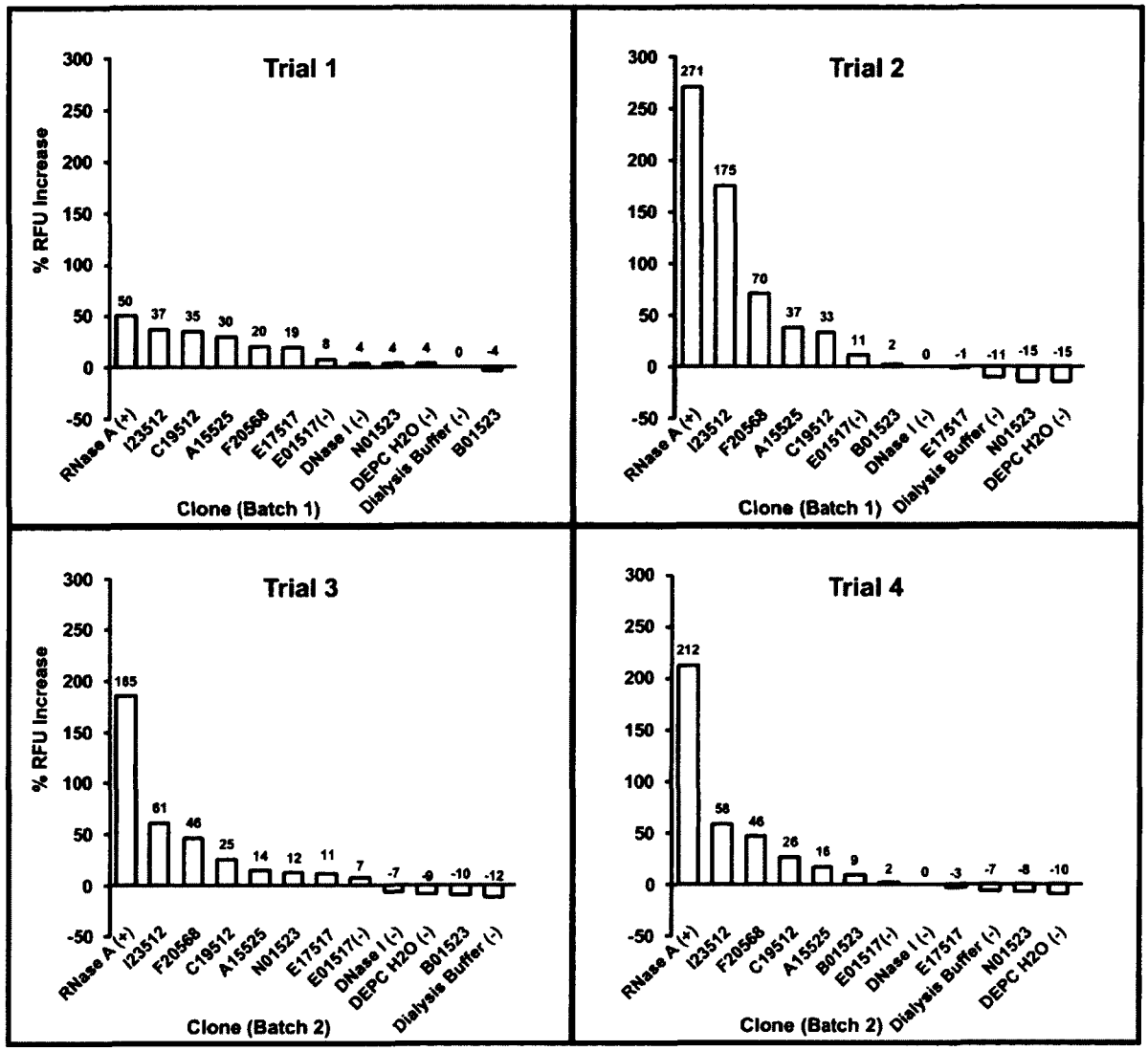

Figure 18. Secondary screen for endoribonuclease activity. Purified proteins (1μg) of candidate clones were subjected to fluorescence assay using miR155 as a substrate. Clones are arranged from the highest to the lowest % RFU increase in the graphs. Two batches of each retested clones were purified and two trials were performed with each batch of clones.

4.3.4 Identity and Integrity of Clones

DNA sequences were translated into protein sequences from six reading frames with ExPASy. Identities were determined using BLASTx (NCBI) with DNA sequences and

BLASTp (NCBI) with translated protein sequences that contained 6 histidines (Table 15). The results of clone A15525 obtained from the DNA sequence and the translated protein sequence with 6 histidines did not match with each other. The identity of the A15525 DNA sequence was identical to a protein sequence from one of the reading frames that did not contain the 6-His tag. We determined that the insert of A15525 was shifted and out of frame with the His-tag. Therefore, this clone was eliminated from further analysis.

Table 15. Identity, protein size and expected protein size of positive clones.

Clone MPMGp 800..	Protein Identity	Expressed protein size estimated by SDS-PAGE (kDa)	Predicted protein size
C19512	Caskin-1	~15	61 kDa
I23512	40S Ribosomal Protein S2	~15	32 kDa
A15525	No match (not in-frame)	19	N/A
F20568	Translationally controlled Tumor Protein	29	19 kDa

Note: Expected protein sizes were obtained from UniProt Database. "N/A" data not applicable.

4.3.5 Characterization of candidate enzymes using electrophoretic endoribonuclease assay

Translationally controlled tumour protein (TCTP, clone F20568)

The RFU signal of recombinant TCTP (clone F20568) toward the fluorogenic substrate appeared to be lower than that of RPS2 (Figure 18). When subjected to electrophoretic assay, TCTP appeared to have ribonucleolytic activity toward both substrates (Figure 19 and 20). Major cleavage site generated by TCTP on miR155_13nt was 5UC, while weak cleavages were at 9GA, 11UA and 12AG (Figure 19). Appearance

of laddering pattern in both miR155_13nt (Figure 19A Lane 6) and miR155_24nt (Figure 20A Lane 3-4) suggested that TCTP may possess exoribonucleolytic activity.

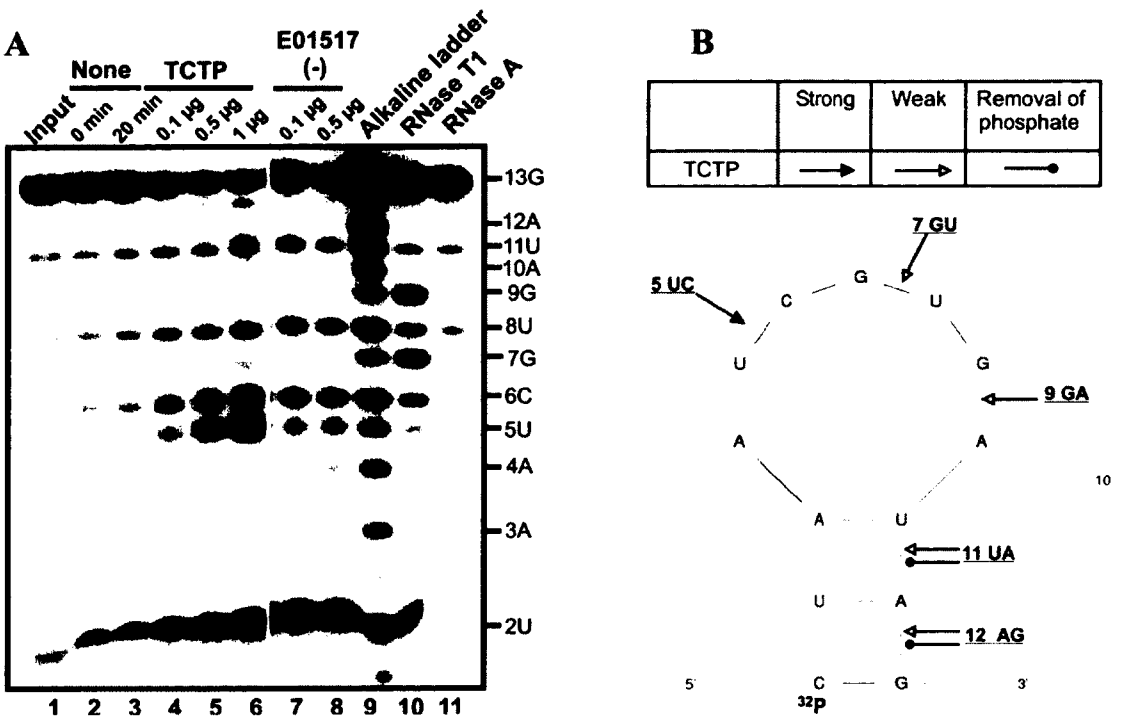

Figure 19. Electrophoretic endoribonuclease assay and cleavage pattern of TCTP toward 5'-labeled miR155_13nt. (A) Increasing amount of TCTP and negative clone E01517 were tested against miR155_13nt for 20 minutes at 37°C in a standard electrophoretic endoribonuclease assay. **(B)** The RNA secondary structure of miR155_13nt shows the location of cleavage by TCTP.

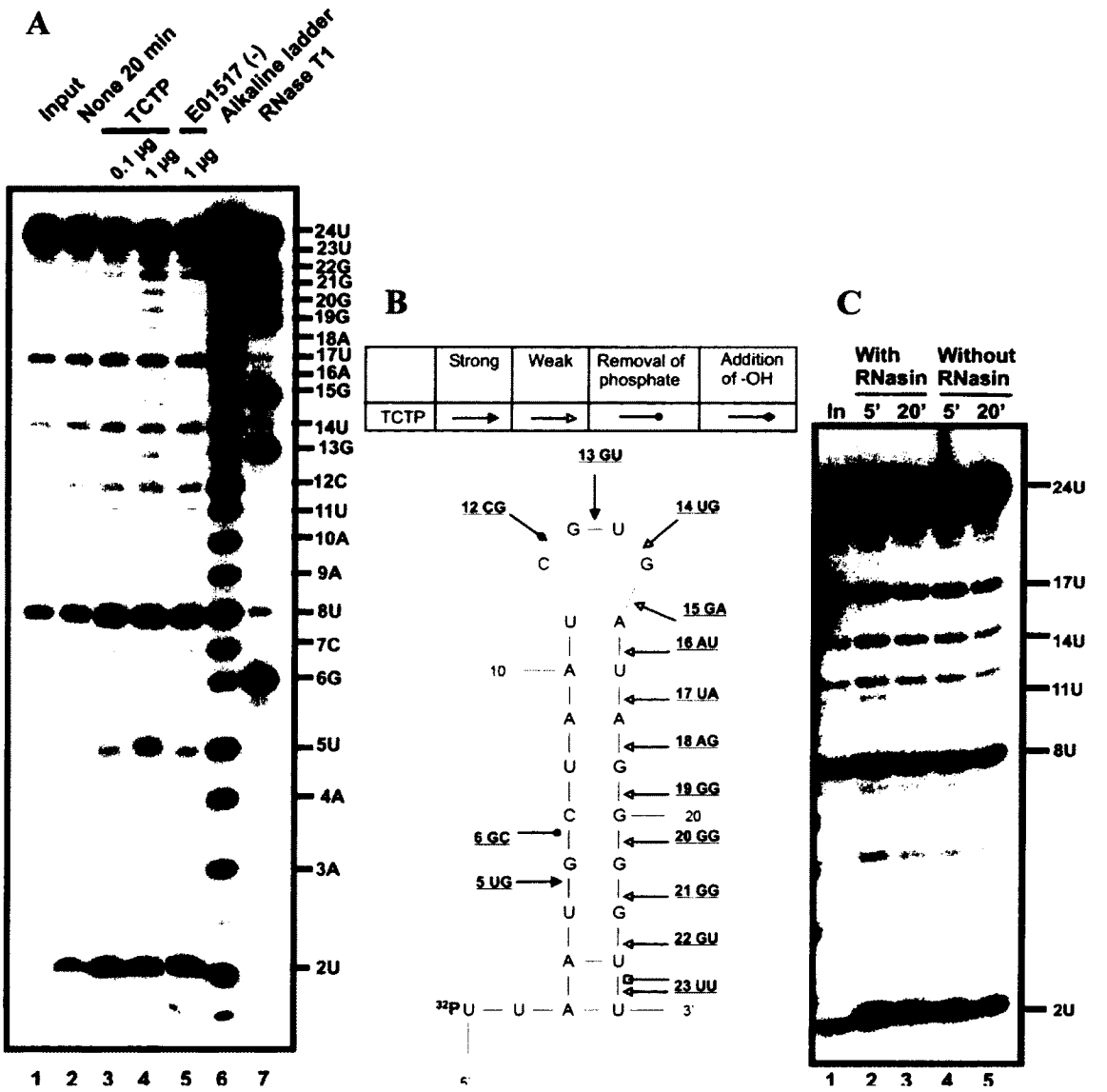

Figure 20. Electrophoretic endoribonuclease assay of TCTP toward 5'-labeled miR155_24nt and "None" negative controls with and without 3U RNasin®. (A) Increasing amount of TCTP and 1 µg of negative clone E01517 were tested against miR155_24nt for 20 minutes at 37°C in a standard electrophoretic endoribonuclease assay. **(B)** The RNA secondary structure of miR155_24nt shows the location of cleavage by TCTP. **(C)** No difference is found between "None" with and without 3U of RNasin®.

The substrate miR155_24nt appeared to be unstable in the electrophoretic assay as shown in Figure 20 A (Lanes 1 and 2), C and Figure 21 (Lanes 1 and 2). If the miR155_24nt folded as the most stable predicted structure (Figure 14B), 19G, 21G and

22G should have been paired as shown in Figure 14B. However, it was observed that the cleavage product at these G sites appeared in the RNase T1 ladder reaction. This observation led us to suspect that the substrate did not stay in one secondary structure constantly when the reaction took place. To determine the possibility of RNase A contamination in our assay, a time-dependent test was performed by incubating 1μL of labeled miR155_24nt in each reaction mixture with or without RNasin® Plus RNase Inhibitor (Promega, Madison, WI). One unit of RNasin® was shown previously to be able to inhibit the activity of 5ng of RNase A by 50% (Promega, Madison, WI). As observed in Figure 20C, miR155_24nt incubated with or without 3U RNasin® were significantly degraded at all of the U sites. The band intensities of these two conditions were almost identical. Addition of RNasin did not change the appearance of cleavage at U sites. Furthermore, the U site is a known natural self-cleaving site. Taken together, the cleavage product at U sites was not a result of contamination from common ribonuclease sensitive to RNasin®, such as RNase A, but maybe due to the unstable nature of the substrate.

Caskin-1 (clone C19512)

Clone C19512, which was identified to be caskin-1 or CASK interacting protein, did not exhibit strong expression (Figure 21, Lane 8). It also appeared to have extra bands being purified at 72, 60, 31 and 29 kDa along with the major band at 15 kDa. The 15 kDa band appeared to be more intense than the rest of the bands in Figure 17; it was more likely to be the recombinant protein bands. If this 15 kDa band was the recombinant Caskin-1, with the complete sequence of Caskin-1 being 157 kDa (1433 AA), the truncated form of caskin-1 that we purified was only 1/10 of the full length protein.

CH 4 POST SCREENING ANALYSIS

Based on the four fluorescence-based assay replicates, this truncated caskin-1 was able to generate an increase in RFU signal in all 4 trials of fluorescence assay comparing to the negative control E01517 (Figure 18). Caskin-1 appeared to cleave full length miR155 substrate strongly at 4AU and 5UG (Figure 21). However, these strong cleavage bands may be due to the higher amount of substrate present as the intensity of the uncleaved substrate appeared to be higher in Lane 4 of Figure 21. We are aware of the uneven radioactivity presented in Figure 21, even though the amount of radiolabeled substrate for each sample was normalized before loading to the gel.

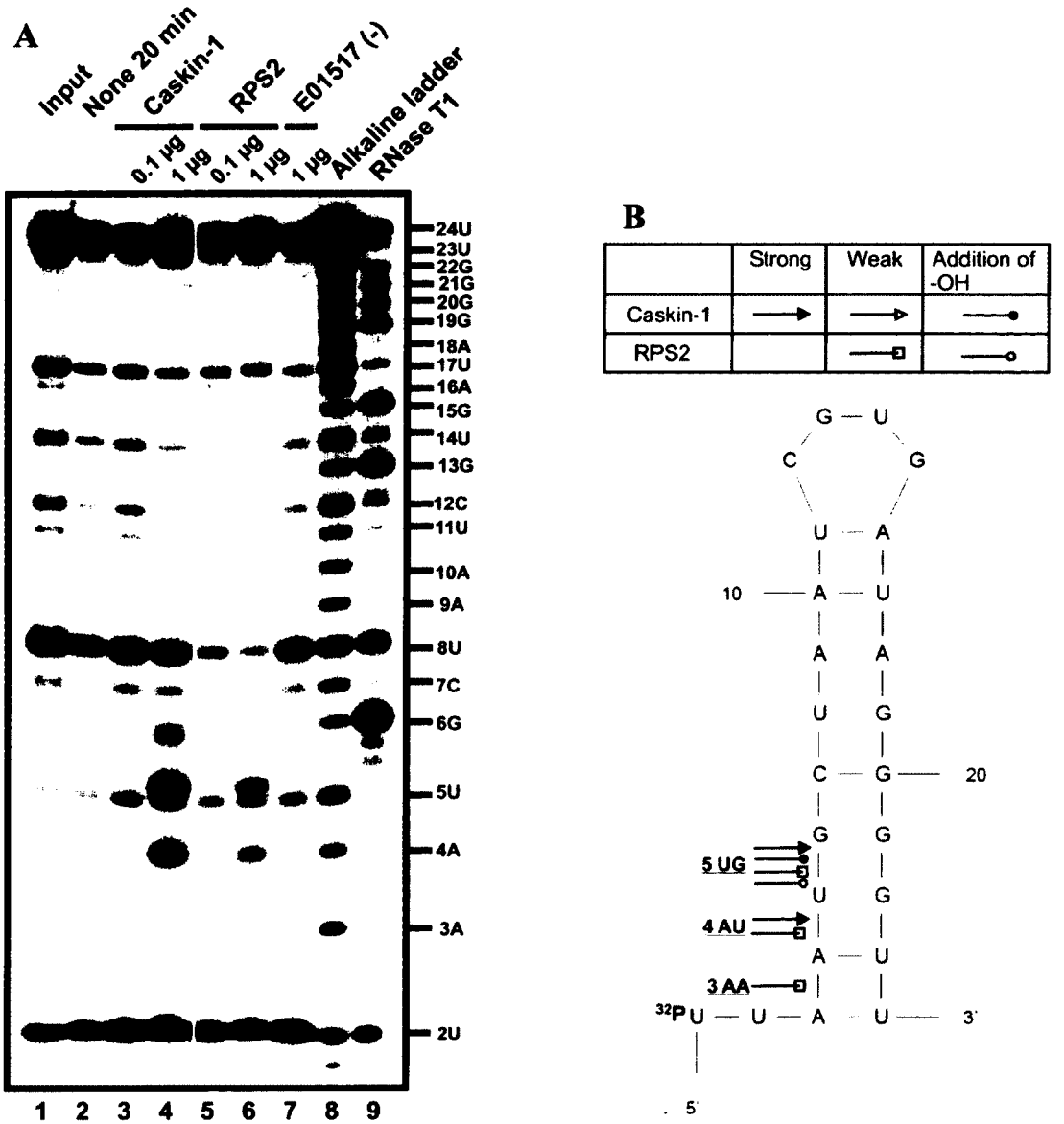

Figure 21. Electrophoretic endoribonuclease assay and cleavage pattern of Caskin-1 and RPS2 toward 5'-labeled miR155_24nt. (A) Increasing amount of Caskin-1 and RPS2, and 1 µg of negative clone E01517 were tested against miR155_24nt for 20 minutes at 37°C in a standard electrophoretic endoribonuclease assay. Stronge cleavage and removal of the phosphate group at 5U are shown on the gel. **(B)** The RNA secondary structure of miR155_24nt shows the location of cleavage by Caskin-1 and RPS2.

CH 4 POST SCREENING ANALYSIS

40S ribosomal protein S2 (RPS2, Clone I23512)

As seen on the SDS-PAGE (Figure 17, Lane 8), RPS2 had distinctive single bands with notably high purity. The size of this clone as estimated from the SDS-PAGE was about 15 kDa which was half of its predicted full length size of 32 kDa (293 AA). Based on the fluorescence assay in the secondary screen, RPS2 had the strongest activity to cleave the miR155 substrate by generating the highest percentage change of RFU and highest last RFU value in four trials. RPS2 was further tested *in vitro* for both endoribonuclease and exoribonuclease activities using the miR155_13nt and Poly $(A)_{15}$ substrate.

1) RPS2 cleaves 5' radiolabeled miR155_13nt

As shown in Figure 22A, two different batches of RPS2 consistently cleaved sites at 4AU and 5UC. To further assess the endoribonucleolytic activity of the stronger batch of RPS2 (Lane 3-4 of Figure 22A), we repeated the concentration-dependent electrophoretic endonuclease assay with this batch of RPS2 twice. A representative of the repeated experiment is shown in Figure 22B. A cleavage product at 5UC intensifies as the amount of protein in the reaction increases from 0.1 μg to 1 μg (Figure 22B, Lane 3-4). A smaller and weaker cleavage product is shown at a slightly lower position of 4AU. It is suspected that this cleavage product is generated by a cleaving in between 4AU dinucleotide followed by a removal of the phosphate group. When compared with TCTP that cleaves strongly at 5UC and weakly at 7GU, 9GA, 11UA and 12AG (Figure 19), RPS2 appeared to have a slightly different cleavage pattern. This evidence supports the argument that the cleavages seen in these two reactions were generated by two different enzymes.

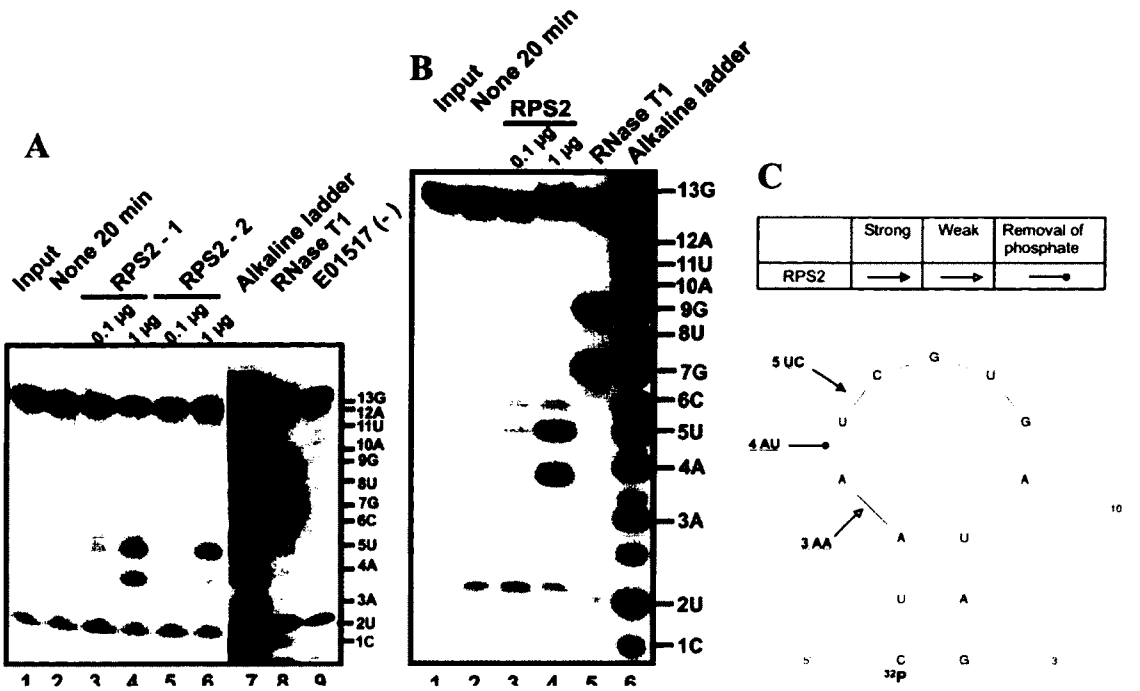

Figure 22. Electrophoretic endoribonuclease assay and cleavage pattern of RPS2 toward 5'-labeled miR155_13nt. (A) Increasing amount of two batches of RPS2 and 1 µg of negative clone E01517 were tested against miR155_13nt for 20 minutes at 37°C in a standard electrophoretic endoribonuclease assay. Both batches of RPS2 showed cleavage, but the first batch exhibit stronger activity. **(B)** Representative gel of repeated electrophoretic endoribonuclease assay using first batch of RPS2. **(C)** Cleavage locations at the predicted secondary structure of miR155_13nt.

In the primary screen, RPS2 was selected as a positive hit that had cleaving activity towards the13-nt miR155 substrate but not toward Oligo CU and CG. To further assess the substrate specificity observed in the screen, RPS2 was subjected to electrophoretic assay using a control substrate Oligo CU-aR.

As anticipated, no cleavage appeared at 10CU site of the Oligo CU-aR (Figure 23). This was consistent with the primary screen observation that RPS2 was not able to cleave the CU dinucleotide. Interestingly, two very weak products were observed in between 5G

and 4G, and 4G and 3A. It is possible that the phosphate groups were removed from the cleaved products at 5GU and 4GG.

It is interesting to note that RPS2 cleaved between UC dinucleotide in miR155_13nt substrate but not in the Oligo CU_aR substrate. Conversely, RPS2 cleaved between GU dinucleotide in Oligo CU_aR but not in miR155_13nt. Both of these sites are in the loop region of both substrates. Taken all together, it is difficult to discern any sequence specificity of RPS2. Further experimentation is needed to investigate the ability of RPS2 to cleave in a sequence-specific manner.

Unlike the electrophoretic assay using miR155_13nt, there was no distinctive cleavage pattern of RPS2 on the full length substrate miR155_24nt (Figure 21). Although RPS2 were able to generate cleavage at 4AU and 5UG, this pattern is identical to those generated by Caskin-1.

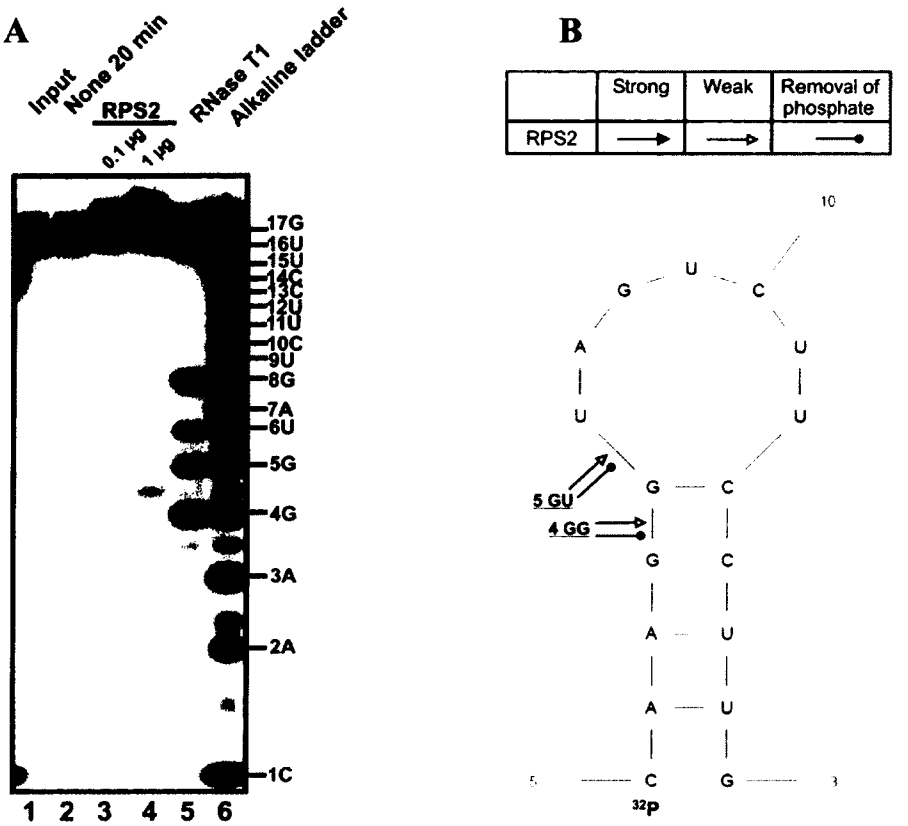

Figure 23. Electrophoretic assay and cleavage pattern of RPS2 toward control substrate Oligo CU. Weak cleavage and removal of the phosphate group at 5G and 4G are shown on the gel. **(A)** Increasing amount of RPS2 was tested against Oligo CU for 20 minutes at 37°C in a standard electrophoretic endoribonuclease assay. **(B)** Cleavage locations at the predicted secondary structure of Oligo CU.

2) Time dependent effect of RPS2 on 5'-radiolabeled miR155_13nt

To further study the ability of RPS2 to cleave miR155, the miR155_13nt was used as a substrate to investigate the enzyme kinetics, as it is more stable than miR155_24nt. A representative picture of the time-course experiment, which was repeated three times, is shown in Figure 24. Over a period of 40 minutes, a significant increase of cleavage product cut at 5UC was observed. Along with the 5UC cleavage site product, another time-dependent cleavage was observed just one nucleotide shorter at 4AU. It was observed that

an extra band gradually appeared below the 4AU band as the incubation time increased. According to this observation, RPS2 appeared to be able to cut at 4AU weakly, and remove the phosphate group from the 3'-end of the cleavage product.

We used the cleavage product at 5UC which was the most distinct decay product to determine the time course of the enzymatic activity which is shown in Figure 24A. A relative increase in radioactivity was obtained by measuring the band intensity of 5UC against a selected background. As observed, the enzymatic activity represented by the 5U band was increased over a period of 60 minutes.

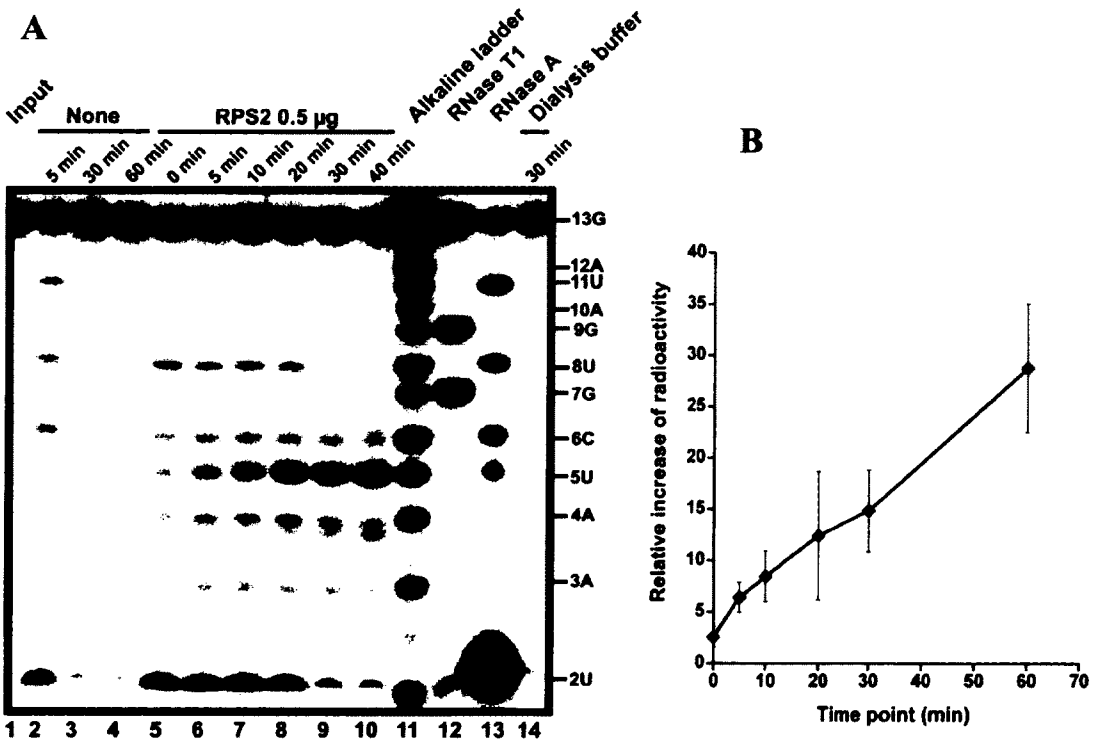

Figure 24. Time-dependent experiment and kinetic analysis of RPS2 toward 5'-labeled miR155_13nt. (A) 0.5 µg of RPS2 were tested against miR155_13nt for increasing time period at 37°C in a standard electrophoretic endoribonuclease assay. **B)** The relative increase of radioactivity was indicated by the increase of band intensity at 5UC cleavage site. The intensity of band was measured using OptiQuant Software. The increase of band intensity was calculated by using the band intensity at a particular time point against the intensity of a randomly selected background. Results presented represent averaged data ± standard deviation from three experiments.

CH 4 POST SCREENING ANALYSIS

3) Effect of RPS2 on 3'- radiolabeled miR155_13nt

To further investigate the cleavage pattern observed in electrophoretic assays with the 5'-labeled miR155_13nt was in fact due to the endoribonuclease activity of RPS2; the assay was repeated using a 3'-labeled miR155_13nt substrate (England *et al.* 1980). If RPS2 did possess only endoribonuclease activity, the cleavage product from 3'-labeled substrate would match the cleavage pattern observed in Figure 22. As shown in Figure 25, the corresponding 5UC dinucleotide cleavage was not observed in the 3'-labeled substrate. Interestingly, a laddering pattern of the substrate was observed, possibly indicating exoribonuclease activity in the 5'-3' direction.

The experiment with 3'-labeled substrate was conducted only once to evaluate whether the cleavage patterns of 5'- and 3'-labeled substrates match with each other. Therefore no reliable conclusion could be drawn from this single experiment. Nonetheless, this experiment with the 3'-labeled substrate warrants future investigations on exoribonucleolytic activity of RPS2.

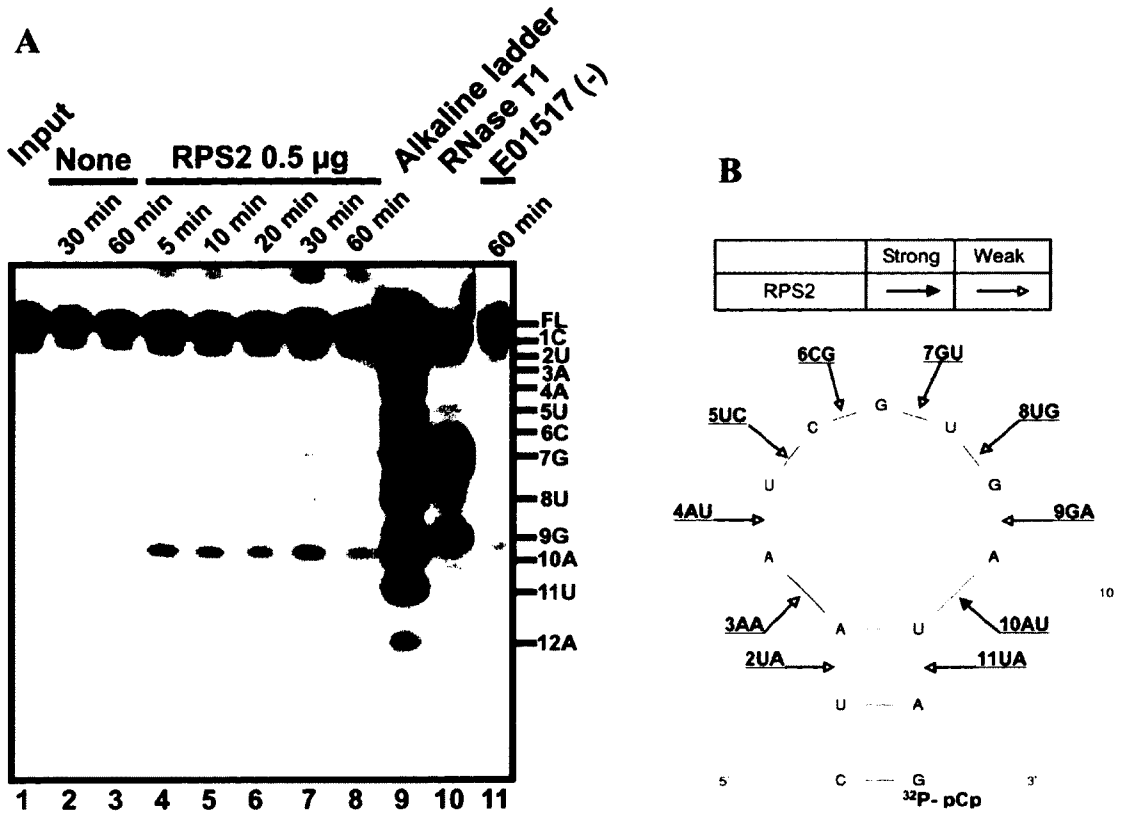

Figure 25. Time-dependent experiment of RPS2 toward 3'-labeled miR155_13nt showing weak exoribonuclease activity. (A) 0.5 µg of RPS2 were tested against 3'-labeled miR155_13nt for increasing time period at 37°C in a standard electrophoretic endoribonuclease assay. Nucleotide labelling corresponds to the 3'-end of the cleavage site. "FL" uncleaved full length substrate. **(B)** Cleavage locations at the predicted secondary structure of miR155_13nt.

4) RPS2 showed weak exoribonucleolytic cleavage toward 3'- labeled Poly(A)$_{15}$ substrate

To further investigate the potential that RPS2 exhibits 5'-3' exoribonuclease activity, a 3'-labeled Poly (A)$_{15}$ substrate was used in the enzymatic assay. As observed in Figure 26, the 3'-radiolabeled Poly(A)$_{15}$ appeared to be degraded from the 5'-end in the presence of 0.5 µg RPS2 (Lane 5-7). All sample lanes with RPS2 (Lane 4-7) had the appearance of several bands with light intensity at the bottom of the gel, indicating that the

substrate was degraded in the 5'-3' direction. This suggests that RPS2 may have weak exoribonuclease activity.

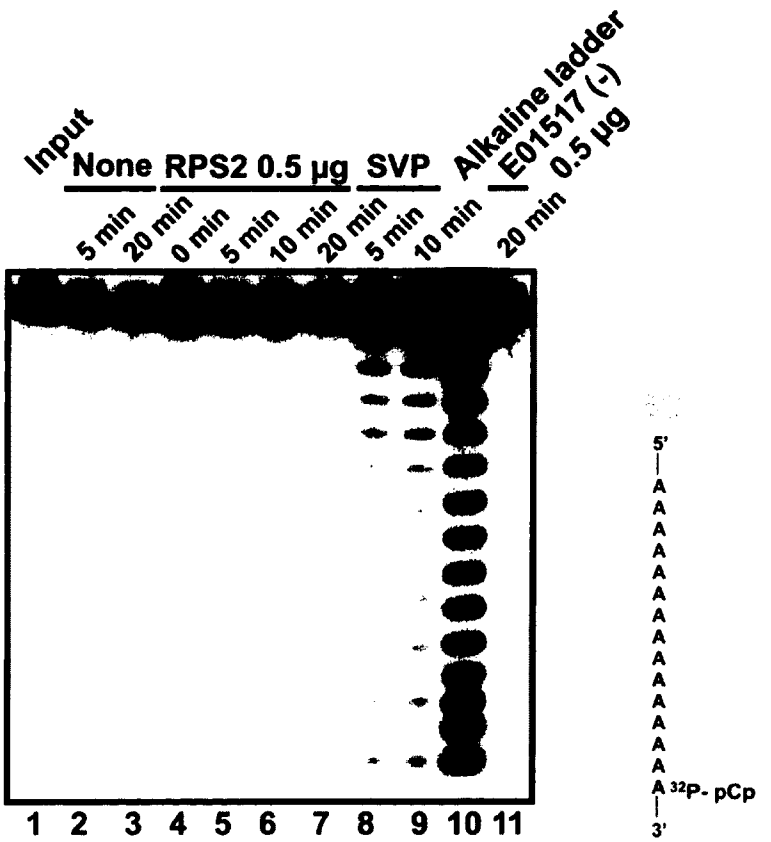

Figure 26. Weak exoribonucleolytic activity by RPS2 toward 3'-labeled PolyA substrate. 0.5 µg of RPS2 were tested against 3'-labeled Poly $(A)_{15}$ substrate for increasing time period at 37°C in a standard electrophoretic assay. Light intensity cleavage bands reveal the exoribonucleolytic activity of RPS2 toward 3'-labeled Poly A substrate.

5) RPS2 showed weak exoribonucleolytic cleavage toward 5' labeled Poly$(A)_{15}$ substrate

To determine if RPS2 has 3'-5' exoribonuclease activity, we challenged recombinant RPS2 with 5'-radiolabeled Poly $(A)_{15}$ substrate (Figure 27). However the activity was detectable but very weak as compared to the strong cleavage by snake venom protein (SVP) that cleaved Poly A from the 3'-end. Directional exoribonucleolytic cleavage

was indicated by the ladder patterns of bands at different time points. SVP cleaves from the 3'-end. The increase in the amount of shorter cleavage products was more pronounced 10 minutes after the start of the reaction. RPS2 started to show visible pattern at 5 minutes; this pattern remained constant at 10 and 20 minutes, while the negative control E01517 did not generate any cleavage even at 20 minute time point. Thus, this observation suggests that RPS2 may have weak 3'-5' exoribonuclease activity towards Poly$(A)_{15}$.

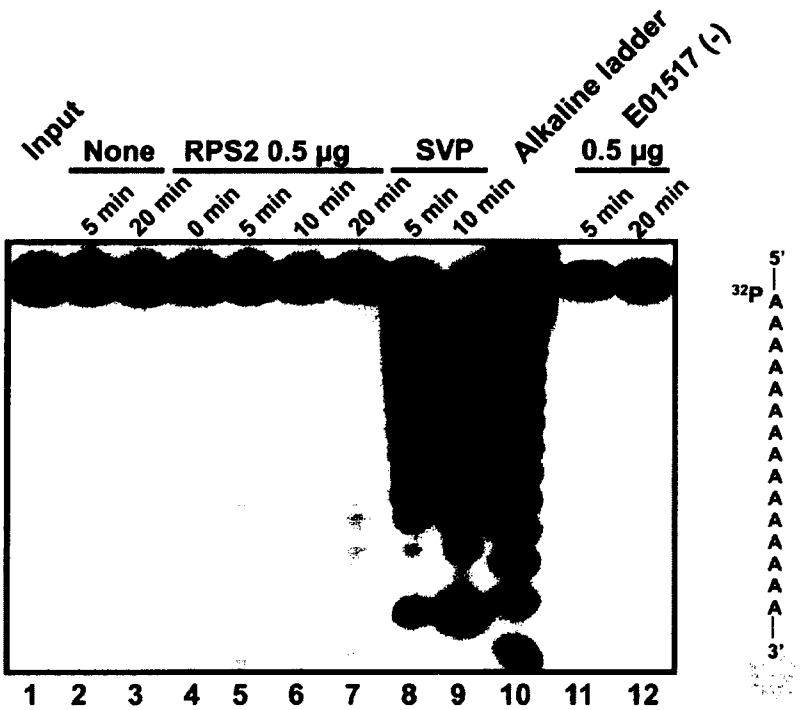

Figure 27. Weak exoribonucleolytic activity by RPS2 toward 5'-labeled PolyA substrate. 0.5 µg of RPS2 and negative control clone E01517 were tested against 5'-labeled Poly $(A)_{15}$ substrate for increasing time period at 37°C in a standard electrophoretic assay. Light intensity cleavage bands reveal the exoribonucleolytic activity of RPS2 toward 5'-labeled Poly $(A)_{15}$ substrate.

Chapter 5

General discussion

5.1 General overview

MicroRNAs have been receiving increasing attention as an important factor that controls expression of many genes including those implicated in cancer. Just like mRNAs, microRNA turnover is likely to be a crucial step in regulating their function (Parker and Song, 2004; Krol *et al*, 2010). Degradation of both mRNA and microRNA has been thought to be carried out mainly by exoribonucleases (Krol *et al*, 2010). However, exoribononucleases do not exhibit the specificity that endoribonucleases possess. Since very few human endoribonucleases have been characterized as compared to other model species such as *E.coli*, we hypothesize that there are many yet unidentified human endoribonucleases that can cleave mRNAs and the functional mature form of microRNAs.

To date, no functional screen has been developed for endoribonuclease activity established outside our laboratory. The main goal of this MSc thesis was to develop a high-throughput functional screening method to identify new human endoribonucleases that cleave miR155. Overall, this study has established a high-throughput experimental protocol to screen library of human recombinant proteins for possible ribonuclease activity. Using this protocol, we have identified a list of new candidate human ribonucleases.

5.2 Significance of finding endoribonucleases that degrade microRNA

The fate of a particular microRNA has great influence on the regulatory ability, as a single type of microRNA can control the expression of up to thousands of mRNA. For

example, the number of gene targets of human miR155 is approximately 5445 predicted by miRanda program (John *et al.* 2004). Many of these target genes also play essential roles in cancer. The oncogenic microRNA and tumour suppresser microRNA regulate the abundance of enzymes implicated in cancer by controlling the number of mRNA copy. In mammalians cells, microRNA acts on target mRNA very specifically by degrading only the complimentary target (Su, 2009). This unique feature of microRNA has been the key to its regulatory function. Thus, if we understand what the determining factors for selective microRNA degradation are (e.g., in specific tissue or in cancer cells), we can better understand the global regulation of gene expression.

Studies on microRNA have been largely focused on the function and targets of microRNAs. To date, there has been limited information on how microRNAs are degraded. Only a handful of factors have been identified as the key players in microRNA turnover. They are exoribonucleases, RBP and adenylase (Das *et al.* 2010; Bail *et al.* 2010; Ramachandran and Chen 2008; Chatterjee and Großhans 2009; Buratti *et al.* 2010). However, these enzymes do not possess sequence specificity, and thus can not explain the precise specificity of microRNA regulation. Therefore, there likely exist other key players such as endoribonucleases that are responsible for the highly regulated characteristic of microRNA turnover.

5.3 The HTS functional screen

The fluorescence-based assay, originally developed in our laboratory, has proven to be valid for the detection of the endoribonuclease activity of APE1 (Kim *et al.* 2010). To extend its further use, we have developed a functional screening-based method on the

principle of the previous fluorescence-based assay. An HTS functional screen using microRNA as the substrate has been developed during the course of this thesis. At the same time, we are aware of some potential problems using miR155_13nt for the sensitive fluorescence-based screen. Compared to the substrate design of Oligo UA, the miR155_13nt differs in several respects that may help us understand the potential problem in the screen (Kim *et al.* 2010). Using miR155_13nt, several improvements have been made during this project.

First, the substrate used in the primary and secondary screen, miR155_13nt, is an all RNA design, whereas in Oligo UA there is only one ribonucleotide. There are advantage and disadvantage in having only one possible cleavage site in the substrate. Making a hybrid DNA-RNA substrate may help eliminate hits that have exoribonuclease activity. However, by doing this, potential proteins that cleave the double stranded part of the substrate will be eliminated. Moreover, if we limit the possible cleavage sites to the one or two particular ribonucleotide sites, we may fail to detect other potential endoribonucleases.

Second, the secondary structure of miR155_13nt has a free energy of 9.2 kJ / mol, while it is – 9.1 kJ / mol for the Oligo UA based on the folded DNA structure. The lower the free energy, the more stable the structure is. The original rationale of using miR155 was the wide association of this microRNA in various cancers. As long as we continue to use miR155 as a template, the problems we encountered will still exist.

Third, the Oligo UA has a stronger stem than miR155_13nt, by having more CG base pairs on a longer stem. An extra nucleotide was artificially added to the 5'- and 3'-

end to create an extra CG pair at the end and a more stable structure. If we continue using the same microRNA, miR155, additional CG complimentary pair at the end may increase the stability. Nonetheless, we were able to obtain a list of positive hits despite the imperfect design of the original substrate miR155_13nt.

We used the combination of selection method by last RFU (method 2 as described in Section 3.3.2) and elimination method that omit non-unique clones toward miR155 (Section 3.3.3). Eliminating mutual positive hits with other oligonucleotides may not be the most suitable elimination method. As it may exclude true positive clones that cleave in between CG, CU or UA, only a portion of the potential true positives was covered and survived from the elimination. Furthermore, most of the positive hits that were selected using this elimination method generally had weak positive signals in fluorescence-based assay (Table 9). Therefore, future studies focusing on the positive hits using other selection and elimination methods can help us to determine which one is the best to eliminate false positives.

5.4 From primary screen to secondary screen

As summarized in Table 16, clones that showed positive results in both primary and secondary screen did show cleavage on RNA substrates in the electrophoretic assay (i.e. RPS2 and TCTP). Negative control, clone E01517, which did not appear to be cleaving the fluorogenic substrate in the secondary fluorescence-based assay, also did not show noticeable cleavage products in electrophoretic assay.

The 24-nucleotide full length microRNA substrate was problematic because of its sensitivity to general degradation as observed at the U sites (Figure 20 and 21). Although

miR155_24nt required less free energy for forming the three possible secondary structures than the 13-nucleotide substrate (miR155_13nt), it was more sensitive to the natural cleavage sites. This also provides an answer as to why the full length substrate is not suitable for both fluorescence-based assay and electrophoretic assay.

Table 16. Comparison between results from primary and secondary screen.

Clone MPM Gp 800..	Identity	Primary Screen		Post screening analysis		
				Secondary screen	Electrophoretic Assay	
		Signal	Repeatable		13nt	24nt
C19512	CASK interacting protein (Caskin-1)	M	N/A	+	N/A	+
I23512	RPS2	M	N/A	+	+	+
F20568	TCTP	H	Yes	+	+	+
E01517	Negative control	-	Yes	-	-	-

Note: "-" non-detectable level of activity; "N/A" data is not available or inconclusive.

According to the results herein, both remaining candidates RPS2 and TCTP were positive from the primary screen to electrophoretic assay. As none of these clones have previously been shown to have ribonuclease activity, the results obtained in this study may be of importance and warrant futher investigation.

In Eukaryotes, RPS2 belongs to the 40S small subunit of 80S ribosome. The ribosome is a primary place for protein synthesis, where the 40S small subunit is responsible for holding the mRNA for translation. An *in vitro* study has found the correlation of RPS2 with increased cell proliferation (Kowalczyk *et al.* 2002). RPS2 is known to bind to mRNA as a ribosomal protein; it also binds to microRNA (Wang *et al.* 2011). Recent study shows that RPS2 binds to pre-let-7a-1 to prevent the expression of tumour suppressor microRNA let-7a in human prostate cancer (Wang *et al.* 2011). Future

studies can focus on finding out the RNA binding ability of RPS2 toward miR155 to add more information to its microRNA binding characteristic. Results shown in Chapter 4 indicate that RPS2 is possibly a ribonuclease with both endoribonuclease and exoribonuclease activity. Combining these results together, it is suggested that RPS2 may preferably cleave after unpaired U and A closer to the 5'-end, and carry out weak exoribonuclease activity from both 5'-3' and 3'-5' directions after the endoribonucleolytic cleavage. These activities may play a surveillance role in keeping any aberrant mRNA from being translated.

In the past, TCTP has been linked to cell growth and malignant transformation, and is generally more abundant in tumours (Bommer and Thiele 2004; Li *et al.* 2010; Tuynder *et al.* 2002). Interestingly, it is involved in a very rare cellular event called tumour reversion (Marce, 2004). The molecular functions of TCTP that have been identified so far include calcium-binding activity (reviewed in Bommer *et al.* 2002) and tubulin-binding activity (Kim *et al.* 2000). Although, the previous findings of RPS2 and TCTP suggest that they may be oncogenic and not involved in the turnover of oncogenic miR155, their identification in this project may suggest a more complex role they play in regulating miR155 function. Since RPS2 and TCTP had different cleavage patterns, it was very likely that they were two different enzymes. Thus, more careful work is still required to establish their specific function toward miR155.

Some shared cleavage sites that RPS2 and TCTP generated led us to suspect that it might be a bacterial ribonuclease that caused the appearances of the same bands at 3AA, 4AU and 5UC of miR155_13nt. However, comparison of the purity of these three proteins (Figure 17) with the lower purity of the negative clone (E01517) made us question about

this speculation. If the recombinant RPS2 and TCTP were contaminated, why would these cleavages not appear in the reaction using a less pure E01517? It would be worth retesting RPS2 toward 3'-labeled miR155 and confirm the results seen in Figure 27. Since TCTP has shown exoribonuclease-like activity toward miR155_24nt (Figure 20 A and B), conducting an electrophoretic assay with Poly $(A)_{15}$ substrate would help us to clarify this. In addition, tests like Electromobility Shift Assay (EMSA) would be helpful to determine whether RPS2 and TCTP have RNA binding ability toward miR155.

5.5 Establishment of HTS procedure

Compared to the original designed procedure, the established procedure to discover new human endoribonucleases has been slightly modified to maximize the chance of capturing novel enzymes. To summarize the modified HTS experimental procedure, a schematic diagram is shown in Figure 28. Several changes made to the initial design of the experiment (Figure 28). First, increasing the culture volume can improve the low yield in high-throughput protein purification. Second, repeating the primary screen and checking the reproducibility of positive hits may be a good tool to eliminate false positive. As shown in Chapter 3 and 4, reproducibility of a few clones supported this statement. Positive status of clone E17517 was not repeatable in the primary screen and did not survive the secondary screen. Clone F20528 with repeatable positive signal in primary screen survived in the secondary screen and showed enzymatic activity in the electrophoretic assay. The negative signal of negative control E01517 was repeatable in primary screen and was confirmed in the electrophoretic assay. However, since primary screen of some clones was conducted once, there was not enough evidence to prove that reproducibility can predict true positive. Therefore, for the future screen, repeating the primary screen step can provide

more insights. Third, other selection methods still remain untested. Subjecting positive hits by other selection method to further analysis can provide information on choosing the best selection method. Fourth, substrate miR155_24nt is excluded due to it being unstable.

Several further improvements can be made in future studies. First, using another library which has more complete information and full length clones will help to speed up the process of identifying positive clones. Second, now that this HTS procedure is established, screening for a higher number of clones will increase the chance of capturing true positive endoribonuclease. Third, using more than one type of microRNA as substrate to compare instead of Oligo CG, CU and UA can increase the chance of identifying new ribonucleases against selected microRNAs.

The results presented in this thesis also allow us to know what to expect when conducting HTS screen using clones in hEx1 library and miR155 as a substrate, and difficulties that one may encounter when conducting future screen. In general, the established HTS procedure has allowed us to get one step closer to finding novel human endoribonucleases *in vitro*.

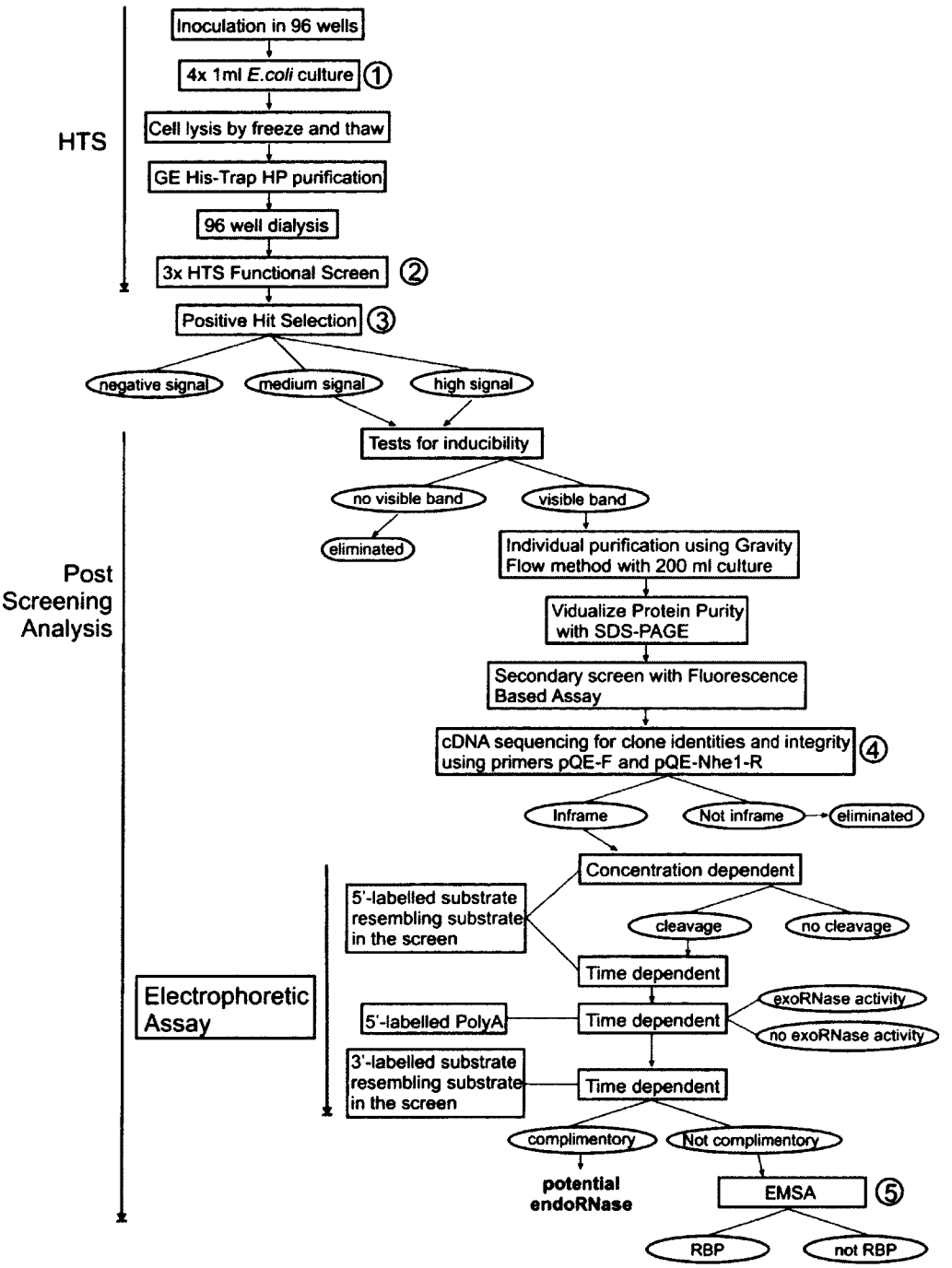

Figure 28. Schematic diagram summarizing the suggested procedure. Modifications: **1.** Culture volume increase from 2x 1mL to 4x 1mL; **2.** Repeat the high-throughput primary screen three times to collect statistic data and determine if reproducibility is an effective tool to select true positive; **3.** Testing positive hits using other untested selection methods can provide more information on choosing the best methods; **4.** cDNA sequencing using primers pQE-F and pQE-Nhe1-R instead of SP6 and T7; **5.** Additional EMSA to find out whether positive hit possess RNA binding activity if ribonuclease activity is not observed.

CH 5 GENERAL DISCUSSION

5.6 Future directions

This MSc project has led to several future research directions. First, the endoribonuclease activity of RPS2 and TCTP must be retested by repeating experiments with 3'-labeled substrate. Second, the combination of selection method using last RFU (second method as described in Section 3.3.2 (1)) and elimination method (eliminating non-unique hits toward miR155_13nt) may have not been the most effective way of selecting strong endoribonucleases as the fluorescent signal for both RPS2 and TCTP did not appear to be very high. Although we might have eliminated false positive hits by selecting unique hits, we may also have eliminated potentially highly active enzymes that cleave between CG, CU or UA. It is highly recommended to investigate the clones which exhibited high increases in fluorescence signal in future studies. In terms of screening for microRNA specific enymes, it may be of value to design a microRNA substrate with a deoxyguanosin monophosphate at one end and a deoxycytidine monophosphate at the other to stabilize the substrate and prevent capturing exoribonuclease since endoribonuclease is the main target of interest.

5.7 Concluding Remarks

This MSc project was intended to develop and validate a high-throughput procedure to screen a library of human recombinant proteins for endoribonucleases that cleave a microRNA substrate. Three major achievements and observations have been made during this project. First, a high-throughput functional screen has been successfully developed through a series of optimization experiments. Potential positive candidates were obtained from the screen. Second, a set of criteria has been established, which can be used to better narrow down the positive list to a shorter list with candidates that have high potential to be

endoribonucleases. With the selection criteria, future false positive candidates can be eliminated. Third, RPS2 was identified as a potential ribonuclease with both endoribonuclease and exoribonuclease activities. Future studies on RPS2 and the rest of the positive hits are expected to bring more insight in understanding the role of endoribonucleases in regulating microRNA functions.

References

Adams B. D., Claffey K. P. & White B. A. (2009) Argonaute-2 expression is regulated by epidermal growth factor receptor and mitogen-activated protein kinase signaling and correlates with a transformed phenotype in breast cancer cells. *Endocrinology* **150,** 14-23.

Ahluwalia J. K., Hariharan M., Bargaje R., Pillai B. & Brahmachari V. (2009) Incomplete penetrance and variable expressivity: Is there a microRNA connection? *Bioessays* **31,** 981-992.

Al-Souhibani N., Al-Ahmadi W., Hesketh J. E., Blackshear P. J. & Khabar K. S. A. (2010) The RNA-binding zinc-finger protein tristetraprolin regulates AU-rich mRNAs involved in breast cancer-related processes. *Oncogene* **29,** 4205-4215.

Ambros V., Lee R. C., Lavanway A., Williams P. T. & Jewell D. (2003) MicroRNAs and other tiny endogenous RNAs in C. elegans. *Current Biology* **13,** 807-818.

Anderson P., Kedersha N. (2008) Stress granules: the Tao of RNA triage. *Trends Biochem. Sci.* **33,** 141-150.

Anderson P., Kedersha N. (2006) RNA granules. *J. Cell Biol.* **172,** 803-808.

Anderson P., Kedersha N. (2002) Visibly stressed: The role of eIF2, TIA-1, and stress granules in protein translation. *Cell Stress and Chaperones* **7,** 213-221.

Baek D., Villén J., Shin C., Camargo F. D., Gygi S. P. & Bartel D. P. (2008) The impact of microRNAs on protein output. *Nature* **455,** 64-71.

Bail S., Swerdel M., Liu H., Jiao X., Goff L. A., Hart R. P. & Kiledjian M. (2010) Differential regulation of microRNA stability. *RNA* **16,** 1032-1039.

Barnes T., Kim W. C., Mantha A. K., Kim S. E., Izumi T., Mitra S. & Lee C. H. (2009) Identification of Apurinic/apyrimidinic endonuclease 1 (APE1) as the endoribonuclease that cleaves c-myc mRNA. *Nucleic Acids Res.* **37,** 3946-3958.

Bashkirov V. I., Scherthan H., Solinger J. A., Buerstedde J. -. & Heyer W. -. (1997) A mouse cytoplasmic exoribonuclease (mXRN1p) with preference for G4 tetraplex substrates. *J. Cell Biol.* **136,** 761-773.

Beintema J. J., Blank A., Schieven G. L., Dekker C. A., Sorrentino S. & Libonati M. (1988) Differences in glycosylation pattern of human secretory ribonucleases. *Biochem. J.* **255,** 501-505.

Biedermann B., Hotz H. R. & Ciosk R. (2010) The quaking family of RNA-binding proteins: Coordinators of the cell cycle and differentiation. *Cell Cycle* **9,** 1929-1933.

Blenkiron C., Goldstein L. D., Thorne N. P., Spiteri I., Chin S. F., Dunning M. J., Barbosa-Morais N. L., Teschendorff A. E., Green A. R., Ellis I. O., Tavaré S., Caldas C. & Miska E. A. (2007) MicroRNA expression profiling of human breast cancer identifies new markers of tumor subtype. *Genome Biol.* **8,** .

Bohn H., Inaba N. & Lueben G. (1981) New placental proteins and their potential diagnostic significance as tumour markers. *Oncodevelopmental Biology and Medicine* **2,** 141-153.

Bohn H., Winckler W. (1980) Isolation and characterization of a new placental tissue protein (PP11). *Arch. Gynecol.* **229,** 293-301.

Bommer U. A., Borovjagin A. V., Greagg M. A., Jeffrey I. W., Russell P., Laing K. G., Lee M. & Clemens M. J. (2002) The mRNA of the translationally controlled tumor protein P23/TCTP is a highly structured RNA, which activates the dsRNA-dependent protein kinase PKR. *RNA* **8,** 478-496.

Bommer U. A., Thiele B. J. (2004) The translationally controlled tumour protein (TCTP). *International Journal of Biochemistry and Cell Biology* **36,** 379-385.

Bruce Alberts, Alexander Johnson, Julian Lewis, Martin Raff, Keith Roberts & Peter Walter. (2002). Molecular biology of the cell. 4th ed. Garland Science, New York.

Buck A. H., Perot J., Chisholm M. A., Kumar D. S., Tuddenham L., Cognat V., Marcinowski L., Dölken L. & Pfeffer S. (2010) Post-transcriptional regulation of miR-27 in murine cytomegalovirus infection. *RNA* **16,** 307-315.

Buratti E., De Conti L., Stuani C., Romano M., Baralle M. & Baralle F. (2010) Nuclear factor TDP-43 can affect selected microRNA levels. *FEBS Journal* **277,** 2268-2281.

Büssow K., Cahill D., Nietfeld W., Bancroft D., Scherzinger E., Lehrach H. & Walter G. (1998) A method for global protein expression and antibody screening on high-density filters of an arrayed cDNA library. *Nucleic Acids Res.* **26,** 5007-5008.

Büssow K., Nordhoff E., Lübbert C., Lehrach H. & Walter G. (2000) A human cDNA library for high-throughput protein expression screening. *Genomics* **65,** 1-8.

Büssow K., Quedenau C., Sievert V., Tischer J., Scheich C., Seitz H., Hieke B., Niesen F. H., Götz F., Harttig U. & Lehrach H. (2004) A catalog of human cDNA expression clones and its application to structural genomics. *Genome Biol.* **5,** .

Cai Y., Yu X., Hu S. & Yu J. (2009) A Brief Review on the Mechanisms of miRNA Regulation. *Genomics, Proteomics and Bioinformatics* **7,** 147-154.

Carpten J., Nupponen N., Isaacs S., Sood R., Robbins C., Xu J., Faruque M., Moses T., Ewing C., Gillanders E., Hu P., Bujnovszky P., Makalowska I., Baffoe-Bonnie A., Faith D., Smith J., Stephan D., Wiley K., Brownstein M., Gildea D., Kelly B., Jenkins R., Hostetter G., Matikainen M., Schleutker J., Klinger K., Connors T., Xiang Y., Wang Z., De Marzo A., Papadopoulos N., Kallioniemi O. -., Burk R., Meyers D., Grönberg H., Meltzer P., Silverman R., Bailey-Wilson J., Walsh P., Isaacs W. & Trent J. (2002) Germline mutations in the ribonuclease L gene in families showing linkage with HPC1. *Nat. Genet.* **30,** 181-184.

Carrasco D. R., Sukhdeo K., Protopopova M., Sinha R., Enos M., Carrasco D., Zheng M., Mani M., Henderson J., Pinkus G. S., Munshi N., Horner J., Ivanova E. V., Protopopov A., Anderson K. C., Tonon G. & DePinho R. A. (2007) The Differentiation and Stress Response Factor XBP-1 Drives Multiple Myeloma Pathogenesis. *Cancer Cell* **11,** 349-360.

Carthew R. W., Sontheimer E. J. (2009) Origins and Mechanisms of miRNAs and siRNAs. *Cell* **136,** 642-655.

Chang A. C. Y., Sohlberg B., Trinkle-Mulcahy L., Claverie-Martin F., Cohen P. & Cohen S. N. (1999) Alternative splicing regulates the production of ARD-1 endoribonuclease and NIPP-1, an inhibitor of protein phosphatase-1, as isoforms encoded by the same gene. *Gene* **240,** 45-55.

Chatterjee S., Großhans H. (2009) Active turnover modulates mature microRNA activity in Caenorhabditis elegans. *Nature* **461,** 546-549.

Chekulaeva M., Filipowicz W. (2009) Mechanisms of miRNA-mediated post-transcriptional regulation in animal cells. *Curr. Opin. Cell Biol.* **21,** 452-460.

Chen J., Chiang Y. C. & Denis C. L. (2002) CCR4, a 3′-5′ poly(A) RNA and ssDNA exonuclease, is the catalytic component of the cytoplasmic deadenylase. *EMBO J.* **21,** 1414-1426.

Chen Y., Zhang S., Chen Y. P. & Lin J. Y. (2006) Increased expression of angiogenin in gastric carcinoma in correlation with tumor angiogenesis and proliferation. *World Journal of Gastroenterology* **12,** 5135-5139.

Chendrimada T. P., Gregory R. I., Kumaraswamy E., Norman J., Cooch N., Nishikura K. & Shiekhattar R. (2005) TRBP recruits the Dicer complex to Ago2 for microRNA processing and gene silencing. *Nature* **436,** 740-744.

Chou K. M., Cheng Y. C. (2002) An exonucleolytic activity of human apurinic/apyrimidinic endonuclease on 3′ mispaired DNA. *Nature* **415,** 655-659.

Claverie-Martin F., Wang M. & Cohen S. N. (1997) ARD-1 cDNA from human cells encodes a site-specific single-strand endoribonuclease that functionally resembles Escherichia coli RNase E. *J. Biol. Chem.* **272,** 13823-13828.

Corcoran D. L., Pandit K. V., Gordon B., Bhattacharjee A., Kaminski N. & Benos P. V. (2009) Features of mammalian microRNA promoters emerge from polymerase II chromatin immunoprecipitation data. *PLoS ONE* **4,** .

Cougot N., Babajko S. & Séraphin B. (2004) Cytoplasmic foci are sites of mRNA decay in human cells. *J. Cell Biol.* **165,** 31-40.

Danilin S., Sourbier C., Thomas L., Lindner V., Rothhut S., Dormoy V., Helwig J. -., Jacqmin D., Lang H. & Massfelder T. (2010) Role of the RNA-binding protein HuR in human renal cell carcinoma. *Carcinogenesis* **31,** 1018-1026.

Das S. K., Sokhi U. K., Bhutia S. K., Azab B., Su Z. -., Sarkar D. & Fisher P. B. (2010) Human polynucleotide phosphorylase selectively and preferentially degrades microRNA-221 in human melanoma cells. *Proc. Natl. Acad. Sci. U. S. A.* **107,** 11948-11953.

Davenport E. L., Moore H. E., Dunlop A. S., Sharp S. Y., Workman P., Morgan G. J. & Davies F. E. (2007) Heat shock protein inhibition is associated with activation of the unfolded protein response pathway in myeloma plasma cells. *Blood* **110,** 2641-2649.

Davies M. P. A., Barraclough D. L., Stewart C., Joyce K. A., Eccles R. M., Barraclough R., Rudland P. S. & Sibson D. R. (2008) Expression and splicing of the unfolded protein response gene XBP-1 are significantly associated with clinical outcome of endocrine-treated breast cancer. *International Journal of Cancer* **123,** 85-88.

De Ruyck K., Szaumkessel M., De Rudder I., Dehoorne A., Vral A., Claes K., Velghe A., Van Meerbeeck J. & Thierens H. (2007) Polymorphisms in base-excision repair and nucleotide-excision repair genes in relation to lung cancer risk. *Mutation Research - Genetic Toxicology and Environmental Mutagenesis* **631,** 101-110.

Dean M. (1998) Cancer as a complex developmental disorder - Nineteenth Cornelius P. Rhoads memorial award lecture. *Cancer Res.* **58,** 5633-5636.

delCardayre S. B., Raines R. T. (1995) A residue to residue hydrogen bond mediates the nucleotide specificity of ribonuclease A. *J. Mol. Biol.* **252,** 328-336.

Denli A. M., Tops B. B. J., Plasterk R. H. A., Ketting R. F. & Hannon G. J. (2004) Processing of primary microRNAs by the Microprocessor complex. *Nature* **432,** 231-235.

Di Donato A., Cafaro V., De Nigris M., Rizzo M. & D'Alessio G. (1993) The determinants of the dimeric structure of seminal ribonuclease are located in its N-terminal region. *Biochemical and Biophysical Research Communications* **194,** 1440-1445.

Dimitriadis E., Trangas T., Milatos S., Foukas P. G., Gioulbasanis I., Courtis N., Nielsen F. C., Pandis N., Dafni U., Bardi G. & Ioannidis P. (2007) Expression of oncofetal RNA-binding protein CRD-BP/IMP1 predicts clinical outcome in colon cancer. *International Journal of Cancer* **121,** 486-494.

Ding X. C., Weiler J. & Großhans H. (2009) Regulating the regulators: mechanisms controlling the maturation of microRNAs. *Trends Biotechnol.* **27,** 27-36.

Doi N., Zenno S., Ueda R., Ohki-Hamazaki H., Ui-Tei K. & Saigo K. (2003) Short-interfering-RNA-mediated gene silencing in mammalian cells requires dicer and eIF2C translation initiation factors. *Current Biology* **13,** 41-46.

Doyle G. A., Bourdeau-Heller J. M., Coulthard S., Meisner L. F. & Ross J. (2000) Amplification in human breast cancer of a gene encoding a c-myc mRNA- binding protein. *Cancer Res.* **60,** 2756-2759.

Dyer K. D., Rosenberg H. F. (2006) The RNase a superfamily: Generation of diversity and innate host defense. *Mol. Divers.* **10,** 585-597.

Eberle A. B., Lykke-Andersen S., Mühlemann O. & Jensen T. H. (2009) SMG6 promotes endonucleolytic cleavage of nonsense mRNA in human cells. *Nature Structural and Molecular Biology* **16,** 49-55.

Economopoulou M. A. I., Fragoulis E. G. & Sideris D. C. (2007) Molecular cloning and characterization of the human RNase κ, an ortholog of Cc RNase. *Nucleic Acids Res.* **35,** 6389-6398.

Elcheva I., Tarapore R. S., Bhatia N. & Spiegelman V. S. (2008) Overexpression of mRNA-binding protein CRD-BP in malignant melanomas. *Oncogene* **27,** 5069-5074.

Esslinger S., Förstemann K. (2009) MicroRNAs repress mainly through mRNA decay. *Angewandte Chemie - International Edition* **48,** 853-855.

Eulalio A., Behm-Ansmant I. & Izaurralde E. (2007) P bodies: At the crossroads of post-transcriptional pathways. *Nature Reviews Molecular Cell Biology* **8,** 9-22.

Fan J., Yang X., Wang W., Wood III W. H., Becker K. G. & Gorospe M. (2002) Global analysis of stress-regulated mRNA turnover by using cDNA arrays. *Proc. Natl. Acad. Sci. U. S. A.* **99,** 10611-10616.

Faraoni I., Antonetti F. R., Cardone J. & Bonmassar E. (2009) miR-155 gene: A typical multifunctional microRNA. *Biochimica Et Biophysica Acta - Molecular Basis of Disease* **1792,** 497-505.

Fillman C., Lykke-Andersen J. (2005) RNA decapping inside and outside of processing bodies. *Curr. Opin. Cell Biol.* **17,** 326-331.

Fortin K. R., Nicholson R. H. & Nicholson A. W. (2002) Mouse ribonuclease III. cDNA structure, expression analysis, and chromosomal location. *BMC Genomics* **3,** .

Franks T. M., Lykke-Andersen J. (2008) The Control of mRNA Decapping and P-Body Formation. *Mol. Cell* **32,** 605-615.

Galicia-Vázquez G., Lindqvist L., Wang X., Harvey I., Liu J. & Pelletier J. (2009) High-throughput assays probing protein-RNA interactions of eukaryotic translation initiation factors. *Anal. Biochem.* **384,** 180-188.

Gallouzi I. E., Brennan C. M., Stenberg M. G., Swanson M. S., Eversole A., Maizels N. & Steitz J. A. (2000) HuR binding to cytoplasmic mRNA is perturbed by heat shock. *Proc. Natl. Acad. Sci. U. S. A.* **97,** 3073-3078.

Gallouzi I. E., Parker F., Chebli K., Maurier F., Labourier E., Barlat I., Capony J. -., Tocque B. & Tazi J. (1998) A novel phosphorylation-dependent RNase activity of GAP-SH3 binding protein: A potential link between signal transduction and RNA stability. *Mol. Cell. Biol.* **18,** 3956-3965.

Gao B., Lee S. M., Chen A., Zhang J., Zhang D. D., Kannan K., Ortmann R. A. & Fang D. (2008) Synoviolin promotes IRE1 ubiquitination and degradation in synovial fibroblasts from mice with collagen-induced arthritis. *EMBO Rep.* **9,** 480-485.

Gao M., Fritz D. T., Ford L. P. & Wilusz J. (2000) Interaction between a poly(A)-specific ribonuclease and the 5' cap influences mRNA deadenylation rates in vitro. *Mol. Cell* **5,** 479-488.

Garneau N. L., Wilusz J. & Wilusz C. J. (2007) The highways and byways of mRNA decay. *Nature Reviews Molecular Cell Biology* **8,** 113-126.

Gironella M., Seux M., Xie M. J., Cano C., Tomasini R., Gommeaux J., Garcia S., Nowak J., Man L. Y., Jeang K. T., Chaix A., Fazli L., Motoo Y., Wang Q., Rocchi P., Russo A., Gleave M., Dagorn J. C., Iovanna J. L., Carrier A., Pébusque M. J. & Dusetti N. J. (2007) Tumor protein 53-induced nuclear protein 1 expression is repressed by miR-155, and its restoration inhibits pancreatic tumor development. *Proc. Natl. Acad. Sci. U. S. A.* **104,** 16170-16175.

Glavan F., Behm-Ansmant I., Izaurralde E. & Conti E. (2006) Structures of the PIN domains of SMG6 and SMG5 reveal a nuclease within the mRNA surveillance complex. *EMBO J.* **25,** 5117-5125.

Gomez B. P., Riggins R. B., Shajahan A. N., Klimach U., Wang A., Crawford A. C., Zhu Y., Zwart A., Wang M. & Clarke R. (2007) Human X-Box binding protein-1 confers both estrogen independence and antiestrogen resistance in breast cancer cell lines. *FASEB Journal* **21,** 4013-4027.

Gregory R. I., Yan K. P., Amuthan G., Chendrimada T., Doratotaj B., Cooch N. & Shiekhattar R. (2004) The Microprocessor complex mediates the genesis of microRNAs. *Nature* **432,** 235-240.

Grundmann U., Romisch J., Siebold B., Bohn H. & Amann E. (1990) Cloning and expression of a cDNA encoding human placental protein 11, a putative serine protease with diagnostic significance as a tumor marker. *DNA Cell Biol.* **9,** 243-250.

Gu M., Fabrega C., Liu S. W., Liu H., Kiledjian M. & Lima C. D. (2004) Insights into the structure, mechanism, and regulation of scavenger mRNA decapping activity. *Mol. Cell* **14,** 67-80.

Gu M., Lima C. D. (2005) Processing the message: Structural insights into capping and decapping mRNA. *Curr. Opin. Struct. Biol.* **15,** 99-106.

Gu W., Wells A. L., Pan F. & Singer R. H. (2008) Feedback regulation between zipcode binding protein 1 and β-catenin mRNAs in breast cancer cells. *Mol. Cell. Biol.* **28,** 4963-4974.

Guichard C., Pedruzzi E., Fay M., Marie J. C., Braut-Boucher F., Daniel F., Grodet A., Gougerot-Pocidalo M. A., Chastre E., Kotelevets L., Lizard G., Vandewalle A., Driss F. & Ogier-Denis E. (2006) Dihydroxyphenylethanol induces apoptosis by activating serine/threonine protein phosphatase PP2A and promotes the endoplasmic reticulum stress response in human colon carcinoma cells. *Carcinogenesis* **27,** 1812-1827.

Guo Z., Qian L., Liu R., Dai H., Zhou M., Zheng L. & Shen B. (2008) Nucleolar localization and dynamic roles of flap endonuclease 1 in ribosomal DNA replication and damage repair. *Mol. Cell. Biol.* **28,** 4310-4319.

Hammer N. A., Hansen T. v., Byskov A. G., Rajpert-De Meyts E., Grøndahl M. L., Bredkjær H. E., Wewer U. M., Christiansen J. & Nielsen F. C. (2005) Expression of IGF-II mRNA-binding proteins (IMPs) in gonads and testicular cancer. *Reproduction* **130,** 203-212.

Han J., Lee Y., Yeom K. H., Kim Y. K., Jin H. & Kim V. N. (2004) The Drosha-DGCR8 complex in primary microRNA processing. *Genes and Development* **18,** 3016-3027.

Hua Y., Zhou J. (2004) Survival motor neuron protein facilitates assembly of stress granules. *FEBS Lett.* **572,** 69-74.

Huntzinger E., Izaurralde E. (2011) Gene silencing by microRNAs: Contributions of translational repression and mRNA decay. *Nature Reviews Genetics* **12,** 99-110.

Hutvagner G., Zamore P. D. (2002) A microRNA in a multiple-turnover RNAi enzyme complex. *Science* **297,** 2056-2060.

Hwang H. W., Wentzel E. A. & Mendell J. T. (2007) A hexanucleotide element directs microRNA nuclear import. *Science* **315,** 97-100.

Inaba N., Ishige H. & Ijichi M. (1982) Immunohistochemical detection of pregnancy-specific protein (SP1) and placenta-specific tissue proteins (PP5, PP10, PP11 and PP12) in ovarian adenocarcinomas. *Oncodevelopmental Biology and Medicine* **3,** 379-389.

Inaba N., Renk T., Daume E. & Bohn H. (1981) Ectopic production of placenta-'specific' tissue proteins (PP5 and PP11) by malignant breast tumors. *Arch. Gynecol.* **231,** 87-96.

Inaba N., Renk T. & Wurster K. (1980) Ectopic synthesis of pregnancy specific β1-glycoprotein (SP1) and placental specific tissue proteins (PP5, PP10, P11, PP12) in nontrophoblastic malignant tumours. Possible markers in oncology. *Klin. Wochenschr.* **58,** 789-791.

Inui M., Martello G. & Piccolo S. (2010) MicroRNA control of signal transduction. *Nature Reviews Molecular Cell Biology* **11,** 252-263.

Ioannidis P., Kottaridi C., Dimitriadis E., Courtis N., Mahaira L., Talieri M., Giannopoulos A., Iliadis K., Papaioannou D., Nasioulas G. & Trangas T. (2004) Expression of the RNA-binding protein CRD-BP in brain and non-small cell lung tumors. *Cancer Lett.* **209,** 245-250.

Ioannidis P., Mahaira L., Papadopoulou A., Teixeira M. R., Heim S., Andersen J. A., Evangelou E., Dafni U., Pandis N. & Trangas T. (2003) 8q24 copy number gains and expression of the c-myc mRNA stabilizing protein CRD-BP in primary breast carcinomas. *International Journal of Cancer* **104,** 54-59.

Ioannidis P., Mahaira L. G., Perez S. A., Gritzapis A. D., Sotiropoulou P. A., Kavalakis G. J., Antsaklis A. I., Baxevanis C. N. & Papamichail M. (2005) CRD-BP/IMP1 expression characterizes cord blood CD34+ stem cells and affects c-myc and IGF-II expression in MCF-7 cancer cells. *J. Biol. Chem.* **280,** 20086-20093.

Iorio M. V., Ferracin M., Liu C. G., Veronese A., Spizzo R., Sabbioni S., Magri E., Pedriali M., Fabbri M., Campiglio M., Ménard S., Palazzo J. P., Rosenberg A., Musiani P., Volinia S., Nenci I., Calin G. A., Querzoli P., Negrini M. & Croce C. M. (2005) MicroRNA gene expression deregulation in human breast cancer. *Cancer Res.* **65,** 7065-7070.

Iwakoshi N. N., Lee A. H., Vallabhajosyula P., Otipoby K. L., Rajewsky K. & Glimcher L. H. (2003) Plasma cell differentiation and the unfolded protein response intersect at the transcription factor XBP-I. *Nat. Immunol.* **4,** 321-329.

Iwawaki T., Hosoda A., Okuda T., Kamigori Y., Nomura-Furuwatari C., Kimata Y., Tsuru A. & Kohno K. (2001) Translational control by the ER transmembrane kinase/ribonuclease IRE1 under ER stress. *Nat. Cell Biol.* **3,** 158-164.

Jakymiw A., Lian S., Eystathioy T., Li S., Satoh M., Hamel J. C., Fritzler M. J. & Chan E. K. L. (2005) Disruption of GW bodies impairs mammalian RNA interference. *Nat. Cell Biol.* **7,** 1167-1174.

Jinek M., Doudna J. A. (2009) A three-dimensional view of the molecular machinery of RNA interference. *Nature* **457,** 405-412.

John B., Enright A. J., Aravin A., Tuschl T., Sander C. & Marks D. S. (2004) Human microRNA targets. *PLoS Biology* **2,** .

Joung H. J., Liao G., Collins J. B., Grissom S. F. & Jetten A. M. (2007) Farnesol-induced apoptosis in human lung carcinoma cells is coupled to the endoplasmic reticulum stress response. *Cancer Res.* **67,** 7929-7936.

Katoh T., Sakaguchi Y., Miyauchi K., Suzuki T., Suzuki T., Kashiwabara S. I. & Baba T. (2009) Selective stabilization of mammalian microRNAs by 3' adenylation mediated by the cytoplasmic poly(A) polymerase GLD-2. *Genes and Development* **23,** 433-438.

Katona T. M., Neubauer B. L., Iversen P. W., Zhang S., Baldridge L. A. & Cheng L. (2005) Elevated expression of angiogenin in prostate cancer and its precursors. *Clinical Cancer Research* **11,** 8358-8363.

Kaufmann I., Martin G., Friedlein A., Langen H. & Keller W. (2004) Human Fip1 is a subunit of CPSF that binds to U-rich RNA elements and stimulates poly(A) polymerase. *EMBO J.* **23,** 616-626.

Kedersha N., Chen S., Gilks N., Li W., Miller I. J., Stahl J. & Anderson P. (2002) Evidence that ternary complex (eIF2-GTP-tRNAi Met)-Deficient preinitiation complexes are core constituents of mammalian stress granules. *Mol. Biol. Cell* **13,** 195-210.

Kedersha N., Stoecklin G., Ayodele M., Yacono P., Lykke-Andersen J., Fitzler M. J., Scheuner D., Kaufman R. J., Golan D. E. & Anderson P. (2005) Stress granules and

processing bodies are dynamically linked sites of mRNP remodeling. *J. Cell Biol.* **169,** 871-884.

Kedersha N. L., Gupta M., Li W., Miller I. & Anderson P. (1999) RNA-binding proteins TIA-1 and TIAR link the phosphorylation of eIF-2α to the assembly of mammalian stress granules. *J. Cell Biol.* **147,** 1431-1441.

Kelemen B. R., Klink T. A., Behlke M. A., Eubanks S. R., Leland P. A. & Raines R. T. (1999) Hypersensitive substrate for ribonucleases. *Nucleic Acids Res.* **27,** 3696-3701.

Kijanka G., IpCho S., Baars S., Chen H., Hadley K., Beveridge A., Gould E. & Murphy D. (2009) Rapid characterization of binding specificity and cross-reactivity of antibodies using recombinant human protein arrays. *Journal of Immunological Methods* **340,** 132-137.

Kim M., Jung Y., Lee K. & Kim C. (2000) Identification of the Calcium Binding Sites in Translationally Controlled Tumor Protein. *Arch. Pharm. Res.* **23,** 633-636.

Kim M. M., Wiederschain D., Kennedy D., Hansen E. & Yuan Z. M. (2007) Modulation of p53 and MDM2 activity by novel interaction with Ras-GAP binding proteins (G3BP). *Oncogene* **26,** 4209-4215.

Kim S. E., Gorrell A., Rader S. D. & Lee C. H. (2010) Endoribonuclease activity of human apurinic/apyrimidinic endonuclease 1 revealed by a real-time fluorometric assay. *Anal. Biochem.* **398,** 69-75.

Kim V. N., Han J. & Siomi M. C. (2009) Biogenesis of small RNAs in animals. *Nature Reviews Molecular Cell Biology* **10,** 126-139.

Kim W. C., Lee C. H. (2009) The role of mammalian ribonucleases (RNases) in cancer. *Biochimica Et Biophysica Acta - Reviews on Cancer* **1796,** 99-113.

Kolev N. G., Yario T. A., Benson E. & Steitz J. A. (2008) Conserved motifs in both CPSF73 and CPSF100 are required to assemble the active endonuclease for histone mRNA 3′-end maturation. *EMBO Rep.* **9,** 1013-1018.

Kowalczyk P., Woszczyński M. & Ostrowski J. (2002) Increased expression of ribosomal protein S2 in liver tumors, posthepactomized livers, and proliferating hepatocytes in vitro. *Acta Biochim. Pol.* **49,** 615-624.

Kraus M., Malenke E., Gogel J., Müller H., Rückrich T., Overkleeft H., Ovaa H., Koscielniak E., Hartmann J. T. & Driessen C. (2008) Ritonavir induces endoplasmic reticulum stress and sensitizes sarcoma cells toward bortezomib-induced apoptosis. *Molecular Cancer Therapeutics* **7,** 1940-1948.

Krol J., Loedige I. & Filipowicz W. (2010) The widespread regulation of microRNA biogenesis, function and decay. *Nature Reviews Genetics* **11,** 597-610.

Lai P. F. H., Mohamed F., Monge J. -. & Stewart D. J. (2003) Downregulation of eNOS mRNA expression by TNFα: Identification and functional characterization of RNA-protein interactions in the 3'UTR. *Cardiovasc. Res.* **59,** 160-168.

Laneve P., Gioia U., Ragno R., Altieri F., Di Franco C., Santini T., Arceci M., Bozzoni I. & Caffarelli E. (2008) The tumor marker human placental protein 11 is an endoribonuclease. *J. Biol. Chem.* **283,** 34712-34719.

Lau P. W., MacRae I. J. (2009) The molecular machines that mediate microRNA maturation. *J. Cell. Mol. Med.* **13,** 54-60.

Le Roy F., Bisbal C., Silhol M., Martinand C., Lebleu B. & Salehzada T. (2001) The 2-5A/RNase L/RNase L Inhibitor (RNI) Pathway Regulates Mitochondrial mRNAs Stability in Interferon α-treated H9 Cells. *J. Biol. Chem.* **276,** 48473-48482.

Lebreton A., Tomecki R., Dziembowski A. & Séraphin B. (2008) Endonucleolytic RNA cleavage by a eukaryotic exosome. *Nature* **456,** 993-996.

Lee F. S., Vallee B. L. (1989) Characterization of ribonucleolytic activity of angiogenin towards tRNA. *Biochem. Biophys. Res. Commun.* **161,** 121-126.

Lee K., Tirasophon W., Shen X., Michalak M., Prywes R., Okada T., Yoshida H., Mori K. & Kaufman R. J. (2002) IRE1-mediated unconventional mRNA splicing and S2P-mediated ATF6 cleavage merge to regulate XBP1 in signaling the unfolded protein response. *Genes and Development* **16,** 452-466.

Leeds P., Kren B. T., Boylan J. M., Betz N. A., Steer C. J., Gruppuso P. A. & Ross J. (1997) Developmental regulation of CRD-BP, an RNA-binding protein that stabilizes c-myc mRNA in vitro. *Oncogene* **14,** 1279-1286.

Li B., Gao B., Ye L., Han X., Wang W., Kong L., Fang X., Zeng Y., Zheng H., Li S., Wu Z. & Ye L. (2007) Hepatitis B virus X protein (HBx) activates ATF6 and IRE1-XBP1 pathways of unfolded protein response. *Virus Res.* **124,** 44-49.

Li C., Qiu L., Ning X., Chen A., Qin S., Wu H. & Zhao J. (2010) The first molluscan TCTP in Venerupis philippinarum: Molecular cloning and expression analysis. *Fish and Shellfish Immunology* **29,** 530-533.

Li W. M., Barnes T. & Lee C. H. (2010) Endoribonucleases-enzymes gaining spotlight in mRNA metabolism. *FEBS Journal* **277,** 627-641.

Li Y., Song M. G. & Kiledjian M. (2008) Transcript-specific decapping and regulated stability by the human Dcp2 decapping protein. *Mol. Cell. Biol.* **28,** 939-948.

Lian S., Jakymiw A., Eystathioy T., Hamel J. C., Fritzler M. J. & Chan E. K. L. (2006) GW bodies, microRNAs and the cell cycle. *Cell Cycle* **5,** 242-245.

Liang S. L., Quirk D. & Zhou A. (2006) RNase L: Its biological roles and regulation. *IUBMB Life* **58,** 508-514.

Licata L. A., Hostetter C. L., Crismale J., Sheth A. & Keen J. C. (2010) The RNA-binding protein HuR regulates GATA3 mRNA stability in human breast cancer cell lines. *Breast Cancer Res. Treat.* **122,** 55-63.

Lin J. H., Li H., Yasumura D., Cohen H. R., Zhang C., Panning B., Shokat K. M., LaVail M. M. & Walter P. (2007) IRE1 signaling affects cell fate during the unfolded protein response. *Science* **318,** 944-949.

Little J. L., Wheeler F. B., Fels D. R., Koumenis C. & Kridel S. J. (2007) Inhibition of fatty acid synthase induces endoplasmic reticulum stress in tumor cells. *Cancer Res.* **67,** 1262-1269.

Liu J., Carmell M. A., Rivas F. V., Marsden C. G., Thomson J. M., Song J. -., Hammond S. M., Joshua-Tor L. & Hannon G. J. (2004) Argonaute2 is the catalytic engine of mammalian RNAi. *Science* **305,** 1437-1441.

Lu S., Sun Y. -. & Chiang V. L. (2009) Adenylation of plant miRNAs. *Nucleic Acids Res.* **37,** 1878-1885.

Lueking A., Horn M., Eickhoff H., Büssow K., Lehrach H. & Walter G. (1999) Protein microarrays for gene expression and antibody screening. *Anal. Biochem.* **270,** 103-111.

Lunts Ya. V. (1976) The effect of some imidazol derivatives on the adenosine 3',5' monophosphoric acid phosphodiesterase activity (Russian). *Byulleten Eksperimentalnoi Biologii i Meditsiny* **82,** 1055-1059.

Lynn F. C. (2009) Meta-regulation: microRNA regulation of glucose and lipid metabolism. *Trends in Endocrinology and Metabolism* **20,** 452-459.

MacRae I. J., Ma E., Zhou M., Robinson C. V. & Doudna J. A. (2008) In vitro reconstitution of the human RISC-loading complex. *Proc. Natl. Acad. Sci. U. S. A.* **105,** 512-517.

Madsen B. E., Ramos E. M., Boulard M., Duda K., Overgaard J., Nordsmark M., Wiuf C. & Hansen L. L. (2008) Germline mutation in RNASEL predicts increased risk of head and neck, uterine cervix and breast cancer. *PLoS ONE* **3,** .

Makeyev E. V., Maniatis T. (2008) Multilevel regulation of gene expression by microRNAs. *Science* **319,** 1789-1790.

Mallardo M., Poltronieri P. & D'Urso O. F. (2008) Non-protein coding RNA biomarkers and differential expression in cancers: A review. *Journal of Experimental and Clinical Cancer Research* **27,** .

Mandel C. R., Kaneko S., Zhang H., Gebauer D., Vethantham V., Manley J. L. & Tong L. (2006) Polyadenylation factor CPSF-73 is the pre-mRNA 3'-end-processing endonuclease. *Nature* **444,** 953-956.

Maniataki E., Mourelatos Z. (2005) A human, ATP-independent, RISC assembly machine fueled by pre-miRNA. *Genes and Development* **19,** 2979-2990.

Martînez J., Ren Y. -., Nilsson P., Ehrenberg M. & Virtanen A. (2001) The mRNA Cap Structure Stimulates Rate of Poly(A) Removal and Amplifies Processivity of Degradation. *J. Biol. Chem.* **276,** 27923-27929.

Mattick J. S., Makunin I. V. (2006) Non-coding RNA. *Hum. Mol. Genet.* **15 Spec No 1,** R17-29.

Melo S. A., Ropero S., Moutinho C., Aaltonen L. A., Yamamoto H., Calin G. A., Rossi S., Fernandez A. F., Carneiro F., Oliveira C., Ferreira B., Liu C. -., Villanueva A., Capella G., Schwartz Jr. S., Shiekhattar R. & Esteller M. (2009) A TARBP2 mutation in human cancer impairs microRNA processing and DICER1 function. *Nat. Genet.* **41,** 365-370.

Mitchell P., Petfalski E., Shevchenko A., Mann M. & Tollervey D. (1997) The exosome: A conserved eukaryotic RNA processing complex containing multiple 3'→5' exoribonucleases. *Cell* **91,** 457-466.

Morita M., Suzuki T., Nakamura T., Yokoyama K., Miyasaka T. & Yamamoto T. (2007) Depletion of mammalian CCR4b deadenylase triggers elevation of the p27 Kip1 mRNA level and impairs cell growth. *Mol. Cell. Biol.* **27,** 4980-4990.

Mouratou B., Rouyre S., Pauillac S. & Guesdon J. -. (2002) Development of nonradioactive microtiter plate assays for nuclease activity. *Anal. Biochem.* **309,** 40-47.

Mukherjee D., Gao M., O'Connor J. P., Raijmakers R., Pruijn G., Lutz C. S. & Wilusz J. (2002) The mammalian exosome mediates the efficient degradation of mRNAs that contain AU-rich elements. *EMBO J.* **21,** 165-174.

Nicholson R. H., Nicholson A. W. (2002) Molecular characterization of a mouse cDNA encoding Dicer, a ribonuclease III ortholog involved in RNA interference. *Mammalian Genome* **13,** 67-73.

Noubissi F. K., Elcheva I., Bhatia N., Shakoori A., Ougolkov A., Liu J., Minamoto T., Ross J., Fuchs S. Y. & Spiegelman V. S. (2006) CRD-BP mediates stabilization of βTrCP1 and c-myc mRNA in response to β-catenin signalling. *Nature* **441,** 898-901.

Noubissi F. K., Goswami S., Sanek N. A., Kawakami K., Minamoto T., Moser A., Grinblat Y. & Spiegelman V. S. (2009) Wnt signaling stimulates transcriptional outcome of the hedgehog pathway by stabilizing GLI1 mRNA. *Cancer Res.* **69,** 8572-8578.

O'Carroll D., Mecklenbrauker I., Das P. P., Santana A., Koenig U., Enright A. J., Miska E. A. & Tarakhovsky A. (2007) A Slicer-independent role for Argonaute 2 in hematopoiesis and the microRNA pathway. *Genes and Development* **21,** 1999-2004.

Oh H. S. (2009) To Identify Novel Human Endoribonucleases that cleave CG Oligo I Using High-throughput System. CHEM 499 – Independent Research. UNBC.

Orii A., Masutani H., Nikaido T., Zhai Y. -., Kato K., Kariya M., Konishi I., Yodoi J. & Fujii S. (2002) Altered post-translational modification of redox factor 1 protein in human uterine smooth muscle tumors. *J. Clin. Endocrinol. Metab.* **87,** 3754-3759.

Ovcharenko D., Kelnar K., Johnson C., Leng N. & Brown D. (2007) Genome-scale microRNA and small interfering RNA screens identify small RNA modulators of TRAIL-induced apoptosis pathway. *Cancer Res.* **67,** 10782-10788.

Ozsolak F., Poling L. L., Wang Z., Liu H., Liu X. S., Roeder R. G., Zhang X., Song J. S. & Fisher D. E. (2008) Chromatin structure analyses identify miRNA promoters. *Genes and Development* **22,** 3172-3183.

Pardini B., Naccarati A., Novotny J., Smerhovsky Z., Vodickova L., Polakova V., Hanova M., Slyskova J., Tulupova E., Kumar R., Bortlik M., Barale R., Hemminki K. & Vodicka P. (2008) DNA repair genetic polymorphisms and risk of colorectal cancer in the Czech Republic. *Mutation Research - Fundamental and Molecular Mechanisms of Mutagenesis* **638,** 146-153.

Parker F., Maurier F., Delumeau I., Duchesne M., Faucher D., Debussche L., Dugue A., Schweighoffer F. & Tocque B. (1996) A Ras-GTPase-activating protein SH3-domain-binding protein. *Mol. Cell. Biol.* **16,** 2561-2569.

Parker R., Sheth U. (2007) P Bodies and the Control of mRNA Translation and Degradation. *Mol. Cell* **25,** 635-646.

Parker R., Song H. (2004) The enzymes and control of eukaryotic mRNA turnover. *Nature Structural and Molecular Biology* **11,** 121-127.

Paroo Z., Ye X., Chen S. & Liu Q. (2009) Phosphorylation of the Human MicroRNA-Generating Complex Mediates MAPK/Erk Signaling. *Cell* **139,** 112-122.

Proudfoot M., Kuznetsova E., Sanders S. A., Gonzalez C. F., Brown G., Edwards A. M., Arrowsmith C. H. & Yakunin A. F. (2008) High throughput screening of purified proteins for enzymatic activity. *Methods Mol. Biol.* **426,** 331-341.

Pryzbylkowski P., Obajimi O. & Keen J. C. (2008) Trichostatin A and 5 Aza-2' deoxycytidine decrease estrogen receptor mRNA stability in ER positive MCF7 cells through modulation of HuR. *Breast Cancer Res. Treat.* **111,** 15-25.

Raghavan A., Ogilvie R. L., Reilly C., Abelson M. L., Raghavan S., Vasdewani J., Krathwohl M. & Bohjanen P. R. (2002) Genome-wide analysis of mRNA decay in resting and activated primary human T lymphocytes. *Nucleic Acids Res.* **30,** 5529-5538.

Rai D., Karanti S., Jung I., Dahia P. L. M. & Aguiar R. C. T. (2008) Coordinated expression of microRNA-155 and predicted target genes in diffuse large B-cell lymphoma. *Cancer Genet. Cytogenet.* **181,** 8-15.

Raijmakers R., Schilders G. & Pruijn G. J. M. (2004) The exosome, a molecular machine for controlled RNA degradation in both nucleus and cytoplasm. *Eur. J. Cell Biol.* **83,** 175-183.

Rajasethupathy P., Fiumara F., Sheridan R., Betel D., Puthanveettil S. V., Russo J. J., Sander C., Tuschl T. & Kandel E. (2009) Characterization of Small RNAs in Aplysia Reveals a Role for miR-124 in Constraining Synaptic Plasticity through CREB. *Neuron* **63,** 803-817.

Ramachandran V., Chen X. (2008) Degradation of microRNAs by a family of exoribonucleases in Arabidopsis. *Science* **321,** 1490-1492.

Robins P., Pappin D. J. C., Wood R. D. & Lindahl T. (1994) Structural and functional homology between mammalian DNase IV and the 5'- nuclease domain of Escherichia coli DNA polymerase I. *J. Biol. Chem.* **269,** 28535-28538.

Rodgers N. D., Wang Z. & Kiledjian M. (2002) Characterization and purification of a mammalian endoribonuclease specific for the α-globin mRNA. *J. Biol. Chem.* **277,** 2597-2604.

Rosenberg U. B., Preiss A. & Seifert E. (1985) Production of phenocopies by Kruppel antisense RNA injection into Drosophila embryos. *Nature* **313,** 703-706.

Ross J., Lemm I. & Berberet B. (2001) Overexpression of an mRNA-binding protein in human colorectal cancer. *Oncogene* **20,** 6544-6550.

Ryan B. M., Robles A. I. & Harris C. C. (2010) Genetic variation in microRNA networks: The implications for cancer research. *Nature Reviews Cancer* **10,** 389-402.

Ryan K., Calvo O. & Manley J. L. (2004) Evidence that polyadenylation factor CPSF-73 is the mRNA 3′ processing endonuclease. *RNA* **10,** 565-573.

Saxena S. K., Rybak S. M., Davey Jr. R. T., Youle R. J. & Ackerman E. J. (1992) Angiogenin is a cytotoxic, tRNA-specific ribonuclease in the RNase A superfamily. *J. Biol. Chem.* **267,** 21982-21986.

Schaeffer D., Tsanova B., Barbas A., Reis F. P., Dastidar E. G., Sanchez-Rotunno M., Arraiano C. M. & Van Hoof A. (2009) The exosome contains domains with specific endoribonuclease, exoribonuclease and cytoplasmic mRNA decay activities. *Nature Structural and Molecular Biology* **16,** 56-62.

Schneider C., Leung E., Brown J. & Tollervey D. (2009) The N-terminal PIN domain of the exosome subunit Rrp44 harbors endonuclease activity and tethers Rrp44 to the yeast core exosome. *Nucleic Acids Res.* **37,** 1127-1140.

Sethi P., Lukiw W. J. (2009) Micro-RNA abundance and stability in human brain: Specific alterations in Alzheimer's disease temporal lobe neocortex. *Neurosci. Lett.* **459,** 100-104.

Shapiro R., Riordan J. F. & Vallee B. L. (1986) Characteristic ribonucleolytic activity of human angiogenin. *Biochemistry (N. Y.)* **25,** 3527-3532.

Shen B., Nolan J. P., Sklar L. A. & Park M. S. (1996) Essential amino acids for substrate binding and catalysis of human flap endonuclease. *J. Biol. Chem.* **271,** 9173-9176.

Shuda M., Kondoh N., Imazeki N., Tanaka K., Okada T., Mori K., Hada A., Arai M., Wakatsuki T., Matsubara O., Yamamoto N. & Yamamoto M. (2003) Activation of the ATF6, XBP1 and grp78 genes in human hepatocellular carcinoma: A possible involvement of the ER stress pathway in hepatocarcinogenesis. *J. Hepatol.* **38,** 605-614.

Siomi H., Siomi M. C. (2010) Posttranscriptional Regulation of MicroRNA Biogenesis in Animals. *Mol. Cell* **38,** 323-332.

Snow B. E., Erdmann N., Cruickshank J., Goldman H., Gill R. M., Robinson M. O. & Harrington L. (2003) Functional conservation of the telomerase protein Est1p in humans. *Current Biology* **13,** 698-704.

Sparanese D., Lee C. H. (2007) CRD-BP shields c-myc and MDR-1 RNA from endonucleolytic attack by a mammalian endoribonuclease. *Nucleic Acids Res.* **35,** 1209-1221.

Stevens A. (1998) Endonucleolytic cleavage of RNA at 5' endogenous stem structures by human flap endonuclease 1. *Biochem. Biophys. Res. Commun.* **251,** 501-508.

Stevens A., Wang Y., Bremer K., Zhang J., Hoepfner R., Antoniou M., Schoenberg D. R. & Maquat L. E. (2002) β-globin mRNA decay in erythroid cells: UG site-preferred endonucleolytic cleavage that is augmented by a premature termination codon. *Proc. Natl. Acad. Sci. U. S. A.* **99,** 12741-12746.

Stoecklin G., Stubbs T., Kedersha N., Wax S., Rigby W. F. C., Blackwell T. K. & Anderson P. (2004) MK2-induced tristetraprolin:14-3-3 Complexes prevent stress granule association and ARE-mRNA decay. *EMBO J.* **23,** 1313-1324.

Su H., Trombly M. I., Chen J. & Wang X. (2009) Essential and overlapping functions for mammalian argonautes in microRNA silencing. *Genes and Development* **23,** 304-317.

Tam W., Dahlberg J. E. (2006) miR-155/BIC as an oncogenic microRNA. *Genes Chromosomes and Cancer* **45,** 211-212.

Tell G., Damante G., Caldwell D. & Kelley M. R. (2005) The intracellular localization of APE1/Ref-1: More than a passive phenomenon? *Antioxidants and Redox Signaling* **7,** 367-384.

Thomas M. G., Tosar L. J. M., Loschi M., Pasquini J. M., Correale J., Kindler S. & Boccaccio G. L. (2005) Staufen recruitment into stress granules does not affect early mRNA transport in oligodendrocytes. *Mol. Biol. Cell* **16,** 405-420.

Tirasophon W., Welihinda A. A. & Kaufman R. J. (1998) A stress response pathway from the endoplasmic reticulum to the nucleus requires a novel bifunctional protein kinase/endoribonuclease (Ire1p) in mammalian cells. *Genes and Development* **12,** 1812-1824.

Tomecki R., Dziembowski A. (2010) Novel endoribonucleases as central players in various pathways of eukaryotic RNA metabolism. *RNA* **16,** 1692-1724.

Tomecki R., Kristiansen M. S., Lykke-Andersen S., Chlebowski A., Larsen K. M., Szczesny R. J., Drazkowska K., Pastula A., Andersen J. S., Stepien P. P., Dziembowski A. & Jensen T. H. (2010) The human core exosome interacts with differentially localized processive RNases: HDIS3 and hDIS3L. *EMBO J.* **29,** 2342-2357.

Tong A. W., Nemunaitis J. (2008) Modulation of miRNA activity in human cancer: A new paradigm for cancer gene therapy? *Cancer Gene Ther.* **15,** 341-355.

Tourrière H., Chebli K., Zekri L., Courselaud B., Blanchard J. M., Bertrand E. & Tazi J. (2003) The RasGAP-associated endoribonuclease G3BP assembles stress granules. *J. Cell Biol.* **160,** 823-831.

Tourrière H., Gallouzi I. E., Chebli K., Capony J. P., Mouaikel J., Van der Geer P. & Tazi J. (2001) RasGAP-associated endoribonuclease G3BP: Selective RNA degradation and phosphorylation-dependent localization. *Mol. Cell. Biol.* **21,** 7747-7760.

Tuynder M., Susini L., Prieur S., Besse S., Fiucci G., Amson R. & Telerman A. (2002) Biological models and genes of tumor reversion: Cellular reprogramming through tpt1/TCTP and SIAH-1. *Proc. Natl. Acad. Sci. U. S. A.* **99,** 14976-14981.

van den Berg A., Mols J. & Han J. (2008) RISC-target interaction: Cleavage and translational suppression. *Biochimica Et Biophysica Acta - Gene Regulatory Mechanisms* **1779,** 668-677.

Van Dijk E. L., Sussenbach J. S. & Holthuizen P. E. (2000) Distinct RNA structural domains cooperate to maintain a specific cleavage site in the 3'-UTR of IGF-II mRNAs. *J. Mol. Biol.* **300,** 449-467.

Vihinen P., Kallioinen M., Vuoristo M. S., Ivaska J., Syrjänen K. J., Hahka-Kemppinen M., Kellokumpu-Lehtinen P. L. & Pyrhönen S. O. (2007) Serum angiogenin levels predict treatment response in patients with stage IV melanoma. *Clinical and Experimental Metastasis* **24,** 567-574.

Vikesaa J., Hansen T. V. O., Jønson L., Borup R., Wewer U. M., Christiansen J. & Nielsen F. C. (2006) RNA-binding IMPs promote cell adhesion and invadopodia formation. *EMBO J.* **25,** 1456-1468.

Wang D., Luo M. & Kelley M. R. (2004) Human apurinic endonuclease 1 (APE1) expression and prognostic significance in osteosarcoma: Enhanced sensitivity of osteosarcoma to DNA damaging agents using silencing RNA APE1 expression inhibition. *Molecular Cancer Therapeutics* **3,** 679-686.

Wang M., Hu Y., Amatangelo M. D. & Stearns M. E. (2011) Role of ribosomal protein RPS2 in controlling let-7a expression in human prostate cancer. *Molecular Cancer Research* **9,** 36-50.

Wang N. R., Hergenrother P. J. (2007) A continuous fluorometric assay for the assessment of MazF ribonuclease activity. *Anal. Biochem.* **371,** 173-183.

Wiemer E. A. C. (2007) The role of microRNAs in cancer: No small matter. *Eur. J. Cancer* **43,** 1529-1544.

Wilczynska A., Aigueperse C., Kress M., Dautry F. & Weil D. (2005) The translational regulator CPEB1 provides a link between dcp1 bodies and stress granules. *J. Cell. Sci.* **118,** 981-992.

Wolff D. J., Datto G. A. & Samatovicz R. A. (1993) The dual mode of inhibition of calmodulin-dependent nitric-oxide synthase by antifungal imidazole agents. *J. Biol. Chem.* **268,** 9430-9436.

Woo Y. H., Ravi Rajagopalan P. T. & Benkovic S. J. (2005) A nonradioactive DNA methyltransferase assay adaptable to high-throughput screening. *Anal. Biochem.* **340,** 336-340.

Woodbeck R. (2010) Identification of Heat Shock Protein 70 as a candidate Mammalian endoribonuclease. CHEM 499 – Independent Research. UNBC .

Wulczyn F. G., Smirnova L., Rybak A., Brandt C., Kwidzinski E., Ninnemann O., Strehle M., Seiler A., Schumacher S. & Nitsch R. (2007) Post-transcriptional regulation of the let-7 microRNA during neural cell specification. *FASEB Journal* **21,** 415-426.

Yang Z. Z., Chen X. H. & Wang D. (2007) Experimental study enhancing the chemosensitivity of multiple myeloma to melphalan by using a tissue-specific APE1-silencing RNA expression vector. *Clinical Lymphoma and Myeloma* **7,** 296-304.

Yi R., Fuchs E. (2010) MicroRNA-mediated control in the skin. *Cell Death Differ.* **17,** 229-235.

Yu B., Yang Z., Li J., Minakhina S., Yang M., Padgett R. W., Steward R. & Chen X. (2005) Methylation as a crucial step in plant microRNA biogenesis. *Science* **307,** 932-935.

Yue J., Tigyi G. (2006) MicroRNA trafficking and human cancer. *Cancer Biology and Therapy* **5,** 573-578.

Zhang B., Pan X., Cobb G. P. & Anderson T. A. (2007) microRNAs as oncogenes and tumor suppressors. *Dev. Biol.* **302,** 1-12.

Zhang H., Kolb F. A., Jaskiewicz L., Westhof E. & Filipowicz W. (2004) Single processing center models for human Dicer and bacterial RNase III. *Cell* **118,** 57-68.

Zhang H. Z., Liu J. G., Wei Y. P., Wu C., Cao Y. K. & Wang M. (2007) Expression of G3BP and RhoC in esophageal squamous carcinoma and thier effect on prognosis. *World Journal of Gastroenterology* **13,** 4126-4130.

Zhang K., Dion N., Fuchs B., Damron T., Gitelis S., Irwin R., O'Connor M., Schwartz H., Scully S. P., Rock M. G., Bolander M. E. & Sarkar G. (2002) The human homolog of yeast SEP1 is a novel candidate tumor suppressor gene in osteogenic sarcoma. *Gene* **298,** 121-127.

Zheng D., Ezzeddine N., Chen C. Y. A., Zhu W., He X. & Shyu A. B. (2008) Deadenylation is prerequisite for P-body formation and mRNA decay in mammalian cells. *J. Cell Biol.* **182,** 89-101.

Zuker M. (2003) Mfold web server for nucleic acid folding and hybridization prediction. *Nucleic Acids Res.* **31,** 3406-3415.